

## Feed stream mixing in stirred tank reactors

**Citation for published version (APA):**

Verschuren, I. L. M. (2001). *Feed stream mixing in stirred tank reactors*. [Phd Thesis 1 (Research TU/e / Graduation TU/e), Chemical Engineering and Chemistry]. Technische Universiteit Eindhoven.  
<https://doi.org/10.6100/IR547715>

**DOI:**

[10.6100/IR547715](https://doi.org/10.6100/IR547715)

**Document status and date:**

Published: 01/01/2001

**Document Version:**

Publisher's PDF, also known as Version of Record (includes final page, issue and volume numbers)

**Please check the document version of this publication:**

- A submitted manuscript is the version of the article upon submission and before peer-review. There can be important differences between the submitted version and the official published version of record. People interested in the research are advised to contact the author for the final version of the publication, or visit the DOI to the publisher's website.
- The final author version and the galley proof are versions of the publication after peer review.
- The final published version features the final layout of the paper including the volume, issue and page numbers.

[Link to publication](#)

**General rights**

Copyright and moral rights for the publications made accessible in the public portal are retained by the authors and/or other copyright owners and it is a condition of accessing publications that users recognise and abide by the legal requirements associated with these rights.

- Users may download and print one copy of any publication from the public portal for the purpose of private study or research.
- You may not further distribute the material or use it for any profit-making activity or commercial gain
- You may freely distribute the URL identifying the publication in the public portal.

If the publication is distributed under the terms of Article 25fa of the Dutch Copyright Act, indicated by the "Taverne" license above, please follow below link for the End User Agreement:

[www.tue.nl/taverne](http://www.tue.nl/taverne)

**Take down policy**

If you believe that this document breaches copyright please contact us at:

[openaccess@tue.nl](mailto:openaccess@tue.nl)

providing details and we will investigate your claim.

# **FEED STREAM MIXING IN STIRRED TANK REACTORS**

PROEFSCHRIFT

ter verkrijging van de graad van doctor aan de  
Technische Universiteit Eindhoven, op gezag van de  
Rector Magnificus, prof. dr. R.A. van Santen, voor een  
commissie aangewezen door het College voor  
Promoties in het openbaar te verdedigen  
op donderdag 13 september 2001 om 16.00 uur

door

Iris Lean Marieke Verschuren

geboren te Beek en Donk

Dit proefschrift is goedgekeurd door de promotoren:

prof. dr. ir. J.T.F. Keurentjes

en

prof. dr. ir. G.J.F. van Heijst

© 2001, Iris L.M. Verschuren

Omslagontwerp: Dion van Rijswijk

CIP-DATA LIBRARY TECHNISCHE UNIVERSITEIT EINDHOVEN

Verschuren, Iris L.M.

Feed stream mixing in stirred tank reactors / by Iris L.M. Verschuren. -

Eindhoven : Technische Universiteit Eindhoven, 2001.

Proefschrift. - ISBN 90-386-2942-7

NUGI 841

Trefwoorden: turbulente menging / geroerde reactoren / toevoerstroam /

chemische-reactieselectiviteit

Subject headings: turbulent mixing / stirred reactors / feed stream /

chemical reaction selectivity

Voor mijn ouders



## Chapter 1

---

### **EFFECT OF MIXING ON THE SELECTIVITY OF CHEMICAL REACTIONS**

1	Introduction	2
2	Mixing-sensitive reactions	2
3	Overview of mixing models	4
4	Outline of this thesis	8
	Nomenclature	10
	References	10

## Chapter 2

---

### **THE EFFECT OF MIXING ON THE PRODUCT QUALITY IN SEMI-BATCH STIRRED TANK REACTORS**

	Abstract	13
1	Introduction	14
2	Mixing model	15
3	Hydrodynamic parameters	19
3.1	Energy dissipation rate and velocity length scale	19
3.2	Location of a fluid element	23
4	Experimental verification of the model	24
5	Results and discussion	26
6	Conclusions	31
	Nomenclature	33
	References	34

## Chapter 3

### **MEAN CONCENTRATIONS AND CONCENTRATION FLUCTUATIONS IN A STIRRED TANK REACTOR**

Abstract	37
1 Introduction	38
2 Model for the mean concentration and concentration variance of an passive tracer fed to a stirred tank reactor	39
3 Local energy dissipation rates and mean velocities	44
3.1 LDV experiments	44
3.2 LDV data processing	47
3.3 Results of the LDV experiments	49
4 Mean concentration and concentration variance of an passive tracer fed to a stirred tank reactor	52
4.1 PLIF experiments	52
4.2 PLIF data processing	53
4.3 Results of the PLIF experiments and comparison between simulations and experiments	55
5 Conclusions and application of the main results	64
Nomenclature	66
References	68

## Chapter 4

### **LARGE-SCALE OSCILLATIONS OF A FEED STREAM INSIDE A STIRRED TANK REACTOR**

Abstract	71
1 Introduction	72
2 Theory	73
3 Experimental	76
3.1 Geometry of the vessel	77
3.2 Experimental determination of the flow field characteristics	78
3.3 Experimental determination of the displacements of the centres-of-mass	80

4 Results and Discussion	83
5 Conclusions and practical application	89
Nomenclature	90
References	91

Chapter 5

**DETERMINATION OF THE MIXING RATE OF A HIGH VELOCITY FEED STREAM IN AGITATED VESSELS**

Abstract	93
1 Introduction	94
2 Turbulent dispersion of a feed stream	95
3 Experimental	99
3.1 Determination of the turbulent kinetic energy and the length scale of the velocity fluctuations	99
3.2 Determination of the characteristic length scale for turbulent dispersion and the turbulent dispersion time	102
4 Results and Discussion	103
4.1 Turbulent kinetic energy, integral length scale of the velocity fluctuations and the characteristic length scale for turbulent dispersion	103
4.2 Turbulent dispersion time	109
5 Conclusions	112
Nomenclature	113
References	114



## Chapter 6

### **SCALE-UP OF A STIRRED TANK REACTOR EQUIPPED WITH A PFAUDLER TYPE IMPELLER**

Abstract	117
1 Introduction	118
2 Micromixing model	118
3 Experiments	120
3.1 Experimental determination of the energy dissipation rate	120
3.2 Experimental determination of the product distribution of a mixing-sensitive reaction set	122
4 Results and Discussion	123
4.1 Results of the LDV and torque measurements	123
4.2 Results of the reactive experiments	126
5 Conclusions	130
Nomenclature	131
References	131

## Chapter 7

### **DESIGN AND SCALE-UP OF INDUSTRIAL MIXING PROCESSES**

Abstract	133
1 Introduction	134
2 Practical application of mixing models	134
2.1 Lagrangian mechanistic mixing model	134
2.2 Model based on Reynolds decomposition	139
3 Suggestions for future research	142
Nomenclature	146
References	147



Chapter 1

---

# **EFFECT OF MIXING ON THE SELECTIVITY OF CHEMICAL REACTIONS**

## 1. Introduction

Mixing has a large influence on the yield and selectivity of a broad range of chemical processes. Therefore, the design and operation of mixing devices often determines the profitability and environmental acceptability of the whole plant. In this study the interaction between mixing and chemical reactions is investigated for stirred tank reactors with a feed stream operated under turbulent flow conditions. This reactor type is frequently used in the chemical and biochemical industry, which makes it an important research topic. Figure 1 shows three examples of standard stirred tank reactors, i.e. a Pfaudler reactor, a reactor equipped with a Rushton turbine impeller and a Drais reactor (van der Gulik et al., 2001). In the past the design of mixing devices has mainly relied on empiricism and on the experience of the engineer. Nowadays, thanks to the development of high performance computers and improved numerical algorithms, computational modeling and advanced experimental techniques are available to study industrial mixing processes. Mixing models proposed in literature are, however, often based on assumptions, which might not be valid for stirred tank reactors and do not describe all the mixing processes taking place in a stirred tank reactor. The objective of this study is to obtain models and rules applicable to the design and scale-up of stirred tank reactors yielding a defined product quality.

Some examples of mixing-sensitive reactions are given below, followed by an overview of the models currently available to describe mixing in turbulent flows. The final section of this chapter provides an outline of this thesis.

## 2. Mixing-sensitive reactions

Mixing affects the yield and selectivity of fast competitive parallel and competitive consecutive reactions, because slow mixing can retard desired reactions and promote undesired side reactions. An example of a mixing sensitive competitive parallel reaction is the addition of an acid or base to a solution of an organic substrate that degrades in the presence of a low or high pH. Slow mixing limits the neutralization reaction, which will allow the organic substrate to react with the acid or base, thus forming unwanted byproducts (Paul et al., 1992).

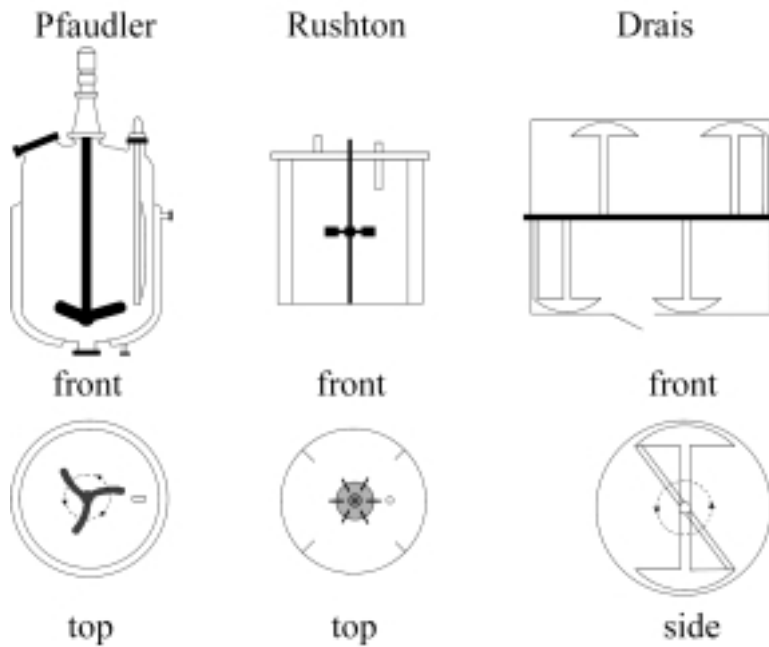
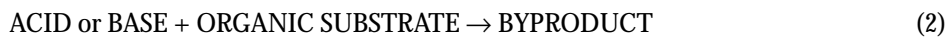
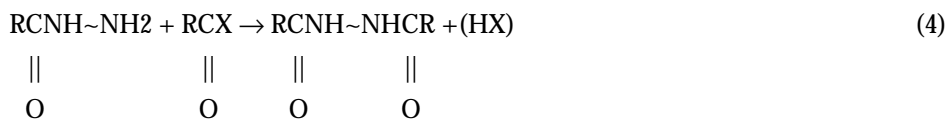
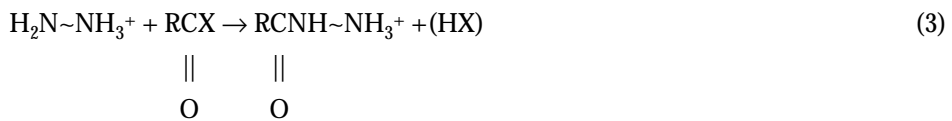


Figure 1: Examples of standard stirred tank reactors, i.e. a Pfaudler reactor, a reactor equipped with a Rushton turbine impeller and a Drais reactor.



An example of a mixing-sensitive consecutive reaction is the monoacylation of symmetrical diamines (Jacobson et al., 1987):



For the synthesis of biologically active agents, such as polyamines, the selective monoacylation of one end of the diamine is required. The monoacylation and diacylation reactions are schematically shown in equations (3) and (4), respectively. The utilization of excess diamine should minimize the diacylation reaction. However, when the transport of the monoacylated product from the reaction zone to the bulk liquid is slow compared to the reaction rate of the diacylation reaction, still predominantly diacyl product will be produced even though the diamine is present in excess in the bulk liquid.

Other examples of mixing sensitive processes are precipitation reactions, e.g. leading to the formation of solid pharmaceuticals, pigments, and catalysts. During a precipitation reaction nucleation takes place in regions where high supersaturation levels are present. An increase in the mixing intensity at low mixing rates will increase the supersaturation, thus increasing the number of nuclei formed. A further increase of the mixing rate will decrease the supersaturation, which will reduce the number of nuclei (Baldyga et al., 1990). Since an increase in the number of nuclei results in smaller particles and vice versa, the obtained product quality is affected by the mixing rate (e.g. Franke and Mersmann, 1995; Philips et al., 1999; Marcant and David, 1991).

### 3. Overview of mixing models

In principle, mixing in turbulent flows is governed by the partial differential equations describing the velocity and scalar fields, which are for an incompressible flow:

$$\frac{\partial u_i}{\partial t} + u_j \frac{\partial u_i}{\partial x_j} = -\frac{1}{\rho} \frac{\partial p}{\partial x_i} + \nu \nabla^2 u_i \quad (5)$$

$$\frac{\partial u_i}{\partial x_i} = 0 \quad (6)$$

$$\frac{\partial c_\alpha}{\partial t} + u_j \frac{\partial c_\alpha}{\partial x_j} = D \nabla^2 c_\alpha + R_\alpha(c) \quad (7)$$

In these equations  $c_\alpha$  is the concentration of a species  $\alpha$ ,  $u_i$  is the velocity,  $D$  is the molecular diffusivity,  $R$  is the chemical source term,  $p$  is the pressure and  $\nu$  is the kinematic viscosity.

Currently, this so-called Direct Numerical Simulation (DNS) can be used for fairly low Reynolds numbers. Figure 2 shows an example of an instantaneous and a time-averaged flow field in a tank stirred by a Rushton turbine impeller simulated with DNS at a Reynolds number of 7275 (Bartels et al., 2000). Reynolds numbers of turbulent reacting flows of practical interest are usually high. A high Reynolds number flow contains a wide range of time and length scales. Due to this variation in time and length scales, DNS requires an excessive computational effort, thus limiting the use of DNS for most practical situations.

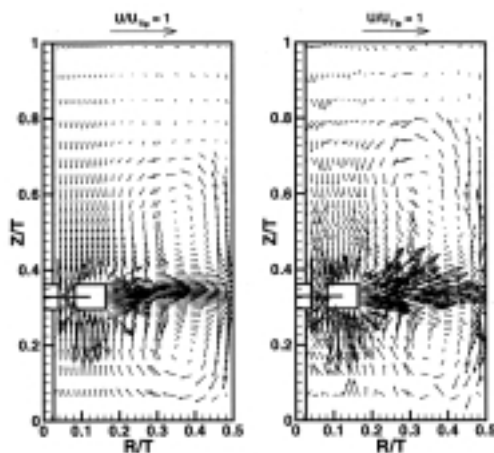


Figure 2: Time-averaged (left) and instantaneous (right) flow field in a reactor equipped with a Rushton turbine impeller calculated with DNS (Bartels et al., 2000).

An alternative to DNS is Large Eddy Simulation (LES). LES exactly solves the equations for the velocity and scalar field using a discretization which is rather coarse. A subgrid scale (SGS) model is used to describe the effect of the small-scale flow phenomena on the large-scale flow phenomena. Figure 3 shows examples of instantaneous flow patterns in a tank equipped with a pitched blade turbine calculated with LES (Bakker, 2000). The shortcoming of LES for reacting flows is the loss of information about flow phenomena below the subgrid scale, as chemical reactions take place at a molecular scale. This means that an SGS-model for the turbulence-chemistry interactions is required. These models are computationally intensive and will be unsuitable for engineering calculations in the near future (Baldyga and Bourne, 1999; Fox, 1996).

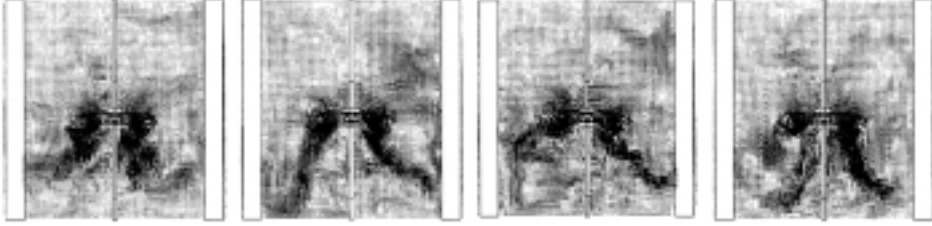


Figure 3: Instantaneous velocity fields in a reactor equipped with a pitched blade turbine calculated with LES (Bakker, 2000).

There are two practical modeling techniques for turbulent reacting flows, i.e. models based on Reynolds decomposition and Lagrangian mechanistic models. Reynolds decomposition describes a property of the turbulent flow with a mean and a fluctuating value:

$$u_i = \bar{u}_i + u'_i \quad (8)$$

$$c = \bar{c} + c' \quad (9)$$

Reynolds decomposition and time averaging generates unclosed terms in the Reynolds-averaged equations for the velocity and scalar fields; the number of unknowns is larger than the number of equations. These unclosed terms need to be modeled. As an example, the Reynolds-averaged equation for the concentration field of a passive tracer is:

$$\frac{\partial \bar{c}}{\partial t} + \bar{u}_j \frac{\partial \bar{c}}{\partial x_j} + \frac{\partial}{\partial x_j} \overline{u'_j c'} = D \frac{\partial^2 \bar{c}}{\partial x^2} \quad (10)$$

This equation contains the unclosed term  $\overline{u'_j c'}$ . This term is usually approximated using the concept of turbulent diffusivity:

$$\overline{u'_j c'} = -D_T \frac{\partial \bar{c}}{\partial x_j} \quad (11)$$

with  $D_T$  being the turbulent dispersion coefficient.



Lagrangian mechanistic mixing models follow a lump of fluid in a Lagrangian frame while it is mixed with the environment. Mixing in a turbulent flow consists of the following processes (Baldyga et. al, 1997) (see Figure 4):

1. Convection with the average velocity
2. Turbulent dispersion by large scale turbulent motions
3. Inertial convective disintegration of large eddies
4. Mixing on a molecular scale by engulfment, deformation and diffusion inside small-scale turbulent motions

In general, in a Lagrangian mechanistic mixing model a complete description of all these processes is not attempted. Instead, one model or a combination of models for these mixing processes is used to calculate the selectivity of mixing sensitive reactions (e.g. Bakker, 1996; Baldyga and Bourne, 1989; Baldyga et al, 1993; David and Villermaux, 1987; Verschuren et al., 2001). Application of these models requires information on turbulent flow parameters inside the studied stirred tank reactor. These parameters can be obtained from measurements, e.g. using Laser Doppler Velocimetry or Particle Image Velocimetry, or can be calculated with one of the models described above.

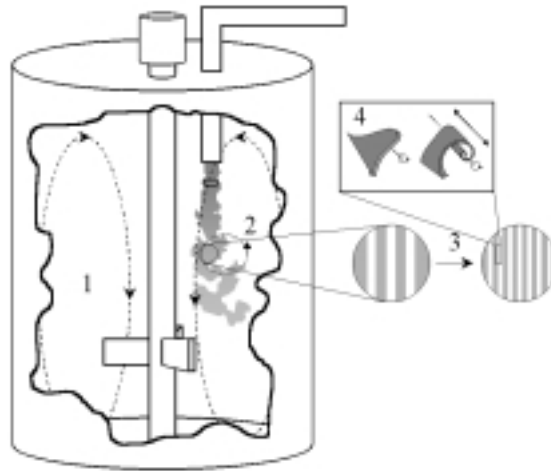


Figure 4: Schematic representation of the mixing processes in a turbulent flow.

#### 4. Outline of this thesis

A Lagrangian mixing model describes the mixing of a fluid element with homogeneous bulk liquid. Therefore, these models can be used to calculate the selectivity of fast chemical reactions creating a localized reaction zone in a reactor. The rate of turbulent dispersion of the reaction zone depends on the radius of the feed stream compared to the size of the large-scale turbulent motions (Lesieur, 1990). The Lagrangian mixing models presented in the literature use a turbulent dispersion coefficient, which can only be applied when the radius of the feed stream is equal to or larger than the size of the turbulent motions. Usually, the radius of a feed stream in a stirred tank reactor is smaller than the length of the large-scale turbulent motions. In Chapter 2, a Lagrangian mixing model is developed with a turbulent dispersion coefficient depending on the radius of the feed stream compared to the size of the large-scale turbulent motions. To calculate the reaction selectivity with this model, information is required on local hydrodynamic parameters inside the reactor. For many industrial processes these hydrodynamic parameters are not known in great detail. Therefore, the required detailing in the description of these hydrodynamic parameters to obtain a good agreement between measured and calculated selectivities has been determined.

A Lagrangian mixing model cannot be used for inhomogeneous flows, where the environment contains partially reacted fluids. For inhomogeneous flows models based on Reynolds decomposition are proposed in the literature. These models have been verified using approximations for the unclosed terms valid when the radius of a scalar cloud is larger than or equal to the length scale of the large-scale turbulent motions (Baldyga, 1989; Baldyga and Henczka, 1997; Hannon et al, 1998). In Chapter 3 models from literature are combined to describe the mean and fluctuating concentration of a feed stream introduced into a stirred tank reactor with an initial length scale much smaller than the length scale of the large-scale turbulent motions. The models have been validated against detailed experimental data and refined to make them more suitable for stirred tank reactors.

Feed streams inside stirred tank reactors have been shown to oscillate (Schoenmakers et al., 1997; Houcine et al., 1999). These oscillations are ignored in the models presented in chapters 2 and 3, because these models are used to describe the mixing of one feed

stream with a relatively homogeneous bulk liquid. Under these circumstances, the oscillations of a feed stream have no effect on the mixing rate. However, when multiple feed points are used these oscillations can cause the feed streams to overlap. Therefore, chapter 4 deals with a description for the large-scale oscillations of a feed stream in a stirred tank reactor.

In chapters 2, 3 and 4 the mixing of feed streams caused by the turbulence generated by the stirrer is considered. However, when the velocity of the incoming feed stream is considerably larger than the local circulation velocity, mixing of the feed stream will be caused by the turbulence generated by the stirrer and by the turbulence generated by the feed stream (Bourne and Hilber, 1990; Thoenes, 1994). Chapter 5 focuses on the mixing of a feed stream due to a combination of feed stream and stirrer generated turbulence.

Application of the models described above requires information on chemical reaction kinetics and on local hydrodynamic parameters inside the stirred tank reactor.

In industry this information is not always available. Therefore, chapter 6 considers the mixing in a stirred tank reactor frequently used in industry for the production of fine chemicals and pharmaceuticals, i.e. a reactor equipped with a Pfaudler impeller-type agitator. In the production of fine-chemicals and pharmaceuticals usually low feed rates are used to prevent a thermal runaway and to control the product distribution. For these low feed rates the mixing rate is controlled by micromixing and the product distribution of mixing-sensitive reactions can be calculated with a micromixing model. In chapter 6 a micromixing model from literature has been used to calculate the selectivity of mixing sensitive reactions in reactors equipped with a Pfaudler impeller. These calculated selectivities have been validated against measured selectivities of mixing sensitive reactions. The hydrodynamic parameters in a baffled reactor equipped with a Pfaudler impeller-type agitator, necessary to calculate the selectivities, have been determined. In addition, a simple scale-up rule for this type of reactor has been obtained.

Finally, chapter 7 discusses the practical applications of the models described in this thesis and suggestions for future research are given. It has been chosen to set-up this thesis in such a way that each individual chapter provides enough information to be read independently from the other chapters. Consequently, some information is repeated in different chapters.

## Nomenclature

c	concentration	[mol m <sup>-3</sup> ]
D	molecular diffusivity	[m <sup>2</sup> s <sup>-1</sup> ]
D <sub>T</sub>	turbulent dispersion coefficient	[m <sup>2</sup> s <sup>-1</sup> ]
p	pressure	[kg m <sup>-2</sup> s <sup>-1</sup> ]
R	reaction rate	[mol m <sup>-3</sup> s <sup>-1</sup> ]
t	time	[s]
u	velocity	[m <sup>2</sup> s <sup>-1</sup> ]
x	coordinate	[-]
v	kinematic viscosity	[m <sup>2</sup> s <sup>-1</sup> ]
ρ	density	[kg m <sup>-3</sup> ]

### subscripts

i, j      coordinate direction

### superscripts

‘      fluctuation

–      average

## References

- Bakker, A., "The use of Large Eddy Simulation to study stirred vessel hydrodynamics", Proc. 10th Europ. Conf. Mixing, 247 (2000)*
- Bakker, R.A. "Micromixing in chemical reactors: models, experiments and simulations", Ph.D. Thesis Delft University of Technology, 1996*
- Baldyga, J. "Turbulent mixer model with application to homogeneous, instantaneous, chemical reactions", Chem. Eng. Sci. 44, 1175 (1989)*
- Baldyga, J., and J.R. Bourne "Simplification of micromixing calculations II. New Applications", Chem. Eng. J., 42, 93 (1989)*
- Baldyga, J., and J.R. Bourne "Turbulent mixing and chemical reactions", John Wiley, Chichester (1999)*

Baldyga, J., J.R. Bourne, and S.J. Hearn "Interaction between chemical reactions and mixing on various scales", *Chem. Eng. Sci.* 52, 457 (1997)

Baldyga, J., Bourne, J. R. and Y. Yang "Influence of feed pipe diameter on mesomixing in stirred tank reactors", *Chem. Eng. Sci.* 48, 3383 (1993)

Baldyga, J., and M. Henczka "Turbulent mixing and parallel chemical reactions in a pipe application of a closure model", *Proc. of the Ninth Europ. Conf. on Mixing 11 (51)*, 341, Paris (1997)

Baldyga, J., Pohorecki, R., Podgorska, W. and B. Marcant "Micromixing effects in semi-batch precipitation", *Proc. 11th Symp. on Industrial Crystallization, Garmisch Partenkirchen* (1990)

Bartels, C., M. Breuer and F. Durst "Comparison between Direct Numerical Simulation and  $k-\epsilon$  predictions of the flow in a vessel stirred by a Rushton turbine", *Proc. 10th Europ. Conf. Mixing*, 239 (2000)

Bourne, J. R. and C.P. Hilber "The productivity of micromixing-controlled reactions: effect of feed distribution in stirred tanks", *Trans. IChemE* 68, 51 (1990)

David, R., and J. Villiermaux "Interpretation of micromixing effects on fast consecutive-competing reactions in semi-batch stirred tanks by a simple interaction model", *Chem. Eng. Commun.*, 54, 333 (1987)

Fox, R. O. "Computational methods for turbulent reacting flows in the chemical process industry", *Revue de l'Institut Français du Pétrole* 51 (1996)

Franke, J. and A. Mersmann "The influence of the operational conditions on the precipitation process", *Chem. Eng. Sci.* 50, 1737 (1995)

Gulik, van der, G.J.S., J.G. Wijers, and J.T.F. Keurentjes "Hydrodynamics in a horizontally stirred tank reactor", *Ind. Eng. Chem. Res.* 40, 785 (2001)

Hannon, J., S. Hearn, L. Marshall, and W. Zhou "Assessment of CFD approaches to predicting fast chemical reactions", *A.I.Ch.E. 1998 Annual Meeting "Chemical and Biological Reactors"* (1998)

Houcine, I., E. Plasari, R. David, and J. Villiermaux "Feedstream jet intermittency phenomenon in a continuous stirred tank reactor", *Chem. Eng. J.* 72, 19 (1999)

Jacobson, A.R., A.N. Makris, and L.M. Sayre "Monoacylation of Symmetrical Diamines", *J. Org. Chem.*, 52, 2592 (1987)

Marcant, B. and R. David "Experimental evidence for and prediction of micromixing effects in precipitation", *AIChE J.* 37, 1698 (1991)

Philips, R., Rohani, S. and J. Baldyga "Micromixing in a single feed semi-batch precipitation process", *AIChE J.* 45, 82 (1999)

*Paul, E. L., J. Mahadevan, J. Foster, and M. Kennedy Midler "The effect of mixing on scale-up of a parallel reaction system", Chem. Eng. Sci. 47, 2837 (1992)*

*Schoenmakers, J. H. A., J. G. Wijers, and D. Thoenes "Determination of feed stream mixing rates in agitated vessels", Proc. 8th Europ. Mix. Conf. (Paris): Récent Progrès en Génie des Procédés 11(52), ed. Lavoisier, 185 (1997)*

*Thoenes, D. "Chemical Reactor Development, Kluwer Academic Publishers", Dordrecht (1994)*

*Verschuren, I.L.M., J.G. Wijers and J.T.F. Keurentjes "Effect of mixing on the product quality in semi-batch stirred tank reactors", accepted for publication in AIChE J. (2001)*

# EFFECT OF MIXING ON THE PRODUCT QUALITY IN SEMI-BATCH STIRRED TANK REACTORS

## Abstract

Semi-batch stirred tank reactors with a turbulent flow field are frequently used in the chemical process industry to accomplish mixing tasks. Mixing in a turbulent flow consists of several processes. Descriptions for these processes from literature are used to construct a model to calculate the selectivity of a mixing-sensitive reaction in a semi-batch stirred tank reactor. The model is validated by determining the effects of various process parameters on the selectivity of the third Bourne reaction. Calculation of the selectivity requires information on the hydrodynamic parameters of the stirred vessel studied. The necessary detailing in the description of these hydrodynamic parameters to obtain a good agreement between measured and calculated selectivities has been determined. The model proved to be successful in predicting the product distribution of a competitive reaction, making it useful for the design and scale-up of stirred tank reactors.

*This chapter has been accepted for publication in A.I.Ch.E. J. as I.L.M. Verschuren, J.G. Wijers and J.T.F. Keurentjes "Effect of mixing on the product quality in semi-batch stirred tank reactors"*

## 1. Introduction

Before a chemical reaction can occur between two or more reactants, the reactants have to be mixed on a molecular scale. When reaction is slow compared to the mixing process, the solution will be homogeneously mixed before reaction takes place and the product distribution will only depend on the chemical kinetics. However, when reaction is fast relative to the mixing rate, also the mixing rate will determine the yield and selectivity of the process. Examples of mixing-sensitive reactions are monoacylation of symmetrical diamines (Jacobson et al., 1987), precipitation reactions (Franke and Mersmann, 1995) and fermentation processes (Larsson et al., 1992).

Because mixing has a large influence on the product quality of a mixing-sensitive reaction, a model for the mixing of reacting flows is a helpful tool in the design of a chemical reactor. In principle, the mixing of fluids is completely described by the partial differential equations describing the momentum, mass and species balances. However, turbulent flows contain a wide range of time and length scales and, therefore, even with the nowadays-available computational recourses the complete exact solution of these differential equations is not possible. Therefore, simplified but tractable models are proposed in the literature to describe the mixing in turbulent flows (see Fox (1996) for a review). The applicability of these models depends on the type of flow and chemical reactions under consideration. Stirred tank reactors with a turbulent flow field are commonly used in chemical and biochemical industries to accomplish mixing tasks. In this paper turbulent mixing of dilute solutions of reactants in a semi-batch stirred tank reactor with a feed stream is considered for fast chemical reactions.

A fast reaction in a stirred tank reactor takes place in a small portion of the whole vessel (Baladyga and Bourne, 1992) and the reaction zone becomes more localized when a stirred tank reactor is scaled-up with a constant power input per unit volume (Bourne and Dell'ava, 1987). For a localized reaction zone the following processes are used to describe the mixing of fluids in a turbulent flow (Ranada and Bourne, 1991):

1. Convection of the reaction zone through the vessel by the average velocity.
2. Spatial evolution of the reaction zone due to turbulent dispersion by large-scale turbulent motions.



3. Mixing of reactants in the reaction zone on a molecular scale inside small-scale turbulent motions by engulfment, deformation and diffusion.

Models for these mixing processes are described in the literature (e.g. Baldyga and Bourne, 1984; Baldyga and Bourne, 1989; David and Villermaux, 1987). In this work a combination of these descriptions will be used to obtain a model for the calculation of the selectivity of a mixing-sensitive reaction set in a semi-batch stirred tank reactor with a feed stream.

The processes of mixing described above are determined by hydrodynamic parameters. Therefore, application of the model requires information on these hydrodynamic parameters inside the stirred vessel. The reactor type used in this study is a cylindrical vessel equipped with a Rushton turbine stirrer and four baffles. The hydrodynamic parameters for this reactor type have been determined extensively by Laser Doppler Velocimetry experiments, as described in previous papers (Kajbic, 1995; Kusters, 1991; Schoenmakers, 1998). However, for many industrial processes these parameters are not known in great detail. Therefore, in this work it is also investigated in how much detail these hydrodynamic parameters have to be known to predict the selectivity of a mixing-sensitive reaction set.

## 2. Mixing model

To validate the model the selectivity of a mixing-sensitive reaction set is determined experimentally for a broad range of process and design variables.

Lagrangian models for the mixing processes in a turbulent flow are used to describe the mixing of the fluid elements in a stirred tank reactor. The engulfment, deformation and diffusion (EDD) model describes micromixing by diffusion within shrinking laminated structures formed by engulfment (Baldyga and Bourne, 1984). Baldyga and Bourne (1989a) have shown that for systems having a Schmidt number less than 4000, engulfment is the rate-determining step of the micromixing process and the EDD-model is simplified to the engulfment model (E-model).

The growth of the micromixed volume according to the E-model is:

$$\frac{dV_{mi}}{dt} = EV_{mi} \quad (1)$$

$$E = 0.058 \sqrt{\frac{\varepsilon}{\nu}} \quad (2)$$

with  $V_{mi}$  the volume mixed on a molecular scale,  $E$  the engulfment rate,  $\varepsilon$  the energy dissipation rate and  $\nu$  the kinematic viscosity.

Mixing of micromixed fluid with micromixed fluid will not lead to growth of the total micromixed volume. The probability of this so-called self-engulfment depends on the volume fraction of micromixed fluid inside the spread feed stream. The growth of the micromixed volume taking into account possible self-engulfment (Baldyga and Bourne, 1989b) is:

$$\frac{dV_{mi}}{dt} = EV_{mi}(1 - V_{mi}/V_{td}) \quad (3)$$

with  $V_{td}$  as the volume of the dispersed feed stream.

The spreading of the feed stream is characterized by a turbulent dispersion coefficient ( $D_t$ ) (Nagata, 1975). David and Villermaux (1987) have used this turbulent dispersion coefficient to describe the growth of the linear dimension ( $L$ ) of a cloud containing an injected scalar:

$$\frac{dL^2}{dt} = D_t \quad \text{or} \quad \frac{dV_{td}}{dt} = \frac{3}{2} D_t V_{td}^{1/3} \quad (4)$$

in which the volume of the cloud is assumed to be equal to  $L^3$  for the sake of simplicity. As noticed by Baldyga and Pohorecki (1995), in a continuous feed stream the concentration gradients in radial direction are much larger than in the direction of the flow. Therefore, only radial dispersion is assumed and the growth of the volume of a slice, with diameter  $L$  and thickness  $\delta$ , is given by (Baldyga and Pohorecki, 1995):

$$\frac{dV_{td}}{dt} = \frac{\pi}{4} \delta \frac{dL^2}{dt} = \frac{\pi}{4} \delta D_t = \frac{V_{td}}{L^2} D_t \quad (5)$$

In this study the mixing of a continuous feed stream in a stirred vessel is investigated. Therefore, equation (5) will probably be more appropriate for our model than equation (4).

The turbulent dispersion coefficient in equation (5), used to describe the growth of  $V_{td}$ , is determined by hydrodynamic parameters. The growth of the diameter of a scalar cloud ( $L$ ), with a diameter smaller or in the order of the velocity length scale ( $L_v$ ), follows a Richardson Law (Lesieur, 1990):

$$\frac{1}{2} \frac{dL^2}{dt} = C\varepsilon^{1/3} L^{4/3} \quad (6)$$

When the scalar cloud diameter is larger than the velocity length scale, the growth of the diameter is described by (Lesieur, 1990):

$$\frac{1}{2} \frac{dL^2}{dt} = C\varepsilon^{1/3} L_v^{4/3} \quad (7)$$

In both equations  $\varepsilon$  is the energy dissipation rate and  $C$  is a constant equal to 2.14 (Lesieur, 1990). The integral length scale of the velocity fluctuations is a measure of the large-scale turbulent flow structures. Combining equations (5), (6) and (7) yields the following equation for the turbulent dispersion coefficient:

$$D_t = 2C\varepsilon^{1/3} \lambda^{4/3} \quad \lambda = L \text{ when } L < L_v \text{ and } \lambda = L_v \text{ when } L > L_v \quad (8)$$

When the momentum of the feed stream is negligible compared to the momentum of the flow in the reactor, the velocity of the feed stream in the reactor will be equal to the local circulation velocity. This is normally the case when the feed velocity is smaller than or comparable to the local circulation velocity (Jeurissen et al., 1994). Under these circumstances the initial diameter of the dispersed feed stream ( $L_0$ ) is given by (Baldyga et al., 1997):

$$Q_f = \frac{\pi}{4} L_0^2 u \quad (9)$$

with  $Q_f$  as the feed flow rate and  $u$  as the feed velocity just beneath the feed pipe.

To calculate the selectivity of a mixing-sensitive reaction set in a semi-batch stirred tank reactor a mass balance is made for each component  $i$  inside a fluid element added to the reactor:

$$\frac{dc_i}{dt} = \frac{1}{V_{mi}} \frac{dV_{mi}}{dt} ((c_i) - c_i) + R_i \quad (10)$$

in which  $c_i$  is the concentration of component  $i$  in the mixed volume,  $\langle c_i \rangle$  is the concentration of component  $i$  in the bulk and  $R_i$  is the specific reaction rate. The growth of the micromixed volume is calculated with equation (3) and depends on the volume of the dispersed feed stream. The volume of the dispersed feed stream is calculated with equations (5) to (9). The concentration in the bulk is assumed to be constant during one circulation time and the added feed liquid is assumed to be homogeneously mixed after one circulation time (Baldyga and Bourne, 1989a; Phillips et al., 1999). Due to this assumption the history of all fluid elements, added to the reactor during one circulation time, will be the same. Therefore, the total feed volume is discretized into fluid elements with a volume ( $V_0$ ) equal to:

$$V_0 = V_{feed} \frac{t_c}{t_{feed}} \quad (11)$$

with  $V_{feed}$  is the total feed volume,  $t_c$  is the circulation time and  $t_{feed}$  is the feed time. The feed time is defined as the total feed volume divided by the feed flow rate. The circulation time inside a stirred tank reactor is given by:

$$t_c = \frac{V_{reactor}}{r_c Q_p} \quad (12)$$

where  $V_{reactor}$  is the volume of the reactor contents,  $r_c$  is the circulation ratio and  $Q_p$  is the pumping capacity of the stirrer. The pumping capacity of the stirrer is:

$$Q_p = N_q N D_{im}^3 \quad (13)$$

in which  $N_q$  is the flow number of the stirrer,  $N$  is the stirrer speed, and  $D_{im}$  is the impeller diameter. The flow number and circulation ratio of a Rushton turbine stirrer are equal to 0.7 and 3, respectively (Schoenmakers, 1998).

### 3. Hydrodynamic parameters

The engulfment rate is a function of the local energy dissipation rate. The turbulent dispersion coefficient depends on the local energy dissipation rate and the local velocity length scale. Therefore, these parameters have to be known for the calculation of the selectivity of a mixing-sensitive reaction. A fluid element added to the reactor is followed as it moves through the reactor. When the hydrodynamic parameters vary throughout the vessel, the location of the added fluid element inside the reactor has to be known. This location is determined by the local average velocity inside the stirred vessel. The energy dissipation rate, the velocity length scale and the local average velocity are dependent on the stirred tank reactor used. For many industrial processes these hydrodynamic parameters are not known in detail. In this study, the necessary degree of complexity in the description of these hydrodynamic parameters to obtain a good agreement between the measured and calculated selectivities is investigated.

#### 3.1 Energy dissipation rate and velocity length scale

The experimental system used in this study is a cylindrical vessel equipped with a Rushton turbine stirrer, illustrated in Figures 1 and 2, respectively.

The hydrodynamic parameters are determined from previous Laser Doppler Velocimetry measurements (Kajbic, 1995; Kusters, 1991; Schoenmakers, 1998). The hydrodynamic parameters are described in three flow maps with different levels of complexity. In these flow maps the local energy dissipation rate is related to the average energy dissipation rate:

$$\bar{\epsilon} = \frac{N_p N^3 D_m^5}{V_{\text{reactor}}} \quad (14)$$

in which  $N_p$  is the power number, equal to 5.3 for the stirrer used in this work (Schoenmakers, 1998).

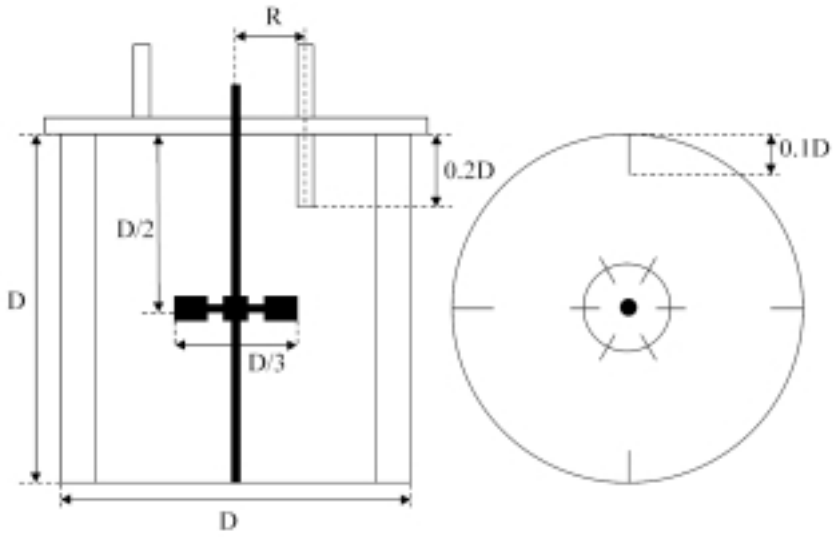


Figure 1: Geometry of the vessels used in this study showing a closed top, four baffles, a feed pipe and an effluent pipe.

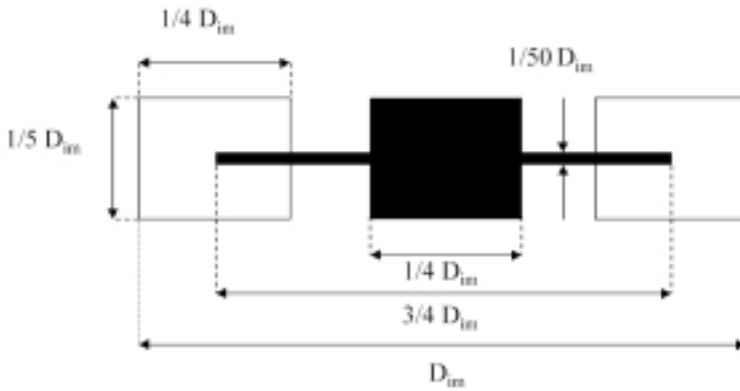


Figure 2: Geometry of the Rushton turbine stirrer used in this work.

### Flow map 1

In the first flow map the hydrodynamic parameters are assumed to be constant throughout the whole vessel. The energy dissipation rate is taken equal to the average energy dissipation rate calculated with equation (13). The velocity length scale is taken equal to the baffle width.

## Flow map 2

In the second flow map, the vessel is divided into three regions as illustrated in Figure 3. The energy dissipation rates in these regions are described by correlations given by Schoenmakers et al. (1996):

$$\text{bulk region: } \varepsilon = 0.13\bar{\varepsilon} \quad (15)$$

$$\text{stirrer region: } \varepsilon = 7.3\bar{\varepsilon} \quad (16)$$

$$\text{wall region: } \varepsilon = 0.63\bar{\varepsilon} \quad (17)$$

In the bulk region, the velocity length scale equals 0.15 times the vessel diameter (Schoenmakers, 1998). The velocity length scale in the stirrer region is equal to the impeller blade width (Kusters, 1991). Experimental data of the velocity length scale in the wall region are not available. As velocity length scales are related to the dimensions of the elements generating the turbulence, the length scale in the wall region is assumed to be equal to the baffle width.

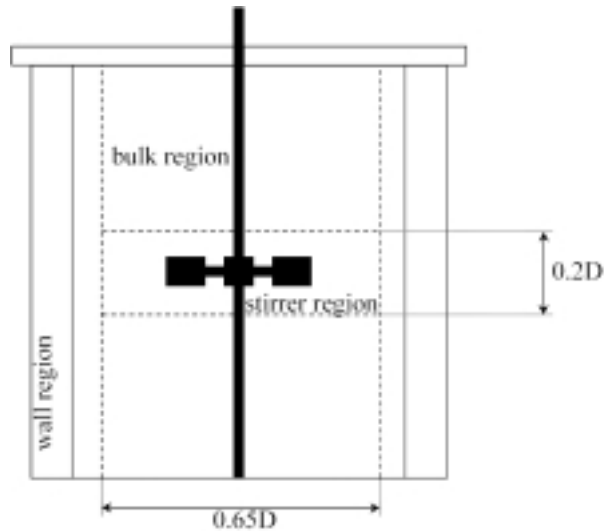


Figure 3: Division of the reactor into three regions having different hydrodynamic parameters.

### Flow map 3

The third flow map is equal to flow map 2 except for the energy dissipation rate in the stirrer region. Due to large gradients in the energy dissipation rate in the stirrer region, in the third flow map a more detailed description of the energy dissipation rate in the stirrer region is used:

$$\varepsilon = \left( 0.414 - 3.462 \cdot \frac{r}{D_{\text{vessel}}} + 8.233 \cdot \left( \frac{r}{D_{\text{vessel}}} \right)^2 \right)^{-1} \cdot \bar{\varepsilon} \quad (18)$$

This equation is obtained by fitting a polynomial function through measured energy dissipation rates. These energy dissipation rates have been measured at a height of  $\frac{1}{2}$  the vessel diameter at nine different radial positions (Kajbic, 1995; Schoenmakers et al., 1996). The measured energy dissipation rates and the fitted polynomial equation are shown in Figure 4.

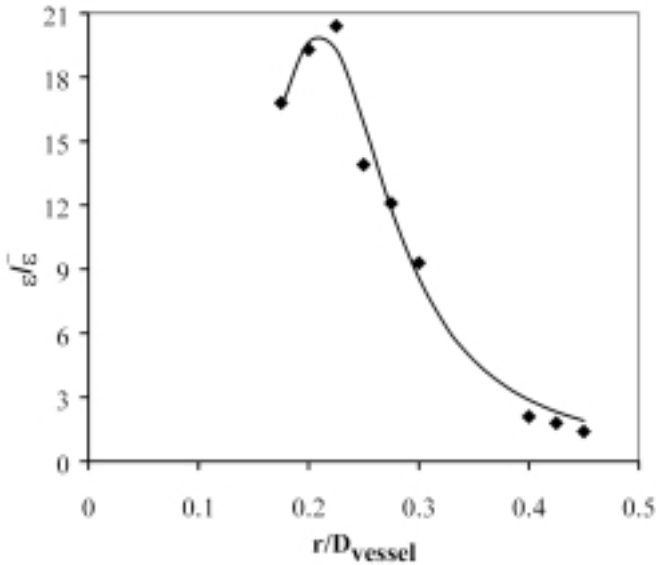


Figure 4: Relative energy dissipation rate profile in the stirrer region. Points are measured energy dissipation rates with Laser Doppler Velocimetry. The curve is obtained by fitting a polynomial equation through the measured data.



### 3.2 Location of a fluid element

When the energy dissipation rate and the velocity length scale vary throughout the vessel, the location of a fluid element added to the reactor has to be known during the reaction time. The reaction time is defined as the time necessary to consume all of the reactants in a fluid element added to the reactor. For the fast chemical reactions considered in this study this reaction time is always smaller than the circulation time. In the reaction time a fluid element is assumed to flow from the feed pipe through the bulk region towards the stirrer, then from the stirrer region into the wall region.

The residence time and location of a fluid element in a region is determined by the local average velocity. The residence time in the bulk region is equal to the distance between the feed point and the stirrer region divided by the average velocity over this distance. The average velocity between the feed point and the stirrer region is equal to 0.15 times the stirrer tip speed ( $\pi ND_{im}$ ) (Schoenmakers, 1998).

Inside the stirrer region the average velocity at every radial position ( $r$ ) is calculated from the pumping capacity of the stirrer:

$$v_{stirrer} = \frac{v_s N_s ND_{se}^3}{0.2D2\pi r} \quad (19)$$

A fluid element is assumed to enter the stirrer region at the radial position of the feed pipe ( $R$ ). With this assumption, the residence time in the stirrer region follows from:

$$t_{stirrer} = \int_R^{\frac{0.65D}{2}} \frac{l}{v_{stirrer}} dr \quad (20)$$

After a fluid element has left the stirrer region, it is assumed to be in the wall region in the remaining reaction time.

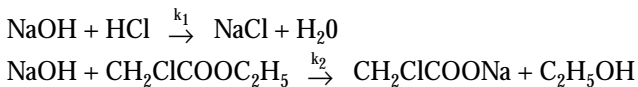
#### 4. Experimental verification of the model

The model presented in section 2 is used in combination with the flow maps presented in the previous section to calculate the selectivity of a mixing-sensitive reaction set.

The calculated selectivities are validated against experimentally determined selectivities for several process and design variables.

The experiments were performed in geometrically similar vessels of 6 L, 19 L and 44 L, respectively, equipped with a Rushton turbine stirrer. The geometry of the vessels is shown schematically in Figure 1. The diameters of the vessels were 0.2 m, 0.288 m and 0.382 m, respectively. The feed pipe diameters for the 6 L, 19 L and 44 L vessel were 5 mm, 8 mm and 10 mm, respectively. The radial position of the feed pipe (R) for the 6 L and the 44 L vessels was 0.2 times the vessel diameter and the radial position of the feed pipe for the 19 L vessel was 0.3 times the vessel diameter. The stirrer Reynolds number ( $ND_{im}^2/\nu$ ) was varied from  $6.7 \cdot 10^3$  to  $4 \cdot 10^4$  in the 6L vessel and from  $1.6 \cdot 10^4$  to  $9.7 \cdot 10^4$  in the 44L vessel. In the 18L vessel the stirrer Reynolds number was equal to  $1.4 \cdot 10^4$  and  $3.7 \cdot 10^4$ . The geometry of the Rushton turbine stirrers is shown schematically in Figure 2.

The mixing-sensitive reaction set used in this work to validate the mixing model was the third Bourne reaction (Bourne and Yu, 1994). The third Bourne reaction consists of the following two competitive reactions:



The second order kinetic constants for this reaction system are (Baldyga and Bourne, 1999):

$$k_1 = 1.3 \cdot 10^8 \text{ m}^3/(\text{mol s}) \text{ at } 298 \text{ K}$$

$$k_2 = 0.030 \text{ m}^3/(\text{mol s}) \text{ at } 298 \text{ K}$$

For engulfment to be the rate determining step of the micromixing process, the Schmidt number must be smaller than 4000. To calculate the Schmidt numbers of the reactants, diffusion coefficients have been estimated using equations (3-34) and (3-32) given in (Perry and Chilton, 1973) valid for electrolytes at infinite dilution and non-electrolytes at low-concentrations, respectively. The Schmidt numbers of hydrochloric acid, sodium

hydroxide and ethyl chloroacetate in water are 300, 470 and 1200, respectively.

Before each experiment the vessel was entirely filled with a solution of 0.09 M ethyl chloroacetate (ECA) and 0.09 M HCl. The feed stream was a solution of 1.8 M NaOH and the feed volume was 1/20 of the vessel volume. When the feed was added, solution left the reactor through an effluent pipe positioned at the top of the vessel as illustrated in Figure1.

The reaction between NaOH and HCl is much faster than the reaction between NaOH and ECA. NaOH will only react significantly with ECA when the reaction between NaOH and HCl is limited by mixing. Therefore, the amount of ethanol produced will increase when the mixing rate decreases. The amount of ethanol and ECA present at the end of an experiment in the reactor and in the solution leaving the reactor were determined chromatographically (HPLC). The mixtures were analyzed immediately to avoid the acid catalyzed hydrolysis of ethyl chloroacetate (Baldyga and Bourne, 1999).

As the reaction between NaOH and HCl is almost instantaneous, the following transformation was used to remove the stiffness from the differential equations and to reduce the number of differential equations to be solved (Baldyga and Bourne, 1989b):

$$\begin{aligned}
 u &= C_{NaOH} - C_{HCl} \\
 C_{NaOH} &= \frac{|u| + u}{2} \\
 C_{HCl} &= \frac{|u| - u}{2}
 \end{aligned} \tag{21}$$

The mass balances for  $u$  and ECA are:

$$\frac{du}{dt} = \frac{1}{V_{tot}} \frac{dV_{tot}}{dt} ((u) - u) - k_2 C_{ECA} \left( \frac{|u| + u}{2} \right) \tag{22}$$

$$\frac{dC_{ECA}}{dt} = \frac{1}{V_{tot}} \frac{dV_{tot}}{dt} ((C_{ECA}) - C_{ECA}) - k_2 C_{ECA} \left( \frac{|u| + u}{2} \right) \tag{23}$$

## 5. Results and discussion

In this section the experimentally determined selectivities are compared with the calculated selectivities. The selectivity is defined as one minus the ethanol yield. The ethanol yield is given as the total amount of ethanol present at the end of an experiment in the reactor and in the solution leaving the reactor divided by the amount of ECA present at the beginning of an experiment.

In Figures 5 and 6 measured and calculated ethanol yields for the 6 L vessel are given as a function of stirrer speed and feed time, respectively. Figure 7 shows a comparison between the measured and calculated ethanol yields versus feed time for the 19 L vessel and two stirrer speeds. In Figure 8 measured and calculated ethanol yields versus stirrer speed are given for the 44 L vessel. From figures 5 to 8 it is concluded that an agreement between the measurements and simulations could not be obtained when using constant hydrodynamic parameters. However, good agreement between the measured and calculated selectivities is obtained when a flow map with three characteristic regions is used. Figures 5, 7 and 8 show an increasing selectivity with increasing stirrer speed. Figures 6 and 8 show that for short feed times the selectivity decreases with decreasing feed time. This is in agreement with a mixing rate that becomes more controlled by the turbulent dispersion process when the feed time is reduced. For the longer feed times the selectivity is independent of feed time.

From figures 5 to 8 it is concluded that the necessary detailing in the description of the hydrodynamic parameters depends on the feed position. The radial feed location was 0.2 times the vessel diameter for the 6 L and 44 L vessel and 0.3 times the vessel diameter for the 19 L vessel. For the 6 L and 44 L vessel a good agreement between the measured and calculated ethanol yields is observed when flow map 3 is used. For the 19 L vessel already a reasonable agreement between the measured and calculated ethanol yields is observed when constant hydrodynamic parameters are used. A good agreement between the measured and calculated ethanol yields is obtained for the 19 L vessel when flow map 2 is used. The calculated ethanol yields with flow map 2 and 3 coincide in figure 7. The influence of the feed position on the necessary degree of complexity in the description of the hydrodynamic parameters will be discussed in more detail below.

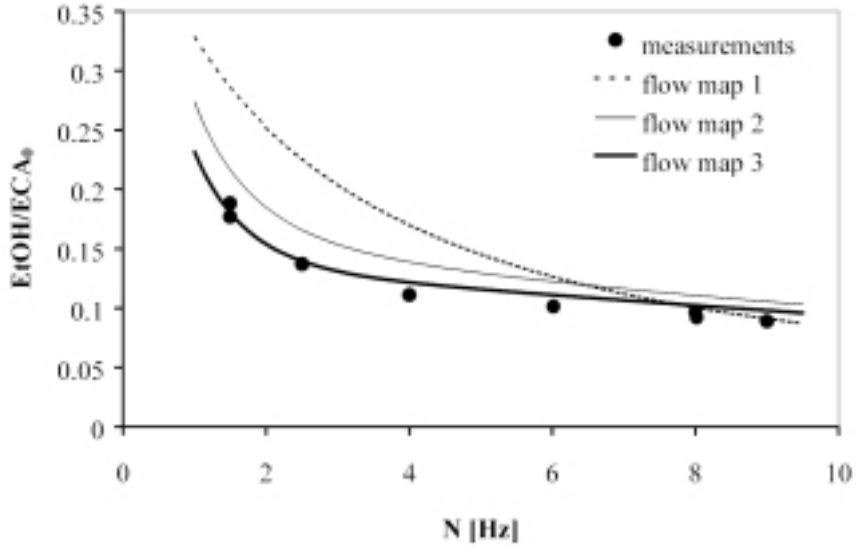


Figure 5: Calculated ethanol yields with the three flow maps and measured ethanol yields versus stirrer speed for the 6 L vessel and a feed rate equal to the local circulation velocity ( $0.15v_{tip}$ ).

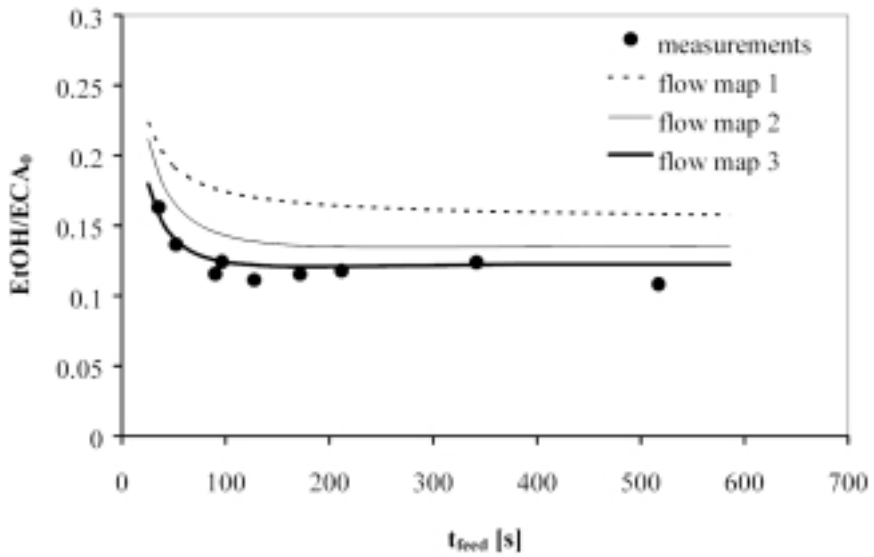


Figure 6: Calculated ethanol yields with the three flow maps and measured ethanol yields as a function of feed time for the 6 L vessel and a stirrer speed of 4 Hz.

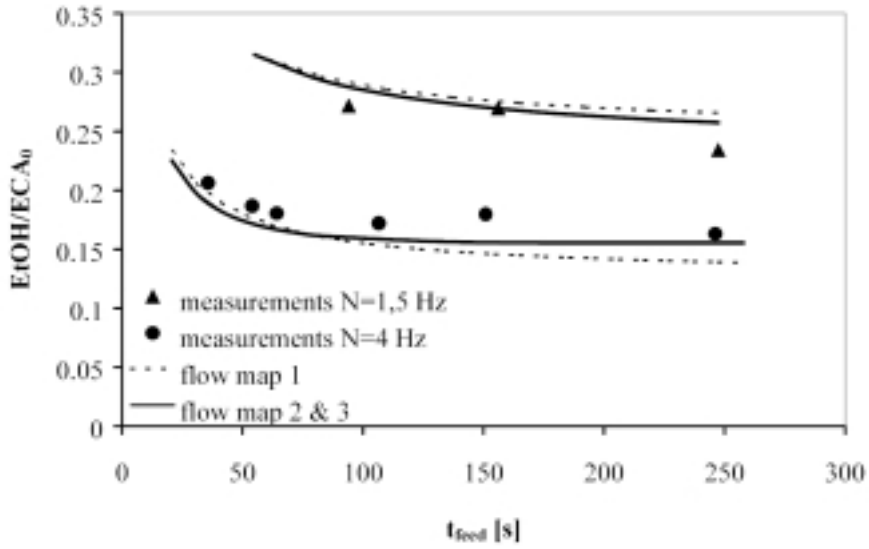


Figure 7: Calculated ethanol yields with the three flow maps and measured ethanol yields as a function of feed time for the 19 L vessel and stirrer speeds of 1.5 Hz and 4 Hz.

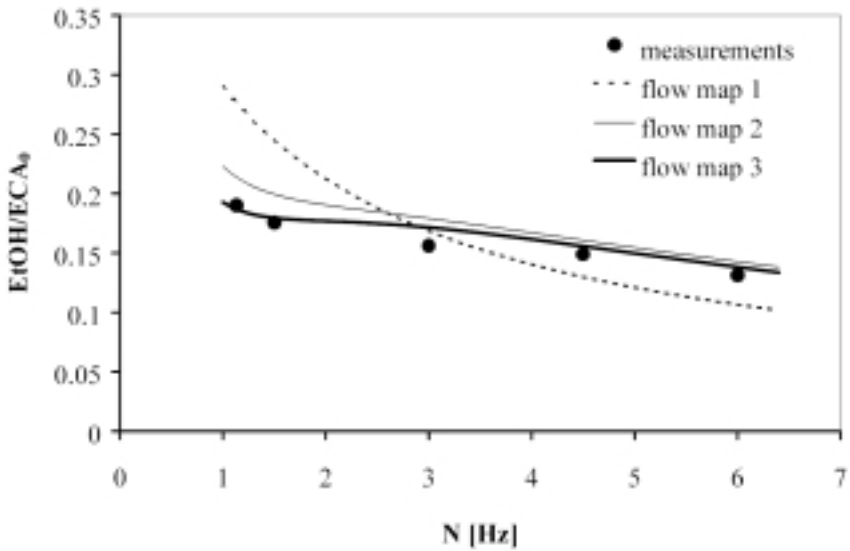


Figure 8: Calculated ethanol yields with the three flow maps and measured ethanol yields versus stirrer speed for the 44 L vessel and a feed rate equal to the local circulation velocity.

In Figures 9 and 10 the growth of the micromixed volume in the feed stream, calculated with the three different flow maps, is plotted versus the dimensionless time ( $t/t_c$ ) for the 6 L and 19 L vessel, respectively. On the lower horizontal axis of these figures, the residence times of a fluid element in the bulk region and in the stirrer region are given. A fluid element is assumed to enter the stirrer region at the radial position of the feed pipe. Therefore, the residence time in the stirrer region for the 19 L vessel is shorter than for the 6 L vessel. In Figure 9 a large deviation between the micromixed volumes in the stirrer region calculated with flow maps 1 and 3 is observed for the 6 L vessel. For the 19 L vessel the residence time in the stirrer region is too short to result in a large difference between these micromixed volumes. For both vessels, large deviations between the micromixed volumes calculated with flow map 1 and flow map 3 are observed in the bulk region. However, in the bulk region the growth of the micromixed volume is small, therefore, only a small amount of ethanol will be produced in this region. Apparently, the residence time in the stirrer region of the 19 L vessel is too short and the amount of ethanol produced in the bulk region too small to generate a large difference between the calculated ethanol yields with flow map 1 and flow map 3, respectively.

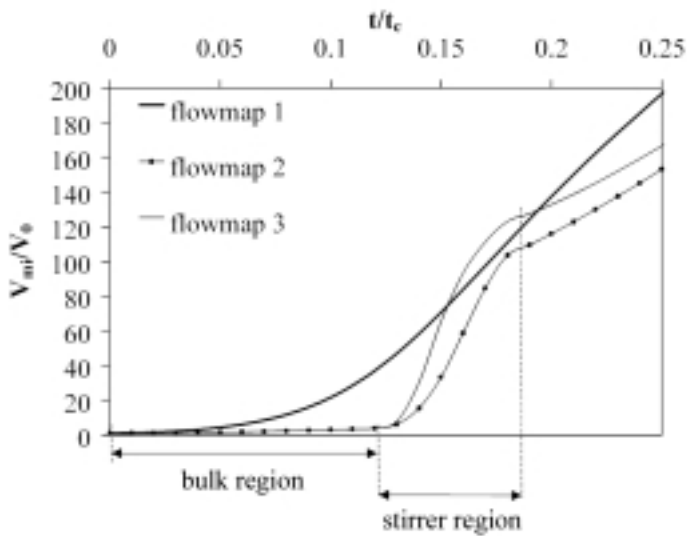


Figure 9: Micromixed volume as a function of dimensionless time ( $t/t_c$ ) for the 6 L vessel, a stirrer speed of 4 Hz and a feed time of 127 s

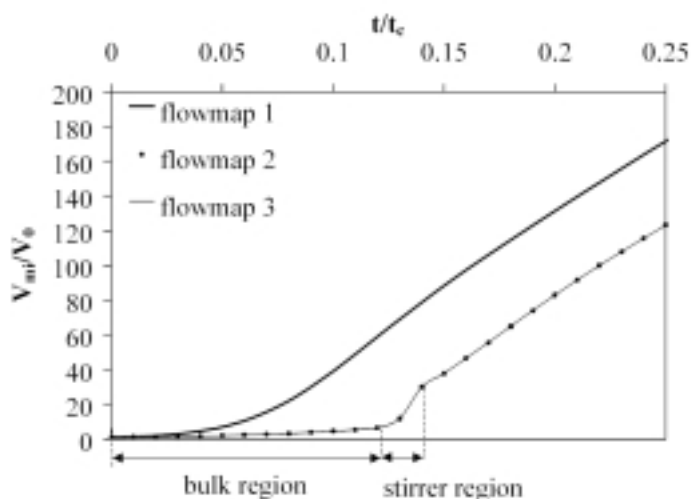


Figure 10: Micromixed volume as a function of dimensionless time ( $t/t_c$ ) for the 19 L vessel, a stirrer speed of 4 Hz and feed time of 103 s.

For the 6 L and 44 L vessel the energy dissipation rate in the stirrer region described by flow map 3 is higher than the average energy dissipation rate in the stirrer region of flow map 2. Consequently, in Figures 5, 6 and 8 the calculated ethanol yields with flow map 3 are lower than the calculated ethanol yields with flow map 2. For the 19 L vessel the energy dissipation rate in the stirrer region described by flow map 3 is almost equal to the average energy dissipation rate in the stirrer region used in flow map 2. Therefore, the ethanol yields calculated with flow map 2 and flow map 3 coincide in Figure 7.

In Figure 11 the dimensionless volume of the dispersed feed stream ( $V_{fd}/V_0$ ) and the dimensionless micromixed volume ( $V_{mi}/V_0$ ) are given as a function of the dimensionless time ( $t/t_c$ ) for several stirrer speeds. These volumes are calculated with flow map 3 with the same process parameters as used to calculate the selectivity in Figure 5. The volume of the dispersed feed stream as a function of the dimensionless time is the same for all stirrer speeds, because  $V_{fd} \sim N$  and  $t_c \sim N^{-1}$ . The micromixed volume as a function of the dimensionless time increases with increasing stirrer speed. Therefore, the volume fraction of micromixed fluid inside the dispersed feed stream increases when the stirrer speed is increased, resulting in more self-engulfment and consequently a smaller increase in the growth rate of the micromixed volume for the higher stirrer speeds. For stirrer speeds above 3 Hz the increase in the growth rate of the micromixed volume with increasing stirrer speed is relatively small.



This effect can also be observed in Figure 5 by a decreasing influence of the stirrer speed on the selectivity for stirrer speeds higher than 3 Hz.

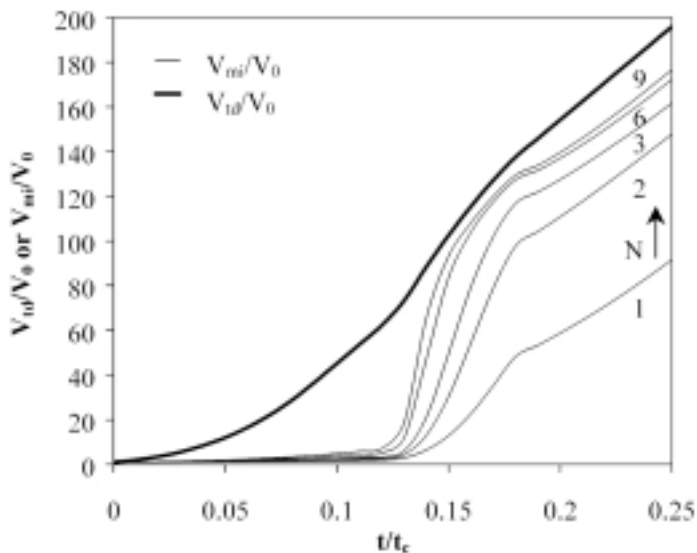


Figure 11: Volume of the dispersed feed stream ( $V_{id}$ ) and the micromixed volume ( $V_{mi}$ ) as a function of dimensionless time ( $t/t_c$ ) and stirrer speed for the 6 L vessel and a feed rate equal to the local circulation velocity ( $0.15v_{ip}$ ).

## 6. Conclusions

In this paper a model is proposed for the prediction of the product quality of fast chemical reactions in semi-batch stirred tank reactors. Application of this model requires information on the energy dissipation rate, the velocity length scale and the average velocity. The local values for these parameters vary throughout the stirred tank and, therefore, the agreement between measured and calculated selectivities depends on the complexity of the flow map describing these hydrodynamic parameters. When these hydrodynamic parameters are described in sufficient detail the proposed mixing model is able to predict the selectivity of a mixing-sensitive reaction. This will allow for the effective design and scale-up of stirred tank reactors in which this type of reactions is carried out.

The model presented in this paper has been validated by determining the product distribution of the third Bourne reaction. During the experiments the feed velocity was smaller than or comparable to the local circulation velocity. Therefore, the influence of the feed stream on the hydrodynamic parameters has been neglected. Under these circumstances, an agreement between the measured and calculated product distributions could not be obtained when using constant hydrodynamic parameters in the entire vessel. However, a flow map with three characteristic regions is sufficient to obtain a good agreement between the measurements and the simulations. In this flow map, the velocity length scale is constant in each region and the energy dissipation rate has a constant value in the bulk region and in the wall region. Since large gradients in the energy dissipation rate are present in the stirrer region, the necessary detailing in the description of the energy dissipation rate depends on the radial position of the feed pipe. When the radial position of the feed pipe is equal to 0.3 times the vessel diameter, a constant energy dissipation rate in the stirrer region can be used. However, when the radial position of the feed pipe is equal to 0.2 times the vessel diameter, a description of the gradient in the energy dissipation rate in the stirrer region is necessary.

## Nomenclature

$c_i$	concentration of component $i$ in the mixed volume	$[\text{mol m}^{-3}]$
$\langle c_i \rangle$	concentration of compound $i$ in the bulk	$[\text{mol m}^{-3}]$
$D_{im}$	impeller diameter	$[\text{m}]$
$D_t$	turbulent dispersion coefficient	$[\text{m}^2 \text{s}^{-1}]$
$D_{\text{vessel}}$	vessel diameter	$[\text{m}]$
$E$	engulfment rate	$[\text{s}^{-1}]$
$k_i$	kinetic constant	$[\text{m}^3 \text{mol}^{-1} \text{s}^{-1}]$
$L$	linear dimension of a scalar cloud	$[\text{m}]$
$L_o$	initial diameter of the dispersed feed stream	$[\text{m}]$
$L_v$	length scale of the velocity fluctuations	$[\text{m}]$
$N$	stirrer speed	$[\text{s}^{-1}]$
$N_p$	power number	$[-]$
$N_q$	stirrer flow number	$[-]$
$Q_p$	stirrer pumping capacity	$[\text{m}^3 \text{s}^{-1}]$
$r$	radial coordinate	$[\text{m}]$
$r_c$	circulation ratio	$[-]$
$R_i$	reaction rate	$[\text{mol m}^{-3} \text{s}^{-1}]$
$t$	time	$[\text{s}]$
$t_c$	circulation time	$[\text{s}]$
$t_{\text{feed}}$	feed time	$[\text{s}]$
$t_{\text{stirrer}}$	residence time in the stirrer region	$[\text{s}]$
$u$	velocity	$[\text{m s}^{-1}]$
$v_{\text{stirrer}}$	velocity in the stirrer region	$[\text{m s}^{-1}]$
$V_0$	volume of a fluid element	$[\text{m}^3]$
$V_{\text{feed}}$	feed volume	$[\text{m}^3]$
$V_{mi}$	volume mixed on a molecular scale	$[\text{m}^3]$
$V_{\text{reactor}}$	volume of the reactor contents	$[\text{m}^3]$
$V_{td}$	volume of the dispersed feed stream	$[\text{m}^3]$
$\delta$	thickness	$[\text{m}]$
$\varepsilon$	energy dissipation rate	$[\text{m}^2 \text{s}^{-3}]$
$\nu$	kinematic viscosity	$[\text{m}^2 \text{s}^{-1}]$

## References

- Baldyga, J., and J.R. Bourne "A fluid mechanical approach to turbulent mixing Part II Micromixing in the light of turbulence theory", *Chem. Eng. Commun.*, 28, 243 (1984)
- Baldyga, J., and J.R. Bourne "Simplification of micromixing calculations I. Derivation and Application of new model", *Chem. Eng. J.*, 42, 83 (1989a)
- Baldyga, J., and J.R. Bourne "Simplification of micromixing calculations II. New Applications", *Chem. Eng. J.*, 42, 93 (1989b)
- Baldyga, J., and J.R. Bourne "Interactions between mixing on various scales in stirred tank reactors", *Chem. Eng. Sci.*, 47, 1839 (1992)
- Baldyga, J., and J.R. Bourne "Turbulent mixing and chemical reactions", John Wiley, Chichester (1999)
- Baldyga, J., J.R. Bourne, and S.J. Hearn "Interaction between chemical reactions and mixing on various scales", *Chem. Eng. Sci.*, 52, 457 (1997)
- Baldyga, J., and R. Pohorecki "Turbulent micromixing in chemical reactors a review", *Chem. Eng. J.*, 58, 183 (1995)
- Bourne, J.R., and P. Dell'ava "Micro- and macro-mixing in stirred tank reactors of different sizes", *Chem. Eng. Res. Des.*, 65, 180 (1987)
- Bourne, J.R., and S. Yu "Investigation of micromixing in stirred tank reactors using parallel reactions", *Ind. Eng. Chem. Res.*, 33, 41 (1994)
- David, R., and J. Villermaux "Interpretation of micromixing effects on fast consecutive-competing reactions in semi-batch stirred tanks by a simple interaction model", *Chem. Eng. Commun.*, 54, 333 (1987)
- Franke, J. and A. Mersmann "The influence of the operation conditions on the precipitation process", *Chem. Eng. Sci.*, 50, 1737 (1995)
- Fox, R.O. "Computational methods for turbulent reacting flows in the chemical process industry", *Revue de L'institut Français du Pétrole*, 51, 215 (1996)
- Jacobson, A.R., A.N. Makris, and L.M. Sayre "Monoacylation of Symmetrical Diamines", *J. Org. Chem.*, 52, 2592 (1987)
- Jeurissen, F., J.G. Wijers, and D. Thoenes "Initial mixing of feed streams in agitated vessels", *I.Chem.E. Symp. Series*, 136, 235 (1994)
- Kajbic, A.F. "Distribution of energy dissipation in stirred vessels for liquids and suspensions" (in Dutch), Eindhoven University of Technology, Institute for Continuing Education, ISBN 90-5282-453-3 (1995)

*Kusters, K.A. "The influence of turbulence on aggregation of small particles in agitated vessels", Ph.D. Thesis, Eindhoven University of Technology (1991)*

*Larsson, G., S. George, and S.O. Enfors "Scale-down reactor model to simulate insufficient mixing conditions during fed batch operation using a biological test system", A.I.Ch.E. Symp. Series, 293, 151 (1992)*

*Lesieur, M. "Turbulence in fluids: Stochastic and numerical modeling", Kluwer Academic Publishers, Dordrecht (1990)*

*Nagata, S. "Mixing", John Wiley, New York (1975)*

*Perry, R.H., and Chilton, C.H. "Chemical Engineers' Handbook", Fifth ed. McGraw-Hill Book Company, New York (1973)*

*Phillips, R., S. Rohani, and J. Baldyga "Micromixing in a single feed semi-batch precipitation process", A.I.Ch.E. J., 45, 82 (1999)*

*Ranade, V.V., and J.R. Bourne "Reactive mixing in agitated tanks", Chem. Eng. Commun., 99, 33 (1991)*

*Schoenmakers, J.H.A. "Turbulent feed stream mixing in agitated vessels", Ph.D. Thesis, Eindhoven University of Technology (1998)*

*Schoenmakers, J.H.A., J.G. Wijers, and D. Thoenes "Simplified stirrer modeling for the prediction of time averaged hydrodynamics in stirred vessels", Proc. Fluid Mixing 5 Conference, 327 (1996)*



# MEAN CONCENTRATIONS AND CONCENTRATION FLUCTUATIONS IN A STIRRED TANK REACTOR

## Abstract

Mixing has a large influence on the product ratio of fast competitive reactions as the product ratio of these reactions is determined by local concentrations. In this study, models from literature have been integrated to describe the mean and fluctuating concentration of a feed stream in a stirred tank reactor. Planar Laser Induced Fluorescence and Laser Doppler Velocimetry experiments have been performed to validate these models and to determine the model parameters. To calculate the mean concentration, the turbulent dispersion coefficient has to be known. In this study, a combination of a theoretical model, measured mean concentrations and LDV measurements is used to determine the turbulent dispersion coefficient. Compared to the literature, the turbulent mixer model requires adjustment of the constant in the production term of the concentration variance to fit the measured concentration variances correctly. The models proved to be able to describe the mean concentration and concentration variance of an passive tracer stream fed to a stirred tank reactor.

*This chapter has been submitted for publication as I.L.M. Verschuren, J.G. Wijers and J.T.F. Keurentjes "Mean concentrations and concentration fluctuations in a stirred tank reactor"*

## 1. Introduction

Before a chemical reaction can take place, the reactants have to be mixed on a molecular scale. Inefficient mixing has large negative effects on the yield and selectivity of a broad range of chemical reactions, because slow mixing can retard desired reactions and promote undesired side reactions. A well-designed and controlled mixing process leads to significant pollution prevention, better usage of raw materials and the prevention of by-product formation avoids expensive separation costs downstream in the process. An example of a mixing-sensitive process is the addition of an acid or base to an organic substrate, which degrades in the presence of a high or low pH. Slow mixing will limit the neutralization reaction, which will allow the organic substrate to react with the acid or base to unwanted byproducts (Paul et al., 1992). Other examples of mixing-sensitive processes are various types of polymerizations, precipitations and fermentations (e.g. Fields and Ottino, 1987; Franke and Mersmann, 1995; Larsson et al., 1992).

The selectivity of a mixing-sensitive reaction depends on local concentrations inside a reactor. This study is focussed on determining local concentrations in stirred tank reactors operated under turbulent flow conditions, as it is often used in the chemical and biochemical industry. In principle, local properties of a flow, such as velocity or concentration, are described by the conservation equations of mass, momentum and energy. Since turbulent flows of practical interest contain a wide range of time and length scales, the complete exact solution of these equations is not possible with the nowadays-available computational resources. Therefore, simplified but tractable models are proposed in the literature to describe the mixing in turbulent flows. The most widely accepted approach for modeling the mixing in a turbulent flow is based on Reynolds decomposition (Fox, 1996). Reynolds decomposition consists of describing a property of the turbulent flow with a mean and a fluctuating value. These models have been verified for a tubular reactor by comparing model predictions with experimentally determined yields of a test reaction (Baldyga, 1989; Baldyga and Henczka, 1997; Hannon et al., 1998). The objective of this work is to integrate models from literature, allowing for the description of the mean and fluctuating concentration of an passive tracer fed to a stirred tank reactor. The models will be validated against experimental data and will be refined to make them more suitable for stirred tank reactors.



The models used to describe the mean concentration and concentration variance require information about local hydrodynamic parameters. In this study, these parameters have been determined for a stirred tank reactor equipped with a Rushton turbine impeller using Laser Doppler Velocimetry. To validate the simulations, mean concentrations and concentration variances of a passive tracer fed to the same stirred tank reactor have been measured with Planar Laser Induced Fluorescence.

## 2. Model for the mean concentration and concentration variance of a passive tracer fed to a stirred tank reactor

Reynolds decomposition and time averaging applied to the mass transfer equation of a passive tracer result in:

$$\frac{D\bar{c}}{Dt} = \frac{\partial}{\partial x_j} \left[ D_m \frac{\partial \bar{c}}{\partial x_j} \right] - \frac{\partial}{\partial x_j} \overline{u'_j c'} \quad (1)$$

where  $\bar{c}$  is the time-averaged concentration of a passive tracer,  $x$  is a space coordinate and  $D_m$  is a molecular diffusion coefficient.

Notice that in equation 1 the term  $\overline{u'_j c'}$  is unclosed. This term is usually approximated using the concept of turbulent diffusivity:

$$-\overline{u'_j c'} = D_T \frac{\partial \bar{c}}{\partial x_j} \quad (2)$$

in which  $D_T$  is the turbulent dispersion coefficient.

Substituting equation (2) into equation (1) leads to the following equation describing the mean concentration field of a passive tracer:

$$\frac{D\bar{c}}{Dt} = \frac{\partial}{\partial x_j} \left[ (D_m + D_T) \frac{\partial \bar{c}}{\partial x_j} \right] \quad (3)$$

In this study equation (3) is used to describe the mean concentration field of a continuous feed stream in a stirred tank reactor. As noticed by Baldyga and Pohorecki (1995), in a continuous feed stream the concentration gradients in the radial direction are much larger than the concentration gradients in the direction of the flow. Therefore, only radial dispersion is assumed. Molecular diffusion has been assumed to be negligible compared to turbulent dispersion.

The turbulent dispersion coefficient depends on the velocity and the length scale of the turbulent motions taking part in the turbulent dispersion process (Tennekes and Lumley, 1972):

$$D_T \approx u(\lambda) \cdot \lambda \quad (4)$$

in which the length scales and the velocities of the turbulent motions are assumed to be described by a characteristic length scale ( $\lambda$ ) and a characteristic velocity ( $u(\lambda)$ ), respectively. The characteristic velocity of a turbulent motion is described by the energy dissipation rate ( $\epsilon$ ) and the characteristic length scale (Tennekes and Lumley, 1972):

$$u(\lambda) \approx (\epsilon \cdot \lambda)^{1/3} \quad (5)$$

Substituting equation (5) into equation (4) leads to the following equation for the turbulent dispersion coefficient:

$$D_T = A \epsilon^{1/3} \lambda^{4/3} \quad (6)$$

with A being a constant.

The value of  $\lambda$  depends on the relative size of the scalar cloud compared to scales of the turbulent flow field (Lesieur, 1990). When the concentration scales are equal to or larger than the scales of the turbulent flow field,  $\lambda$  is equal to the integral velocity length scale and the constant A is equal to 0.1 (Baldyga and Pohorecki, 1995). Usually, a feed stream is introduced into a stirred tank reactor with an initial concentration length scale smaller than the scales of the turbulent flow field. In that case,  $\lambda$  will be equal to a characteristic length scale describing the size of the scalar cloud. In this work  $\lambda$  is

assumed to be equal to the radius of the feed stream when this radius is smaller than the integral velocity length scale. The corresponding value for the constant A has been determined by optimizing the agreement between measured and calculated mean concentration profiles.

The radius of the feed stream is calculated as follows. A scalar length scale (L), such as the radius of a feed stream, which is smaller than the integral velocity length scale follows a Richardson law (Lesieur, 1990):

$$\frac{1}{2} \frac{dL^2}{dt} = C\varepsilon^{1/3} L^{2/3} \quad (7)$$

The value of C depends on the length scale taken into consideration. If L corresponds to a scalar cloud diameter, C is equal to 2.14 (Lesieur, 1990). Integration of equation (7) leads to the following equation for the radius of the feed stream:

$$r = \left( r_0^{2/3} + \frac{2}{3} C \varepsilon^{1/3} t \right)^{3/2} \quad (8)$$

with C equal to 1.35. This value for C corresponds to the growth of the diameter of the feed stream with a constant equal to 2.14.

The initial radius of the feed stream ( $r_0$ ) has been estimated as follows. When the momentum of the feed stream is negligible compared to the momentum of the flow in the reactor, the velocity of the feed stream will, soon after leaving the feed tube, be equal to the local circulation velocity ( $\bar{u}_c$ ). This is normally the case when the feed velocity is smaller than or comparable to the local circulation velocity (Jeurissen et al., 1994). Under these circumstances the initial radius ( $r_0$ ) of the feed stream is given by (Baldyga et al., 1997):

$$r_0 = \sqrt{\frac{Q_{\text{feed}}}{\pi u_c}} \quad (9)$$

with  $Q_{\text{feed}}$  the volumetric flow rate of the feed liquid.

The concentration variance of an passive tracer is described by the turbulent mixer model proposed by Baldyga (1989). In this model the concentration variance ( $\sigma^2$ ) is divided into three parts. Each part corresponds to one of the mixing processes in a turbulent flow for Schmidt numbers much larger than one. These mixing processes and corresponding range of length scales ( $l$ ) are:

1. inertial-convective disintegration of large eddies ( $\sigma_1^2$ ),  $L_v \leq l \leq 12l_k$
2. viscous-convective formation of laminated structures ( $\sigma_2^2$ ),  $12l_k < l \leq l_k$
3. molecular diffusion within the deforming laminated structures ( $\sigma_3^2$ ),  $l < l_k$

The Kolmogorov length scale ( $l_k$ ) is:

$$l_k = \left( \frac{\nu^3}{\varepsilon} \right)^{1/4} \quad (10)$$

where  $\nu$  is the kinematic viscosity ( $\approx 10^{-6}$  for water).

The concentration variance is equal to the sum of these three parts:

$$\sigma^2 = \sigma_1^2 + \sigma_2^2 + \sigma_3^2 \quad (11)$$

The transport equation for each component of the concentration variance is:

$$\frac{D\sigma_i^2}{Dt} = \frac{\partial}{\partial x_j} \left[ (D_m + D_T) \frac{\partial \sigma_i^2}{\partial x_j} \right] + R_{pi} - R_{Di} \quad (12)$$

in which  $R_{pi}$  is a production rate and  $R_{Di}$  is a dissipation rate.

According to Spalding (1971), the production rate of the concentration variance in the inertial- convective subrange of wave numbers ( $\sigma_1^2$ ) is:

$$R_{p1} = C_{g1} D_T \left( \frac{\partial \bar{c}}{\partial x_j} \right)^2 \quad (13)$$

with  $C_{g1}$  being a constant. A commonly used value for this constant is about 2 (Fox, 1996; Baldyga and Henczka, 1997; Spalding, 1971).

The decay of  $\sigma_1^2$  by the inertial-convective disintegration of large eddies is described by Corrsin (1964) and Rosensweig (1964):

$$R_{D1} = \frac{\sigma_1^2}{\tau_s} \quad (14)$$

$$\tau_s = 2 \left( \frac{L_c^2}{\varepsilon} \right)^{1/3} \quad (15)$$

where  $L_c$  is the scalar integral length scale. The initial scalar integral length scale is set equal to the initial radius of the feed stream ( $r_0$ ) (Baldyga et al., 1997). This length scale will grow according to equation (7) with  $C=0.3$  (Lesieur, 1990).

The disintegration of large eddies produces a variance on a smaller scale in the viscous-convective subrange of wave numbers:

$$R_{D2} = R_{D1} \quad (16)$$

The viscous-convective component of the variance ( $\sigma_2^2$ ) decays due to vortices causing the formation of laminated structures (Baldyga and Rohani, 1987):

$$R_{D2} = E \sigma_2^2 \quad (17)$$

$$E = 0.0578 \sqrt{\frac{\varepsilon}{\nu}} \quad (18)$$

The decay of  $\sigma_2^2$  produces the viscous-diffusive variance component ( $\sigma_3^2$ ):

$$R_{D3} = R_{D2} \quad (19)$$

which decays due to molecular diffusion within the deforming laminated structures (Baldyga, 1989):

$$R_{D3} = G_w \sigma_3^2 \quad (20)$$

$$G_w = (0.303 + 17.050 / Sc) E \quad (21)$$

The calculation of mean concentrations and concentration variances with the equations given above requires information about the local energy dissipation rate and local circulation velocity. In this study, local energy dissipation rates and circulation velocities have been determined experimentally using Laser Doppler Velocimetry (LDV) for a stirred tank reactor equipped with a Rushton turbine impeller. To validate the simulations, mean concentrations and concentration variances have been measured with Planar Laser Induced Fluorescence (PLIF) at various axial locations below the feed pipe inside the studied stirred tank reactor. To be able to compare the measured concentrations as a function of axial distance with the calculated concentrations as a function of time, the axial location has been replaced by a Lagrangian time scale:

$$t = \int_0^z \frac{1}{\bar{u}_{ax}} dz \quad (22)$$

in which  $z$  is the axial distance below the feed pipe and  $\bar{u}_{ax}$  is the mean axial velocity below the feed pipe. These mean axial velocities have also been determined from the LDV experiments.

### 3. Local energy dissipation rates and mean velocities

#### 3.1 LDV experiments

Laser Doppler Velocimetry (LDV) was used to determine local velocities and energy dissipation rates. The vessel used for these LDV experiments was made of Perspex and was equipped with a standard six-bladed Rushton turbine impeller, four baffles, a feed pipe and an effluent pipe. The geometry of the tank is schematically shown in Figure 1. The internal diameter of the vessel ( $T$ ) was 0.288 m. The internal diameter of the feed pipe was 8 mm. The wall thickness of the feed pipe was about 1 mm. Details of the impeller geometry are given in Figure 2.

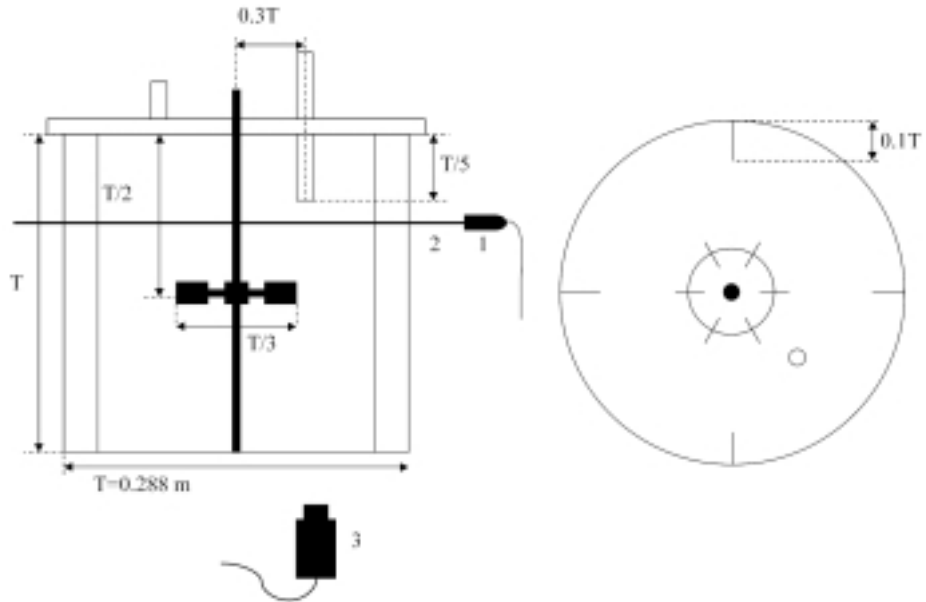


Figure 1: Schematic representation of the stirred vessel and experimental set-up used for the Planar Laser Induced Fluorescence experiments; 1. laser probe, 2. laser light sheet, 3. high speed CCD camera.

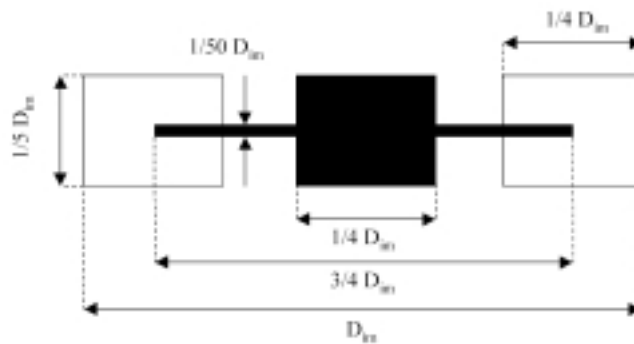
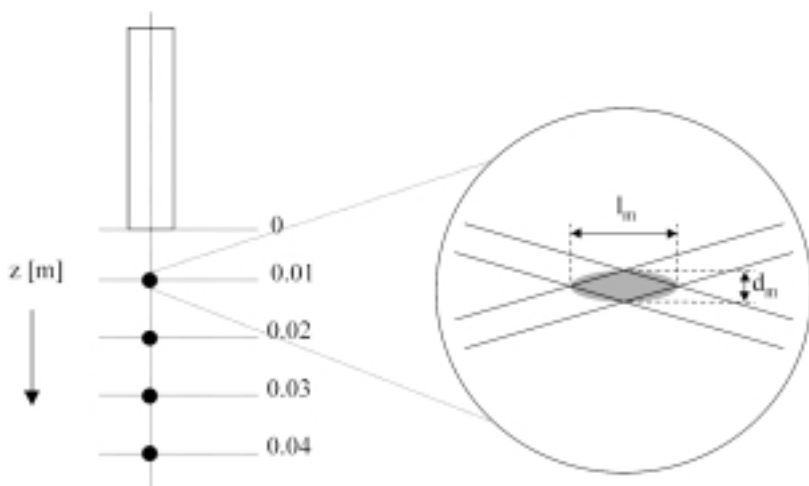


Figure 2: Schematic representation of the Rushton turbine impeller showing the dimensions.

A commercially available LDV set-up was used, operating in the back-scatter mode with two beam pairs. The LDV set-up consisted of a 2W Argon Laser (Stabilite 2017 by Spectra Physics), a color separator, photomultipliers, Burst Spectrum Analyzers (Dantec) and a probe attached to an automated traverse system. The wavelengths of the beam pairs were 488 nm and 514.5 nm, respectively. To be able to discriminate between a positive and a negative direction of the velocity, one beam of each pair was given a frequency shift of 40 mHz. The measuring volume created by the intersection of two laser beams of the same wavelength was 3 mm in length and 0.15 mm in diameter (see Figure 3).



*Figure 3: Measurement positions used for the Laser Doppler Velocimetry experiments and schematic representation of an LDV measurement volume.*

The stirred tank reactor was entirely filled with water and seeded with a small amount of dispersed polystyrene latex with an average particle size of 4  $\mu\text{m}$ . The reactor was placed in a rectangular glass tank filled with water to reduce the diffraction of the laser light due to the curvature of the reactor surface.

LDV measurements were performed for a stirrer speed of 3.1 Hz at 4 positions on a vertical line below the feed pipe as illustrated in Figure 3. The velocities and the energy dissipation rates were normalized with the stirrer tip velocity ( $v_{\text{tip}}$ ) and the average energy dissipation rate inside the stirred tank reactor ( $\bar{\epsilon}$ ), respectively. The average energy dissipation rate inside the stirred tank reactor is estimated with:



$$\varepsilon = \frac{N_p N^3 D_{im}^5}{V_{reactor}} \quad (23)$$

in which  $N_p$  is the power number equal to 5.3 for the Rushton turbine impeller used in this work (Schoenmakers, 1998),  $N$  is impeller speed,  $D_{im}$  is impeller diameter and  $V_{reactor}$  is the liquid volume inside the reactor.

### 3.2 LDV data processing

LDV is based on the measurement of velocities of particles suspended in the flow. The higher measurement probability of particles with a higher velocity yields a velocity distribution biased towards higher values. In order to eliminate this velocity bias, transit time weighting was applied when calculating the mean velocity ( $\bar{u}_i$ ) and the mean square fluctuating velocity ( $\overline{u_i'^2}$ ).

$$\bar{u}_i = \sum_{j=0}^{N-1} \eta_j u_{ij} \quad (24)$$

$$\overline{u_i'^2} = \sum_{j=0}^{N-1} \eta_j (u_{ij} - \bar{u}_i)^2 \quad (25)$$

$$\eta_j = \frac{t_j}{\sum_{k=0}^{N-1} t_k} \quad (26)$$

where  $t_j$  is the transit time of a particle crossing the measurement volume and  $u_{ij}$  is the velocity of this particle.

The energy dissipation rate was estimated with:

$$\varepsilon = \beta \frac{k^{3/2}}{L_v} \quad (27)$$

in which  $\beta$  is a constant, equal to unity (Kusters, 1991),  $k$  is the turbulent kinetic energy and  $L_v$  is the integral velocity length scale.

The turbulent kinetic energy was calculated from the velocity fluctuations in the three orthogonal directions:

$$k = \frac{1}{2} \sum_{i=1}^3 \overline{u_i'^2} \quad (28)$$

Taylor's hypothesis was used to calculate the integral length scale from the integral time scale ( $T_v$ ):

$$L_v = \sqrt{\sum_{i=1}^3 \overline{u_i'^2}} \cdot T_v \quad (29)$$

In which  $T_v$  is the integral time scale equal to the sum of the time scales for the three orthogonal directions ( $T_i$ ):

$$T_v = \sum_{i=1}^3 T_i \quad (30)$$

These time scales were calculated from the energy spectrum of the velocity fluctuations ( $E_i(f)$ ) (Hinze, 1975):

$$T_i = \frac{1}{\overline{u_i'^2}} \lim_{f \rightarrow 0} E_i(f) \quad (31)$$

Integral time scales were approximated from the average of the first points obtained in the horizontal part of energy spectra.

To calculate an energy spectrum, discrete velocity samples have to be evenly distributed in time. To obtain evenly distributed velocity samples from the LDV-measurements, the Sample-Hold technique was used (Adrian and Yao, 1987):

$$u_{SH}(t) = u(t_j) \quad t_j \leq t \leq t_{j+1} \quad (32)$$

The energy spectrum was calculated from the autocovariance of the velocity fluctuations ( $C_{u_i u_i}(\tau)$ ) using Fast Fourier Transformation:

$$C_{v_{i,j}}(\tau) = \lim_{T \rightarrow \infty} \frac{1}{T} \int_0^T (u_i(t) - \bar{u}_i)(u_i(t + \tau) - \bar{u}_i) dt \quad (33)$$

$$E_i(f) = \int_{-\infty}^{\infty} C_{v_{i,j}}(\tau) e^{-i2\pi f\tau} d\tau \quad (34)$$

### 3.3 Results of the LDV experiments

Figure 4 shows the mean velocities in three orthogonal directions and the circulation velocity normalized with the tip velocity as a function of the axial coordinate. The mean velocity in the axial direction is approximately equal to the circulation velocity, whereas the mean velocities in radial and tangential direction are significantly smaller. In Figure 5, turbulent kinetic energies are given as a function of the axial distance below the feed pipe. Velocity length scales have been calculated from integral time scales, which have been approximated from the average of the first points obtained in the horizontal part of the energy spectrum. Figure 6 shows a representative example of an energy spectrum obtained from measured axial velocities at 0.03 m below the feed pipe. In Figure 7, normalized velocity length scales ( $L_v/T$ ) are presented as a function of the axial distance below the feed pipe.

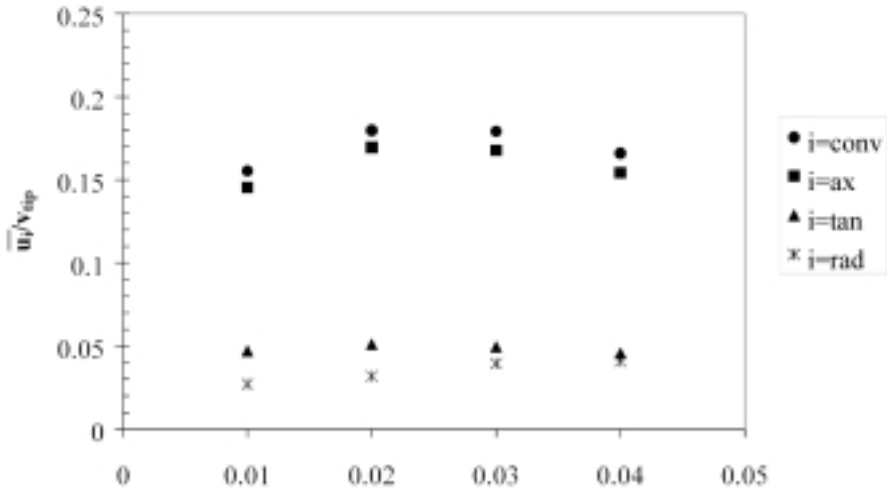


Figure 4: Mean velocities normalized to the stirrer tip speed in the radial, axial and tangential direction and normalized convection velocity as a function of the axial distance below the feed pipe.

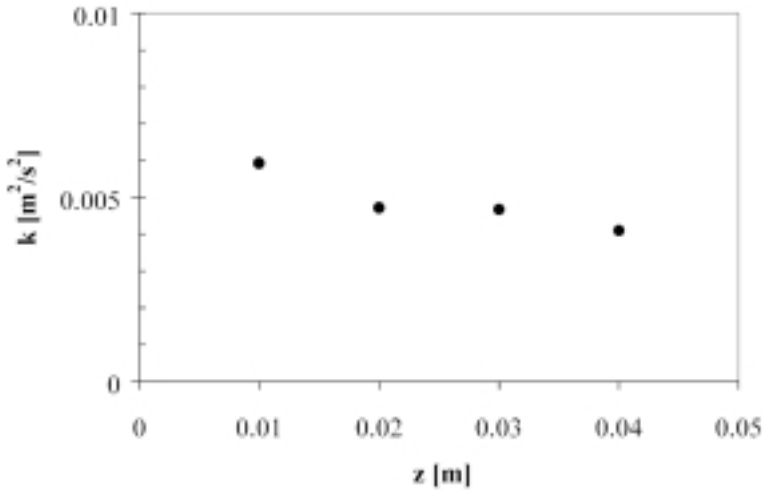


Figure 5: Turbulent kinetic energy below the feed pipe as a function of the axial coordinate, for a stirrer speed of 3.1 Hz.

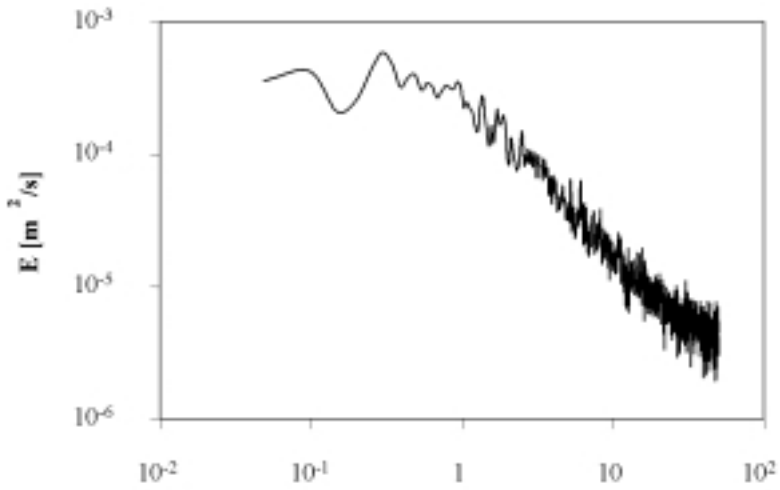


Figure 6: Energy spectrum obtained from measured axial velocities at 0.03 m below the feed pipe

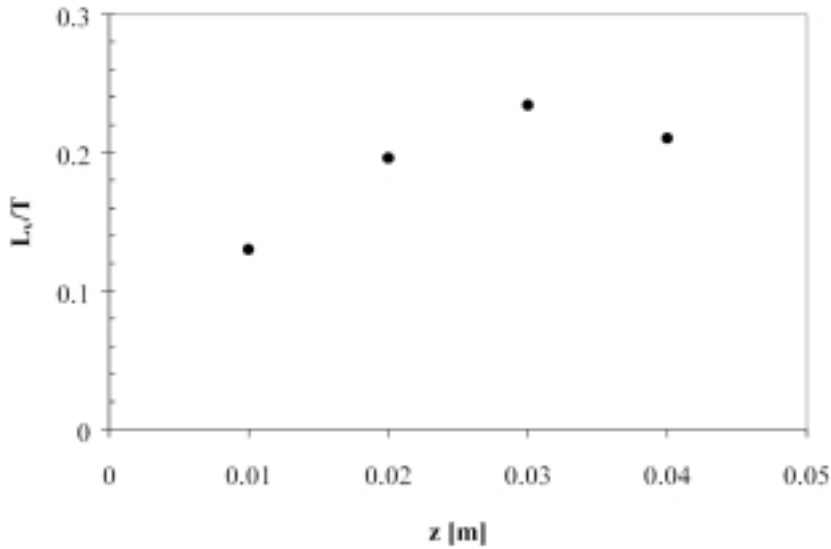


Figure 7: Velocity length scales normalized to the vessel diameter as a function of the axial distance below the feed pipe.

To simplify the calculations, average hydrodynamic parameters below the feed pipe have been used in the models to calculate local mean concentrations and concentration variances. These average hydrodynamic parameters have been obtained by averaging the hydrodynamic parameters measured with LDV and presented in Figures 4, 5 and 7, over the axial distance. The averaged hydrodynamic parameters are given in Table 1. The average energy dissipation rate below the feed pipe has been calculated by substituting the average kinetic energy and the average length scale in equation (27). This average energy dissipation rate normalized to the average energy dissipation rate inside the stirred tank reactor is also given in Table 1.

Table 1. Hydrodynamic parameters averaged over the axial distance below the feed pipe

hydrodynamic parameter	averaged value
$\bar{u}_{ax}$	0.16 $v_{tip}$
$\bar{u}_c$	0.17 $v_{tip}$
k	0.005 $m^2/s^2$
$L_v$	0.19 D
$\epsilon$	0.1 $\bar{\epsilon}$

#### 4. Mean concentration and concentration variance of an passive tracer fed to a stirred tank reactor

##### 4.1 PLIF experiments

Local mean concentrations and concentration variances were measured using Planar Laser Induced Fluorescence (PLIF). The PLIF experiments were performed in the same vessels as used for the LDV experiments.

The principle of PLIF is the measurement of the fluorescence intensity of a tracer dye excited by a laser sheet. As shown in Figure 1, a CCD-camera placed perpendicular to the laser sheet, is used to record the fluorescence intensity and to convert the intensity into a gray value. At low tracer concentrations, the intensity of fluorescence is linearly dependent on the concentration of the dye. When this is the case, the following equation can be used to calculate the instantaneous tracer concentration at position  $x, y$  ( $c(x,y,t)$ ) from the gray values (Houcine et al, 1996):

$$c(x, y, t) = \frac{G(x, y, t) - \bar{G}_B(x, y)}{\bar{G}_{c_{\text{hom}}}(x, y) - \bar{G}_B(x, y)} c_{\text{hom}} \quad (35)$$

with  $G(x,y,t)$  is the local instantaneous gray value,  $\bar{G}_B(x,y)$  is the local average gray value of the background and  $\bar{G}_{c_{\text{hom}}}(x,y)$  is the local average gray value corresponding to a known tracer concentration ( $c_{\text{hom}}$ ) in a homogeneous solution.

The fluorescent dye used in this study was Fluorescein. Preliminary experiments were carried out in the reactor in order to determine the range of linear response between gray value and Fluorescein concentration. In each of these experiments the reactor was filled with a Fluorescein solution of known concentration and gray values were determined at several positions in the tank. These experiments showed that for concentrations of Fluorescein less than  $6 \cdot 10^{-8}$  mol/l, the gray value was linearly related to the Fluorescein concentration.

A laser beam with a wavelength of 488 nm was formed into a sheet of 0.5 mm thickness using a cylindrical lens (Dantec 9080XO.21). The laser sheet was placed horizontally in the vessel as shown in Figure 1. Before each experiment the reactor was entirely filled

with water. During an experiment a Fluorescein solution was injected into the reactor with a velocity approximately equal to the local circulation velocity:

$$v_{feed} = 0.15\pi ND_{in} \quad (36)$$

Measurements were taken at four horizontal cross-sections located at 0.005 m, 0.015 m, 0.03 m and 0.04 m below the feed pipe. The impeller speeds used were 1.5, 3 and 4 Hz. Accordingly, the feed flow rates were  $3.4 \cdot 10^{-6} \text{ m}^3\text{s}^{-1}$ ,  $6.8 \cdot 10^{-6} \text{ m}^3\text{s}^{-1}$  and  $9.0 \cdot 10^{-6} \text{ m}^3\text{s}^{-1}$ , respectively. A CCD-camera (JAI CV-M30) placed perpendicularly to the plane of the laser sheet was used to record 2000 images of the feed stream in 20 circulation times. The following equation was used to calculate the circulation time:

$$t_c = \frac{V_{reactor}}{r_c N_q N D_{in}^3} \quad (37)$$

where  $N_q$  is the pump number and  $r_c$  is the circulation ratio. The pump number and the circulation ratio were 0.7 and 3, respectively, for the Rushton turbine impeller used in this work (Schoenmakers, 1998).

The average background gray value ( $\overline{G_B}$ ) and the average gray value of a homogeneous Fluorescein solution ( $\overline{G_{chom}}$ ) were determined for each experiment. The average background gray value was obtained from 100 recorded images of the reactor filled with water. The average gray value of a homogeneous Fluorescein solution was obtained from 100 recorded images of the reactor filled with a Fluorescein solution of known concentration.

## 4.2 PLIF data processing

Feed streams inside stirred tank reactors have been shown to oscillate (Schoenmakers et al., 1997; Houcine et al., 1999). Large-scale oscillations were also observed visually during the PLIF-experiments described in this paper. These oscillations are ignored in the models presented in the literature, because usually the mixing of one feed stream with a relatively homogeneous bulk liquid is investigated. Under these circumstances, the oscillations of a feed stream will have no effect on the mixing rate. To be able to

compare the measured mean concentrations and concentration variances with the theoretical predictions, the influence of the oscillations on the measured mean concentrations and concentration variances was removed by assuming that the centre-of-mass of an instantaneous radial cross-section of the feed stream was located at a fixed position in the plane of measurement. These centres-of-mass were determined automatically using the commercially available image analysis program Optimas.

Equation (35) was used to calculate the instantaneous Fluorescein concentration at each (i,j) pixel. The mean concentration and concentration variance at each (i,j) pixel were calculated with:

$$\bar{c}(i, j) = \frac{1}{N_c} \sum_{w=1}^{N_c} c(i, j) \quad (38)$$

$$\sigma^2(i, j) = \frac{\sum_{w=1}^{N_c} (\bar{c}(i, j) - c(i, j))^2}{N_c} \quad (39)$$

in which  $N_c$  is the total number of images per experiment.

The concentration variance components and corresponding ranges of length scales have been described in section 2. In Table 2, values for the Kolmogorov length scale ( $l_k$ ) and  $12l_k$  are given together with the spatial resolution of the PLIF-experiments. From Table 2 and the ranges of length scales given in section 2 it is concluded that the spatial resolution of the PLIF-measurements was sufficient to measure the inertial-convective concentration variance component and a part of the viscous-convective concentration variance component. To determine the inertial-convective component of the concentration variance from the PLIF-measurements, the spatial resolution of a PLIF image must be equal to  $12l_k$ . PLIF images with a spatial resolution equal to  $12l_k$  were obtained by averaging the gray values of a number of adjacent pixels. These numbers of adjacent pixels in the x ( $N_x$ ) and y ( $N_y$ ) direction together with the spatial resolution are also given in Table 2.



Table 2. Spatial resolution of the PLIF-images

N [Hz]	$\Delta x$ [10 <sup>-4</sup> m]	$\Delta y$ [10 <sup>-4</sup> m]	$l_k$ [10 <sup>-4</sup> m]	$12l_k$ [10 <sup>-3</sup> m]	$N_x$	$N_y$	$\Delta x_{\text{cor}}$ [10 <sup>-3</sup> m]	$\Delta y_{\text{cor}}$ [10 <sup>-3</sup> m]
1.5	3	6	1.9	2.3	8	4	2.4	2.4
3	3	6	1.1	1.3	4	2	1.2	1.2
4	3	6	0.9	1.1	4	2	1.2	1.2

Independent of background emission, the root-mean-square gray value of the background is 8. This corresponds to a background root-mean-square variance of about 6 % of the maximum corrected gray value, which is the gray value of the initial Fluorescein concentration of the feed liquid minus the gray value of the background ( $\bar{G}_{c_0} - \bar{G}_B$ ). Thus the root-mean-square background variance ( $\sigma_B^2/c_0^2$ ) for the normalized inertial-convective component of the concentration variance ( $\sigma_1^2/c_0^2$ ) is of the order of  $0.06/(N_x N_y)^{1/2}$ . Measured concentration variances were corrected for the background variance:

$$\frac{\sigma_{1c}}{c_0} = \sqrt{\frac{\sigma_1^2}{c_0^2} - \frac{\sigma_B^2}{c_0^2}} \quad (40)$$

#### 4.3 Results of the PLIF experiments and comparison between simulations and experiments

Measured mean concentrations at two horizontal cross-sections located at 0.005 m and 0.03 m below the feed pipe for a stirrer speed of 3 Hz are given in Figures 8a and 8b. Figures 9a and 9b show measured inertial-convective concentration variances at these two horizontal cross-sections for a stirrer of 3 Hz. The mean concentration profiles shown in Figures 8a and 8b are both bell-shaped. Due to mixing with the environment, the height of the concentration profiles decreases and the area occupied by the feed stream increases with increasing distance from the feed pipe. At a distance of 0.005 m below the feed pipe relatively high concentration variances are present in the periphery of the feed stream and at the centre the concentration variances are relatively low. At a distance of 0.03 m below the feed pipe the concentration variance profile is bell-shaped, similar to the mean concentration profile. In the following, 2D cross-sections of these graphs will be used for clarity reasons.

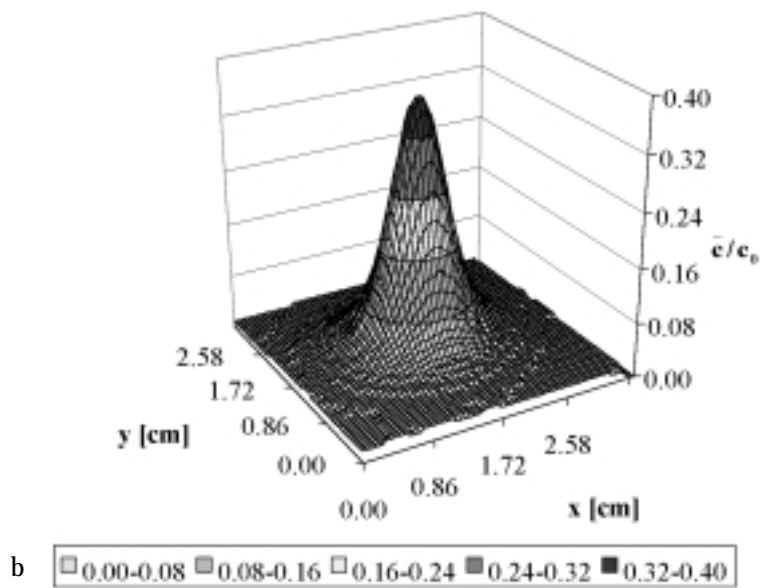
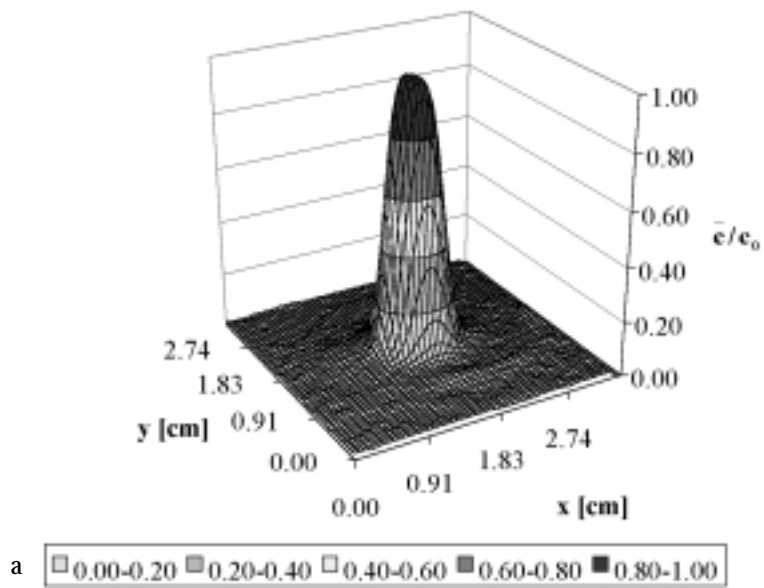


Figure 8: Measured mean concentrations at two horizontal cross-sections located at 0.005 (a) and 0.03 m (b) below the feed pipe for a stirrer speed of 3 Hz.

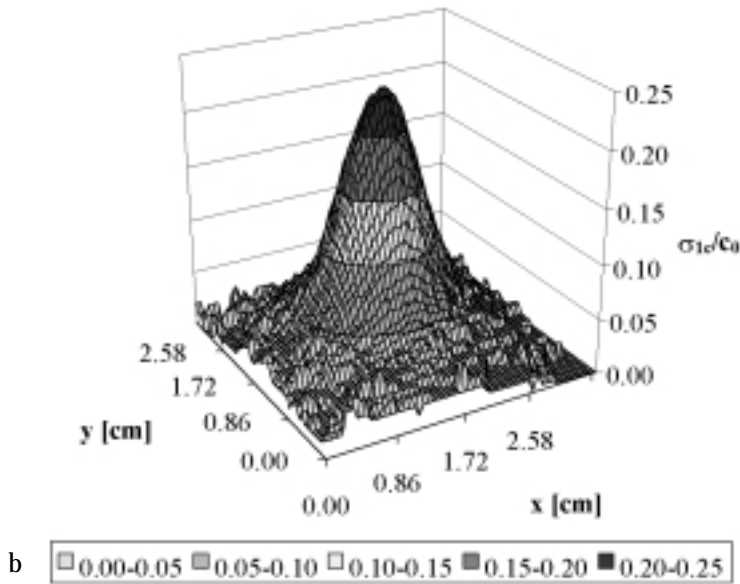
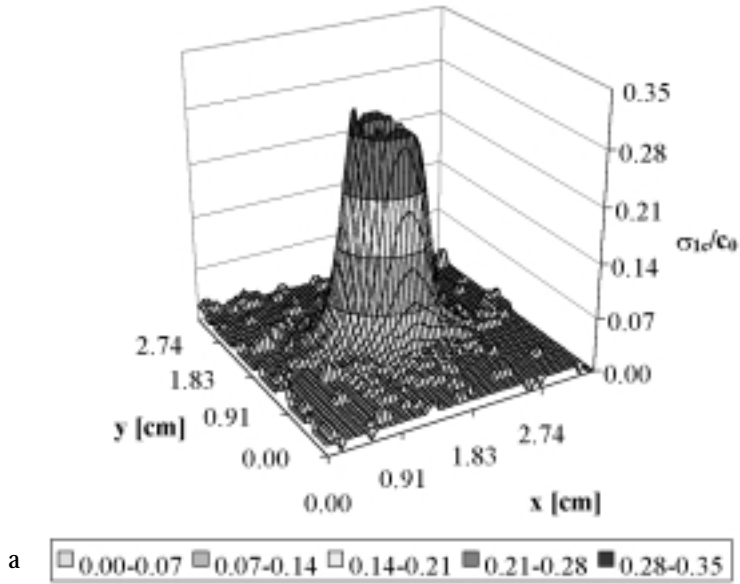


Figure 9: Measured inertial-convective concentration variances at two horizontal cross-sections located at 0.005 (a) and 0.03 m (b) below the feed pipe for a stirrer speed of 3 Hz.

In Figures 10a-d, measured normalized mean concentrations ( $\bar{c}/c_0$ ) are given for three stirrer speeds at axial distances of respectively 0.005, 0.015, 0.03 and 0.04 m below the feed pipe. When comparing the mean concentrations measured at a certain axial distance below the feed pipe at stirrer speeds of 3 and 4 Hz, no significant variation of mean concentration with impeller speed is observed. This is in agreement with predicted mean concentrations, because the turbulent dispersion coefficient scales with the impeller speed ( $N$ ) and the time needed by a fluid element to flow from the feed pipe to a certain axial distance below the feed pipe is proportional to  $N^{-1}$ . However, for a stirrer speed of 1.5 Hz, the mean concentrations presented in Figures 10c and 10d are significantly higher than the mean concentrations for the other two stirrer speeds. This discrepancy may be caused by not fully developed turbulence at this lower stirrer speed, whereas the model is based on fully turbulent flow conditions. Therefore, in the following, simulated mean concentrations and concentration variances will only be compared with experimentally determined values at impeller speeds of 3 and 4 Hz.

For the experimental conditions used in this study, the radius of the feed stream is smaller than the integral velocity length scale. In that case, the length scale ( $\lambda$ ), to be used in equation (4) describing the turbulent dispersion coefficient, is equal to a characteristic concentration length scale of the feed stream. In this study,  $\lambda$  is assumed to be equal to the radius of the feed stream. The value for the constant  $A$  in equation (4) has been determined by optimizing the agreement between the measured and simulated mean concentrations. Figures 10a-d show the comparison between measured and predicted mean concentrations for impeller speeds of 3 and 4 Hz at four axial locations below the feed pipe. With the constant  $A$  equal to 0.1, the predicted mean concentrations correspond reasonably well to the measured mean concentrations. Note that this value for  $A$  is identical with values for  $A$  given in the literature for concentration length scales equal to or larger than the scales of the turbulent flow field (Baladyga and Pohorecki, 1995).

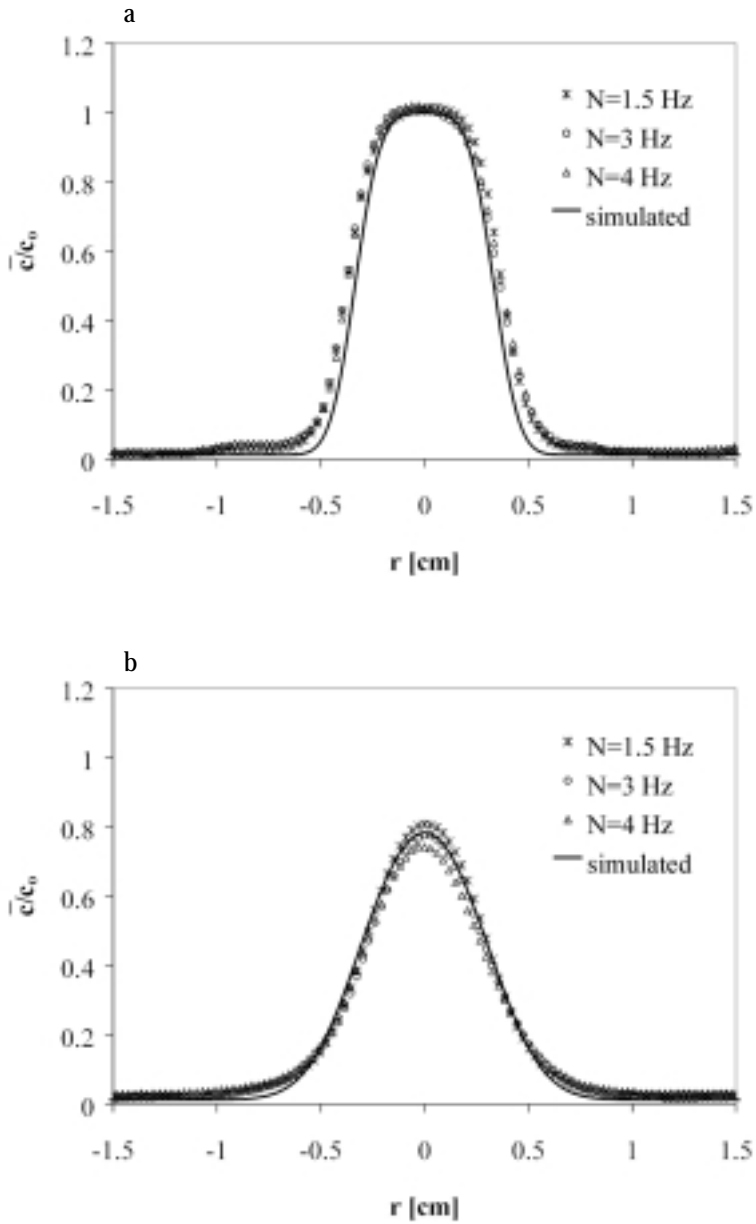


Figure 10: Measured mean concentration profiles for a stirrer speed of 1.5, 3 and 4 Hz and predicted mean concentration profiles for a stirrer speed of 3 and 4 Hz at different axial distances below the feed pipe ( $z$ ). a)  $z=0.005$  m b)  $z=0.015$  m

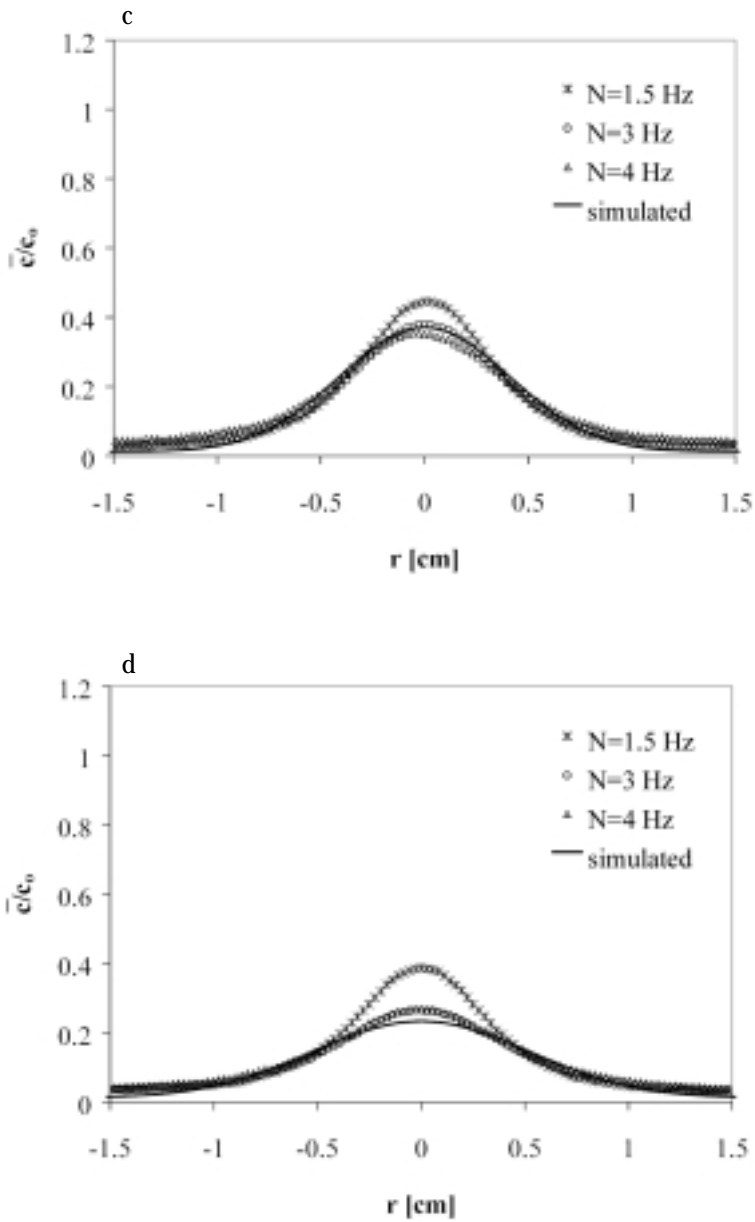
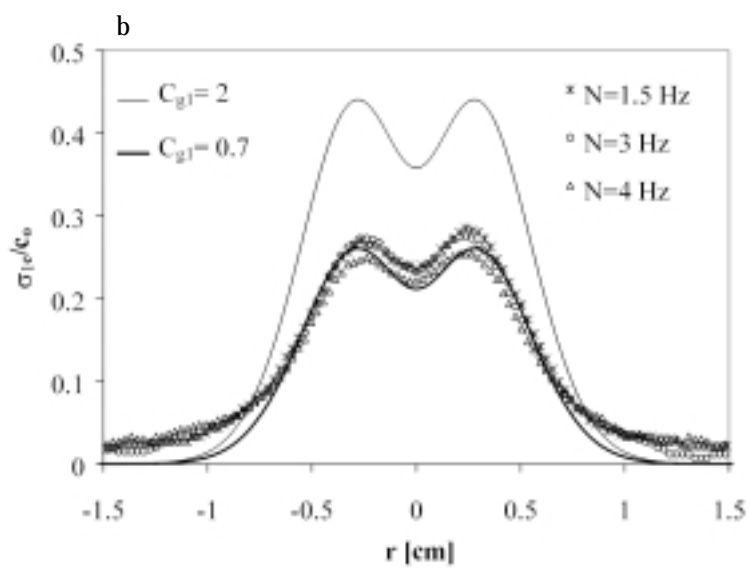
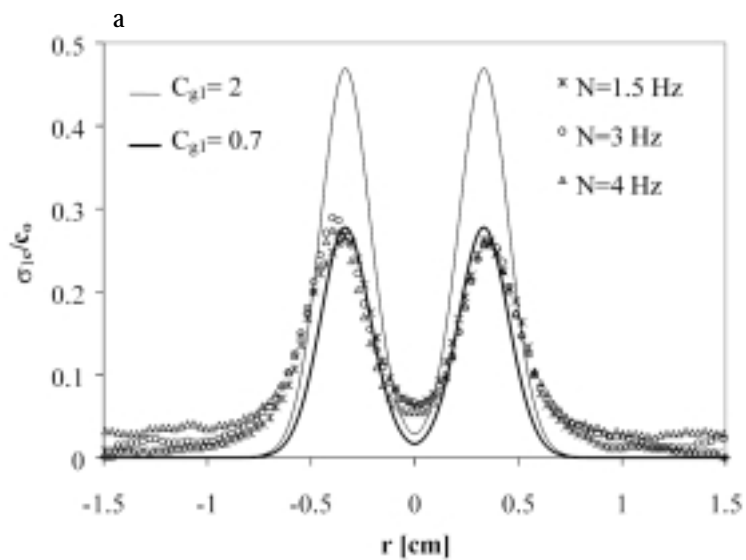


Figure 10: Measured mean concentration profiles for a stirrer speed of 1.5, 3 and 4 Hz and predicted mean concentration profiles for a stirrer speed of 3 and 4 Hz at different axial distances below the feed pipe ( $z$ ). c)  $z=0.03$  m and d)  $z=0.04$  m

The spatial resolution of the PLIF experiments is sufficient to measure the inertial-convective part of the concentration variance. In Figures 11a-d the root square of the measured normalized inertial-convective concentration variances corrected for the background variance ( $\sigma_{1c}/c_0$ ) are given for three stirrer speeds at 0.005, 0.015, 0.03 and 0.04 m below the feed pipe, respectively. At a certain axial distance below the feed pipe, no significant differences between the measured concentration variances for stirrer speeds of 3 and 4 Hz are observed. This is in agreement with the model, because the turbulent dispersion coefficient scales with impeller speed ( $N$ ) and the eddy disintegration time scale ( $\tau_s$ ) and the time needed by a fluid element to flow from the feed pipe to a certain axial distance below the feed pipe is proportional to  $N^{-1}$ .

Figures 11a-d show the comparison between measured and predicted inertial-convective concentration variances for impeller speeds of 3 and 4 Hz at four axial distances below the feed pipe. To calculate these concentration variances, the values 2 and 0.7 have been used for the constant in the production of the concentration variance ( $C_{g1}$ ). As shown in Figures 11a-d, large deviations between calculated and measured concentration variances are obtained when the value for  $C_{g1}$  as proposed in the literature (i.e. equal to 2) is used. Therefore, a value for  $C_{g1}$  equal to 0.7 has been determined by optimizing the agreement between the measured and calculated concentration variance profiles. The calculated concentration variances with  $C_{g1}=0.7$  appear to be in reasonable agreement with the experimental values.





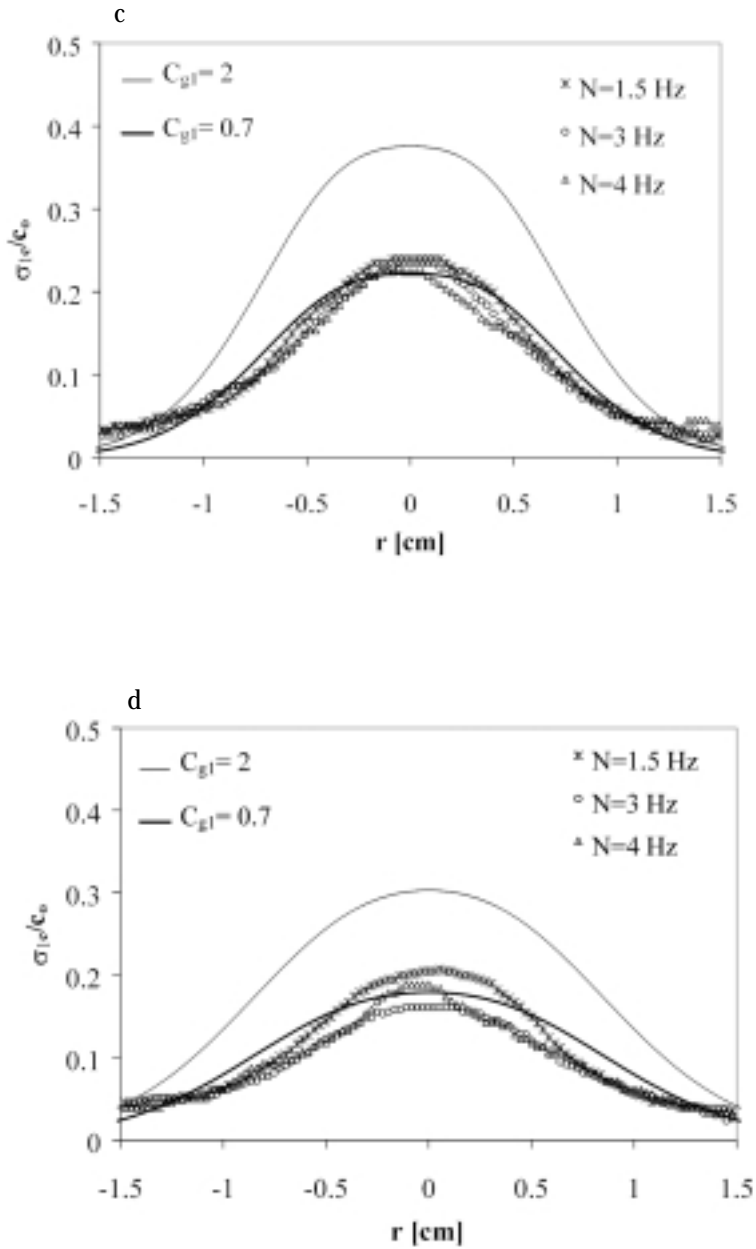


Figure 11: Measured inertial-convective concentration variance profiles for a stirrer speed of 1.5, 3 and 4 Hz and predicted inertial-convective concentration variance profiles for a stirrer speed of 3 and 4 Hz at different axial distances below the feed pipe ( $z$ ).

a)  $z=0.005$  m b)  $z=0.015$  m c)  $z=0.03$  m and d)  $z=0.04$  m

## 5. Conclusions and application of the main results

The Planar Laser Induced Fluorescence technique has been successfully used to measure the mean concentration and inertial-convective concentration variance component of an passive tracer fed to a stirred tank reactor.

For the experimental conditions used, the concentration length scales are smaller than the length scales of the turbulent flow field. Under these circumstances, the characteristic length scale and the corresponding constant to be used in the turbulent dispersion coefficient are not known from literature. In this study, the characteristic length scale is estimated with the radius of the feed stream. A value of 0.1 for the constant in the turbulent dispersion coefficient has been obtained by optimizing the agreement between measured and predicted mean concentrations. When using this length scale and constant A, reasonably good correspondence between the measured and calculated mean concentrations is obtained.

The turbulent mixer model, used to calculate the concentration variance, requires adjustment of the constant in the production of concentration variance ( $C_{g1}$ ) to obtain a reasonable agreement between the measured and predicted concentration variances. With  $C_{g1} = 0.7$ , the turbulent mixer model reasonably predicts the main features of the inertial-convective component of the concentration variance.

The presumed Probability Density Function (PDF) method proposed by Baldyga (1994) enables the calculation of the yield of isothermal single reactions and pairs of reactions from mean concentrations and concentration variances of an passive tracer. This method has been extended to apply to reactions schemes with an arbitrary number of steps, any number of reactants and any reaction order or speed by the Performance Fluid Dynamics Company (Dublin, Ireland). This PDF method in combination with models from literature describing the mean concentration and concentration variance of an passive tracer including the model refinements proposed in this study can be used to calculate the selectivity of mixing sensitive reactions in stirred tank reactors.

To calculate mean concentrations and concentration variances of an passive tracer with the models used in this study, information is required about local energy dissipation

rates, velocity length scales and velocities. A combination between information about these hydrodynamic parameters and the models for the mean concentration and concentration variance can be used to study the effect of several process and design variables on the mixing rate.

## Nomenclature

$A$	constant in the turbulent dispersion coefficient	[-]
$c$	instantaneous concentration	[mol m <sup>-3</sup> ]
$\bar{c}$	mean concentration	[mol m <sup>-3</sup> ]
$c'$	fluctuating concentration	[mol m <sup>-3</sup> ]
$C$	constant in the equation for the scalar length scale	[-]
$C_{g1}$	constant in the production of concentration variance	[-]
$C_{u_i u_i}$	autocovariance of the velocity fluctuations	[m <sup>2</sup> s <sup>2</sup> ]
$D_{im}$	impeller diameter	[m]
$D_m$	molecular diffusion coefficient	[m <sup>2</sup> s <sup>-1</sup> ]
$D_T$	turbulent dispersion coefficient	[m <sup>2</sup> s <sup>-1</sup> ]
$E$	engulfment rate	[s <sup>-1</sup> ]
$E_i(f)$	energy spectrum	[m <sup>2</sup> s <sup>-1</sup> ]
$f$	frequency	[s <sup>-1</sup> ]
$G$	instantaneous gray value	[-]
$\bar{G}$	average gray value	[-]
$G_m$	molecular diffusion rate	[s <sup>-1</sup> ]
$k$	turbulent kinetic energy	[m <sup>2</sup> s <sup>-2</sup> ]
$k_R$	second order reaction rate constant	[m <sup>3</sup> mol <sup>-1</sup> s <sup>-1</sup> ]
$l_k$	Kolmogorov length scale	[m]
$L$	scalar length scale	[m]
$L_c$	integral concentration length scale	[m]
$L_v$	integral velocity length scale	[m]
$N$	impeller speed	[s <sup>-1</sup> ]
$N_e$	number of images	[-]
$N_p$	power number	[-]
$N_q$	pumping capacity	[-]
$Q_{feed}$	volumetric feed flow rate	[m <sup>3</sup> s <sup>-1</sup> ]
$r$	radius of a feed stream	[m]
$r_c$	circulation ratio	[-]
$R_p$	production rate of concentration variance	[mol <sup>2</sup> m <sup>-6</sup> s <sup>-1</sup> ]
$R_D$	dissipation rate of concentration variance	[mol <sup>2</sup> m <sup>-6</sup> s <sup>-1</sup> ]
$r_0$	initial radius of a feed stream	[m]

Sc	Schmidt number ( $\nu/D_m$ )	[-]
t	time	[s]
$t_c$	circulation time	[s]
T	vessel diameter	[m]
$T_i$	integral time scale for direction i	[s]
$T_L$	Lagrangian time scale	[s]
$T_v$	integral velocity time scale	[s]
u	instantaneous velocity	[m s <sup>-1</sup> ]
$\bar{u}$	mean velocity	[m s <sup>-1</sup> ]
u'	fluctuating velocity	[m s <sup>-1</sup> ]
$\overline{u'^2}$	mean square fluctuating velocity	[m <sup>2</sup> s <sup>-2</sup> ]
u( $\lambda$ )	characteristic velocity of a turbulent motion	[m s <sup>-1</sup> ]
$\bar{u}_c$	local circulation velocity	[m s <sup>-1</sup> ]
$v_{\text{feed}}$	feed velocity	[m s <sup>-1</sup> ]
$V_{\text{reactor}}$	reactor volume	[m <sup>3</sup> ]
x	space coordinate	[m]
z	axial coordinate	[m]
$\varepsilon$	energy dissipation rate	[m <sup>2</sup> s <sup>-3</sup> ]
$\bar{\varepsilon}$	average energy dissipation rate	[m <sup>2</sup> s <sup>-3</sup> ]
$\eta$	transit time weighting factor	[-]
$\lambda$	characteristic length scale for turbulent dispersion	[m]
$\sigma^2$	concentration variance	[mol <sup>2</sup> m <sup>-6</sup> ]
$\tau_s$	eddy disintegration time scale	[s]
$\nu$	kinematic viscosity	[m <sup>2</sup> s <sup>-1</sup> ]

#### subscripts

B	background value
$c_{\text{hom}}$	value for a homogeneous tracer solution
i	direction
ax	axial
rad	radial
SH	sample hold
tan	tangential

0	initial value
1	value of variable in the inertial-convective subrange of wave-numbers
2	value of variable in the viscous-convective subrange of wave-numbers
3	value of variable in the viscous-diffusive subrange of wave-numbers

## Nomenclature

*Adrian, R. J., and C. S. Yao "Power spectra of fluid velocities measured by Laser Doppler Velocimetry", Exp. in Fluids 5, 17 (1987)*

*Baldyga, J., "A closure model for homogeneous chemical reactions", Chem. Eng. Sci., 49, 1985 (1994)*

*Baldyga, J. "Turbulent mixer model with application to homogeneous, instantaneous, chemical reactions", Chem. Eng. Sci. 44, 1175 (1989)*

*Baldyga, J., J. R. Bourne, and S. J. Hearn "Interaction between chemical reactions and mixing on various scales", Chem. Eng. Sci. 52, 457 (1997)*

*Baldyga, J., and M. Henczka "Turbulent mixing and parallel chemical reactions in a pipe application of a closure model", Proc. of the Ninth Europ. Conf. on Mixing 11 (51), 341, Paris (1997)*

*Baldyga, J., and R. Pohorecki "Turbulent micromixing in chemical reactors. a review", Chem. Eng. J. 58, 183 (1995)*

*Baldyga, J., and S. Rohani "Micromixing described in terms of inertial-convective disintegration of large eddies and viscous-convective interactions among small eddies", Chem. Eng. Sci. 42, 2597 (1987)*

*Corrsin, S. "Isotropic turbulent mixer", A.I.Ch.E. J. 10, 870 (1964)*

*Fox, R. O. "Computational methods for turbulent reacting flows in the chemical process industry", Revue de l'Institut Français du Pétrole 51, 215 (1996)*

*Fields, S.D. and Ottino, J.M. "Effect of segregation on the course of unpremixed polymerization" A.I.Ch.E.J., 33, 959 (1987)*

*Franke, J. and A. Mersmann "The influence of the operation conditions on the precipitation process", Chem. Eng. Sci., 50, 1737 (1995)*

*Hannon, J., S. Hearn, L. Marshall, and W. Zhou "Assessment of CFD approaches to predicting fast chemical reactions", A.I.Ch.E. 1998 Annual Meeting "Chemical and Biological Reactors" (1998)*

Hinze, J., "Turbulence", 2nd ed., Mc Graw-Hill, Inc., New York (1975)

Houcine, I., E. Plasari, R. David, and J. Villiermaux "Feedstream jet intermittency phenomenon in a continuous stirred tank reactor", *Chem. Eng. J.* 72, 19 (1999)

Houcine, I., H. Vivier, E. Plasari, R. David, and J. Villiermaux "Planar Laser Induced Fluorescence technique for measurement of concentration fields in continuous stirred tank reactors", *Exp. in Fluids* 22, 95 (1996)

Jeurissen, F., J. G. Wijers, and D. Thoenes "Initial mixing of feed streams in agitated vessels", *I.Chem.E. Symp. Series* 136, 235 (1994)

Kusters, K. A. "The influence of turbulence on the aggregation of small particles in agitated vessels", *Ph.D. thesis, Eindhoven University of Technology, The Netherlands* (1991)

Larsson, G., S. George, and S.O. Enfors "Scale-down reactor model to simulate insufficient mixing conditions during fed batch operation using a biological test system", *A.I.Ch.E. Symp. Series*, 293, 151 (1992)

Lesieur, M., "Turbulence in fluids: Stochastic and numerical modeling", *Kluwer Academic Publishers, Dordrecht* (1990)

Lozano, I., I. van Cruyningen, P. Danehy, R. K. and Hanson "Planar Laser Induced Scalar Measurements in a turbulent jet", *Applications of Laser Techniques to Fluid Mechanics*, R. J. Adrian, D. F. G. Durao, and F. Durst, (eds), Springer, 19 (1986)

Paul, E. L., J. Mahadevan, J. Foster, and M. Kennedy Midler "The effect of mixing on scale-up of a parallel reaction system", *Chem. Eng. Sci.* 47, 2837 (1992)

Rosensweig, R. F. "Idealized theory for turbulent mixing in vessels", *A.I.Ch.E. J.* 10, 91 (1964)

Schoenmakers, J. H. A. "Turbulent feed stream mixing in agitated vessels", *Ph.D. Thesis, Eindhoven University of Technology, The Netherlands* (1998)

Schoenmakers, J. H. A., J. G. Wijers, and D. Thoenes "Determination of feed stream mixing rates in agitated vessels", *Proc. 8th Europ. Mix. Conf. (Paris): Récent Progrès en Génie des Procédés* 11(52), ed. Lavoisier, 185 (1997)

Spalding, D. B. "Concentration fluctuations in a round turbulent free jet", *Chem. Eng. Sci.* 26, 95 (1971)

Tennekes, H. and J. L. Lumley, "A First Course in Turbulence", MIT Press, Cambridge (1972)





# LARGE-SCALE OSCILLATIONS OF A FEED STREAM INSIDE A STIRRED TANK REACTOR

## Abstract

Recent studies presented in the literature have shown feed streams inside stirred tank reactors to oscillate. When multiple feed points are used these oscillations can cause feed streams to overlap. The objective of this study is to determine a description for the oscillations that can be used to prevent the feed streams to overlap. The oscillations are analyzed by determining the displacements of the centres-of-mass of a feed stream in radial cross-sections. The growth of the root-mean-square radius of these displacements with time is shown to be linear, which corresponds to the “initial growth stage”. The growth rate of the root-mean-square radius with time proved to be equal to the velocity fluctuations related to turbulent motions with a size larger than the diameter of the feed stream. This indicates that these large-scale turbulent motions are responsible for the large-scale oscillations. With the obtained description for the root-mean-square radius, the minimal distance between two feed pipes necessary to prevent the overlap of the feed streams can be calculated.

*This chapter has been submitted for publication as I.L.M. Verschuren, J.G. Wijers and J.T.F. Keurentjes “Large-scale Oscillations of a feed stream inside a stirred tank reactor”*

## 1. Introduction

Stirred tank reactors with a feed stream are frequently used in the chemical and biochemical industry. When the reaction is slow compared to the mixing process, the feed stream will be homogeneously mixed before reaction takes place and the product distribution will only depend on the chemical kinetics. However, when the time scale for reaction is of the same order of magnitude as the time scale for mixing, the selectivity of a process of competitive reactions will depend on the mixing rate (Rys, 1992).

Because mixing has a large influence on the product quality of fast competitive reactions, various models for feed stream mixing inside stirred tank reactors have been proposed in the literature and feed stream mixing has been the subject of numerous experimental studies. The more recent studies have shown feed streams inside stirred tank reactors to oscillate (Houcine et al., 1999; Schoenmakers et al., 1997). The mixing models proposed in the literature do not take into account these large-scale oscillations. This is because, generally, the mixing of one feed stream with homogeneous bulk liquid is investigated (e.g. Baldyga et al., 1993; Verschuren et al., 2001). Under these circumstances large-scale oscillations of a feed stream will have no effect on the mixing rate.

A method to optimize the selectivity of mixing sensitive reactions is to use sufficiently low feed flow rates so that the selectivity is controlled by micromixing (Baldyga and Bourne, 1999). By increasing the number of feed points the feed flow rate can be decreased without decreasing productivity, provided that the feed points are located at hydrodynamically equivalent positions and the feed streams do not overlap (Baldyga and Bourne, 1999). When the feed points are located closely together the large-scale oscillations of the feed streams can cause the feed streams to come in contact with each other. The objective of this study is to determine a description that can be used to calculate the minimal distance between feed points necessary to prevent feed streams to overlap.

## 2. Theory

Generally, the diameter of the feed stream inside a stirred tank reactor is much smaller than the length scale of the largest turbulent motions. When this is the case, the feed stream is dispersed by turbulent motions with a size comparable to the diameter of the feed stream (Lesieur, 1990). In this study, we will verify the presumption that the larger turbulent motions, i.e. those not taking part in the dispersion process, transport the feed stream bodily, which causes the feed stream to oscillate. This presumption is founded on literature regarding mixing in the atmosphere, which also describes the spreading of a plume in the atmosphere to be the result of these two processes: the dispersion of the plume by small eddies with a size equivalent to the size of the plume and the fluctuation of the entire plume around its mean position due to large-scale turbulent motions (Blackadar, 1996).

The oscillations of a feed stream in a stirred tank reactor will be analyzed by determining the displacements of the centres-of-mass of a feed stream in radial cross-sections, as illustrated in Figure 1. The turbulent movements of the centre-of-mass of a lump of fluid can be considered as a passive marker moving in a turbulent flow field (Baldyga and Bourne, 1999).

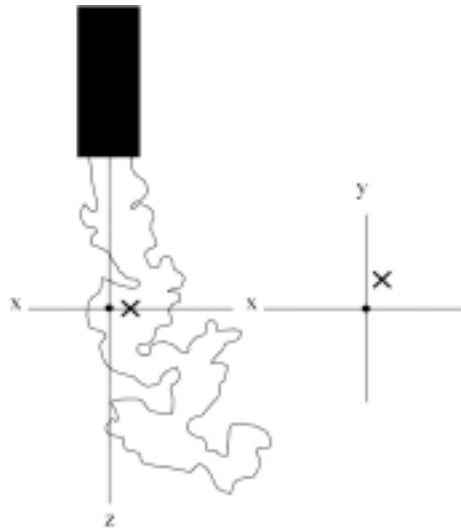


Figure 1: The centre of mass ( $\times$ ) of a radial cross-section of a feed stream.

The mean square displacement of a large number of passive markers in a stationary and homogeneous turbulent flow field without a mean velocity as a function of time ( $t$ ) is derived by Taylor (1921):

$$\overline{X^2} = 2\overline{u_i'^2} \int_0^t (t-\tau) \rho_{ii}(\tau) d\tau \quad (1)$$

with  $\overline{u_i'^2}$  is the mean square turbulent velocity fluctuation in the  $i$ -direction and  $\rho_{ii}$  is the Lagrangian two-time velocity autocorrelation coefficient. This autocorrelation coefficient is defined by:

$$\rho_{ii} = \frac{\overline{u_{i'}(t)u_{i'}(t+\tau)}}{\overline{u_{i'}^2}} \quad (2)$$

The mean square displacement can be calculated with equation (1) when the autocorrelation coefficient is known. Some known features of the autocorrelation coefficient are:

$$\rho_{ii}(\tau) = 1 \quad t \rightarrow 0 \quad (3)$$

$$\int_0^\infty \rho_{ii}(\tau) d\tau = T_L \quad t \rightarrow \infty \quad (4)$$

where  $T_L$  is the Lagrangian time scale.

Substituting equation (3) into equation (1) yields the mean square displacement for short dispersion times:

$$\overline{X^2} = \overline{u_i'^2} t^2 \quad t \rightarrow 0 \quad (5)$$

This equation shows that for short times the root-mean-square (rms) displacement is directly proportional to time, with a growth rate equal to the rms fluctuating velocity. A rms displacement directly proportional to time is marked as the “initial growth stage”. Substituting equation (4) into equation (1) yields the mean square displacement for long dispersion times:

$$\overline{X^2} = 2\overline{u_i'^2} T_L t \quad t \rightarrow \infty \quad (6)$$

From equation (6) it follows that for long dispersion times the rms displacement grows with the square root of time, which is marked as the “random walk regime”.

Consider now the mean square displacement of the centre-of-mass of a feed stream in two directions ( $\overline{X^2}$  and  $\overline{Y^2}$ ), as illustrated in Figure 1. The average position of the centres-of-mass obtained by averaging over many centres-of-mass at an axial location is used as the origin of the coordinate system. Therefore, by definition, the mean velocities  $\overline{u_x}$  and  $\overline{u_y}$  are zero. The mean square displacements in each of the two directions are described by equations (5) or (6) given above. The square radius ( $r^2$ ) of the displacements is equal to:

$$r^2 = \overline{X^2} + \overline{Y^2} = (\overline{u_x'^2} + \overline{u_y'^2}) \cdot t^2 \quad t \rightarrow 0 \quad (7)$$

$$r^2 = \overline{X^2} + \overline{Y^2} = 2T_L (\overline{u_x'^2} + \overline{u_y'^2}) \cdot t \quad t \rightarrow \infty \quad (8)$$

The displacement of a marker in the axial direction ( $z$ ) due to the action of a turbulent motion is assumed to be small compared to the displacement in this direction due to convection with the mean velocity. With this assumption the rms displacement measured at a certain distance  $z$  is equal to the rms displacement at time  $t$  with:

$$t = \int_0^z \frac{1}{u_z} dz \quad (9)$$

As derived by Taylor (1921), the rms displacement of a passive marker is a function of the velocity fluctuations related to the entire range of turbulent motions. This is to be expected because small-scale as well as large-scale turbulent motions move a passive marker in a turbulent flow field. However, only large-scale turbulent motions are assumed to move the centre-of-mass of a feed stream. When this is true, not the velocity fluctuations related to the entire range of turbulent motions, but only the velocity fluctuations related to the large-scale turbulent motions ( $\overline{u_{i,LS}^2}$ ) have to be used in equations (5) and (6) to describe the rms displacement of the centres-of-mass.

The distribution of the intensity of the velocity fluctuations over various length scales is given by the energy spectrum of a velocity signal. The one-dimensional energy spectrum is defined by:

$$\int_0^{\infty} E_v dk = \overline{u'^2} \quad (10)$$

with  $k$  being a wave number, which is proportional to the reciprocal of an eddy size. A schematic representation of an energy spectrum is given in Figure 2. This figure shows three characteristic regions: the low wave number horizontal part which corresponds to the large-scale energy containing eddies, the inertial subrange of wave numbers and the viscous subrange of wave numbers. In this study  $\overline{u'^2}_{i,LS}$  is assumed to be equal to the area below the horizontal part of the energy spectrum.

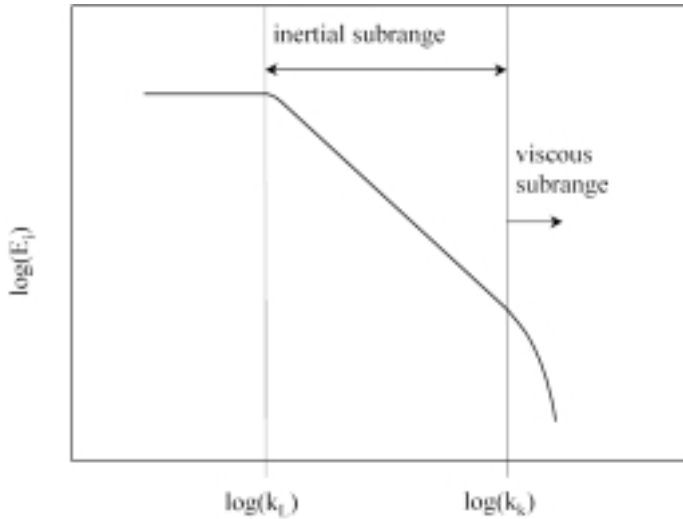


Figure 2: Schematic representation of an energy spectrum of a turbulent velocity signal.

### 3. Experimental

The centres-of-mass of a feed stream in radial cross-sections have been determined at various axial distances below the feed pipe with Planar Laser Induced Fluorescence (PLIF). The axial distance below the feed pipe has been replaced by a Lagrangian time scale, using average velocities below the feed pipe measured with Laser Doppler

Velocimetry. To calculate the rms displacements of the centres-of-mass with the equations given above, information on the turbulent velocity fluctuations needs to be available. These velocity fluctuations have been obtained from LDV-experiments. The LDV- and PLIF-measurements will be discussed in more detail below.

### 3.1 Geometry of the vessel

The geometry of the vessel used for the PLIF and LDV experiments is given in Figure 3. The vessel was made of Perspex, had a flat top and bottom and a height equal to the diameter. The internal diameter of the vessel was 0.288m. The vessel was equipped with four baffles, a feed pipe, an effluent pipe and a Rushton turbine impeller. The feed pipe internal diameter was 0.008 m. Details of the stirrer geometry are given in Figure 4.

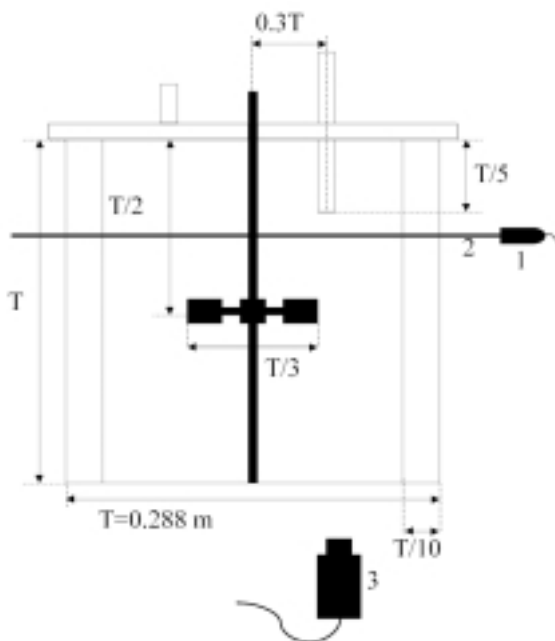


Figure 3: Geometry of the stirred vessel and the experimental set-up used for the Planar Laser Induced Fluorescence experiments, with 1. laser probe, 2. laser light sheet and 3. high speed CCD camera.

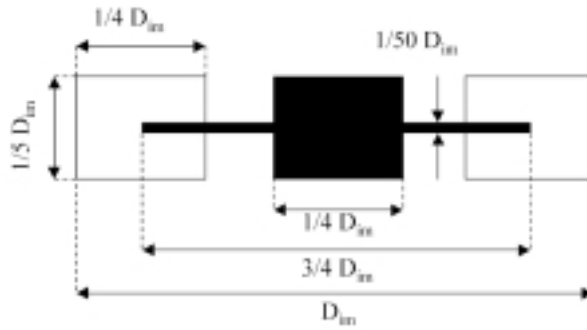


Figure 4: Details of the impeller geometry.

### 3.2 Experimental determination of the flow field characteristics

Laser Doppler Velocimetry was used to determine the local mean and fluctuating velocity. The velocities were measured with a commercial available set-up (Dantec Fiberflow system) operating with two beam pairs. The wavelengths of the laser beams were 514.5 and 488 nm, respectively. One beam of each wavelength was given a frequency shift of 40 MHz. The light source was a 2W-argon Laser (Stabilite 2017 by Spectra Physics). The measurement volume created by the intersection point of two laser beams with the same wavelength, was an ellipsoid with a diameter of about 0.15 mm and a length of about 3.2 mm. A Burst Spectrum Analyzer (Dantec) processed the velocity signals and the results were stored on a computer.

The reactor was entirely filled with water and placed in a square container also filled with water to minimize diffraction of the laser light. For seeding a small amount of dispersed polystyrene latex was used with an average particle size of 4  $\mu\text{m}$ . Radial, axial and tangential velocities were measured at 4 positions on a vertical line below the feed pipe as illustrated in Figure 5, for a stirrer speed of 3.1 Hz.

#### **Processing of velocity data acquired with LDV**

During LDV-experiments the data rate of particles with a higher velocity is higher than the data rate of particles with a lower velocity. Therefore, arithmetic averaging of the velocity signal will bias the results in favour of the higher velocities. In order to eliminate this so-called velocity bias, transit-time-weighting was applied in the calculation of the mean ( $\bar{u}_i$ ) and mean square fluctuating velocity ( $\overline{u_i'^2}$ ):



$$\bar{u}_i = \sum_{j=0}^{N-1} \eta_j u_{ij} \quad (11)$$

$$\overline{u_i^2} = \sum_{j=0}^{N-1} \eta_j (u_{ij} - \bar{u}_i)^2 \quad (12)$$

$$\eta_j = \frac{t_j}{\sum_{k=0}^{N-1} t_k} \quad (13)$$

in which  $t_j$  is the transit time of a particle crossing the measurement volume and  $u_{ij}$  is the velocity of this particle in the  $i$ -direction.

Energy spectra ( $E_i$ ) as a function of frequency ( $f$ ) were calculated from the autocovariance of the velocity fluctuations ( $C_{u_{ii}}(\tau)$ ) using Fast Fourier Transformation:

$$C_{u_{ii}}(\tau) = \lim_{T \rightarrow \infty} \frac{1}{T} \int_0^T (u_i(t) - \bar{u}_i)(u_i(t + \tau) - \bar{u}_i) dt \quad (14)$$

$$E_i(f) = 2 \int_{-\infty}^{\infty} C_{u_{ii}}(\tau) e^{-i2\pi f \tau} d\tau \quad (15)$$

The frequency is proportional to the reciprocal of an eddy lifetime. In the horizontal part and inertial-convective part of an energy spectrum, the spectrum as a function of frequency may be treated as a rearrangement of the spectrum as a function of wave number, because in these regions time scales are monotonously decreasing with wave number (Tennekes and Lumley, 1972).

To calculate an energy spectrum, discrete velocity samples have to be evenly distributed in time. To obtain evenly distributed velocity samples from the LDV-measurements, the Sample-Hold technique proposed by Adrian and Yao (1987) was used:

$$u_{SH}(t) = u(t_j) \quad t_j \leq t < t_{j+1} \quad (16)$$

### 3.3 Experimental determination of the displacements of the centres-of-mass

Planar Laser Induced Fluorescence is based on the measurement of the fluorescence intensity of a tracer excited by a laser sheet. A CCD-camera placed perpendicular to the laser sheet is used to record the fluorescence intensity and to convert the intensity into a gray value. At low tracer concentrations the relationship between the tracer concentration and gray-value is linear and the instantaneous tracer concentration at position  $x, y$  ( $C(x,y,t)$ ) follows from (Houcine et al., 1996):

$$C(x,y,t) = \frac{G(x,y,t) - \bar{G}_B(x,y)}{\bar{G}_{C_{\text{hom}}}(x,y) - \bar{G}_B(x,y)} C_{\text{hom}} \quad (17)$$

with  $G(x,y,t)$  is the local instantaneous gray value,  $\bar{G}_B(x,y)$  is the local average gray value of the background and  $\bar{G}_{C_{\text{hom}}}(x,y)$  is the local average gray value corresponding to a known tracer concentration ( $C_{\text{hom}}$ ) in a homogeneous solution.

The set-up used for the PLIF-experiments is schematically represented in Figure 3. A laser beam with a wavelength of 488 nm was formed into a sheet of 0.5 mm thickness using a cylindrical lens (Dantec 9080XO.21). The laser sheet was placed horizontally in the vessel as shown in Figure 3. Before each experiment the reactor was entirely filled with water. During an experiment a fluorescent dye solution (Fluorescein) was injected into the reactor with a velocity approximately equal to the local circulation velocity just beneath the feed pipe ( $v_{\text{feed}}=0.15\pi ND_{\text{im}}$ ). Measurements were taken at six horizontal cross-sections within the reactor. These cross-sections were located at 0.005 m, 0.015 m, 0.025 m, 0.03 m, 0.035 m and 0.04 m below the feed pipe as illustrated in Figure 5. The impeller speeds used were 1.5, 3 and 4 Hz. Accordingly, the feed flow rates were  $3.4 \cdot 10^{-6} \text{ m}^3/\text{s}$ ,  $6.8 \cdot 10^{-6} \text{ m}^3/\text{s}$  and  $9.0 \cdot 10^{-6} \text{ m}^3/\text{s}$ , respectively. A high-speed camera (JAI CV-M30) was positioned perpendicularly to the laser sheet to record images of the feed stream. During a single experiment the CCD-camera recorded 2000 images in about 20 circulation times.

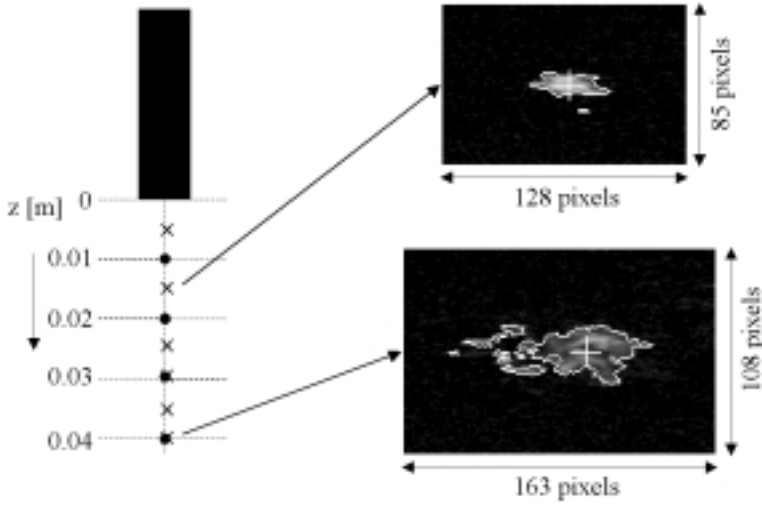


Figure 5: Measurement positions (●) used for the LDV-experiments and PLIF-experiments (×) and PLIF-images of radial cross-sections of a feed stream in a stirred tank reactor measured at a stirrer speed of 3 Hz. These images show the gray-value weighted centre-of-mass of the largest created area (+) in each image at an axial distance below the feed pipe of 0.015 m and 0.04 m, respectively.

The images acquired had a size of 752\*526 pixels. The spatial resolution of the images depended on the distance between the laser sheet and the camera. The spatial resolution in the horizontal directions was:

$$\Delta_x = -7.26 \cdot 10^{-4} z + 3.08 \cdot 10^{-4} \quad (18)$$

with  $z$  the axial distance below the feed pipe. The camera was operated in the interlaced mode, therefore, the spatial resolution in the vertical direction was  $2 \cdot \Delta_x$ .

To enable the calculation of the local instantaneous Fluorescein concentration with equation (17), the average local background gray-value and the average local gray-value of a homogeneous Fluorescein solution were determined for each experiment. The average background gray-value was obtained from 100 recorded images of the reactor filled with water. The average gray-value of a homogeneous Fluorescein solution was obtained from 100 recorded images of the reactor filled with a Fluorescein solution of known concentration.

### **Calibration of the PLIF system**

Preliminary experiments were carried out in the reactor in order to determine the range of linear response between gray value and Fluorescein concentration. In each of these experiments the reactor was filled with a Fluorescein solution of known concentration and the gray-level was determined at several positions in the tank. These experiments showed that for concentrations of Fluorescein less than  $6 \cdot 10^{-8}$  mol/l, the response of gray value to Fluorescein concentration is linear. Therefore, the experiments described above have been carried out using Fluorescein concentrations less than  $6 \cdot 10^{-8}$  mol/l.

### **Processing of data acquired with PLIF**

The centres-of-mass of the feed stream were determined for each of the recorded images. First, each gray value image was converted into a concentration image in which the gray-scale is directly related to the concentration. This was done by calculating the concentration at each pixel position with equation (17). These concentrations were normalized using the initial Fluorescein concentration of the feed liquid and images were reconstructed by assigning a gray-value to each pixel according to:

$$G = \frac{C}{C_0} 200 \quad (19)$$

From a converted image, the centre-of-mass was determined automatically using the commercially available image analysis program Optimas. This program provides algorithms for image analysis. The following sequence of algorithms was used to determine the centre-of-mass. To clearly define the areas containing feed liquid against the background in each image, the threshold function was used to set a range of values as foreground. Areas containing feed liquid were detected using the "CreateArea" function. The centre-of-mass of the feed stream was determined automatically as the gray-value-weighted centre-of-mass from the created areas. When multiple areas were present the gray-value-weighted centre-of-mass from the largest area was used. Two typical examples of PLIF images showing areas containing feed liquid and the gray-value-weighted centre-of-mass of the largest areas are given in Figure 5.

The origin of the coordinate system was taken equal to the average position of the centres-of-mass obtained by linearly averaging over the 2000 centres-of-mass per experiment. The rms radius of the displacements was calculated from the X and Y coordinates of the centres-of-mass:

$$r = \sqrt{\frac{\sum_{i=1}^n X^2}{n} + \frac{\sum_{i=1}^n Y^2}{n}} \quad (20)$$

with n is the number of images per experiment.

#### 4. Results and Discussion

Figures 6 and 7 show the mean and rms fluctuating velocities normalized to the tip speed ( $v_{tip}$ ) as a function of the axial coordinate below the feed pipe. From Figure 6 it is concluded that the average axial velocity is approximately equal to  $0.16v_{tip}$ , independent of position. Figure 7 shows the axial, radial and tangential rms fluctuating velocities to be approximately equal to  $0.05v_{tip}$ ,  $0.06v_{tip}$  and  $0.07v_{tip}$ .

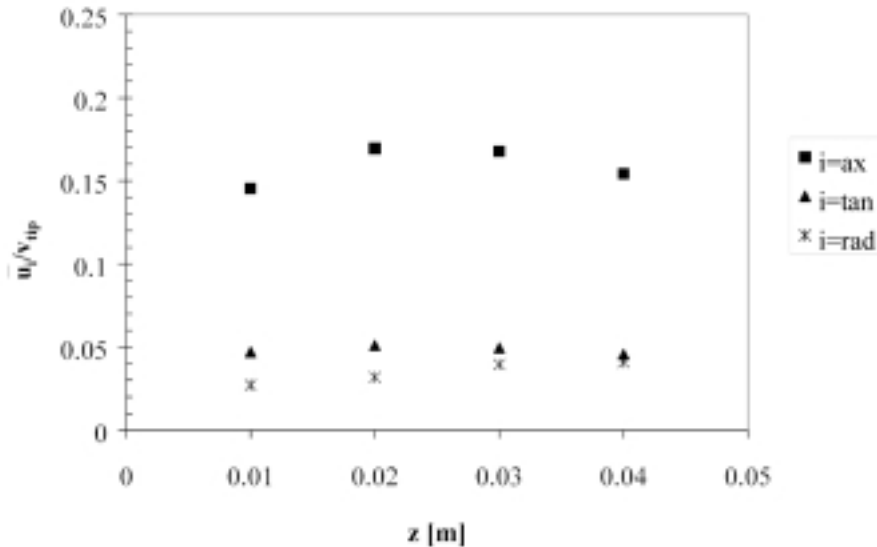


Figure 6: Axial, tangential and radial mean velocities normalized by the tip velocity as a function of the axial coordinate below the feed pipe.

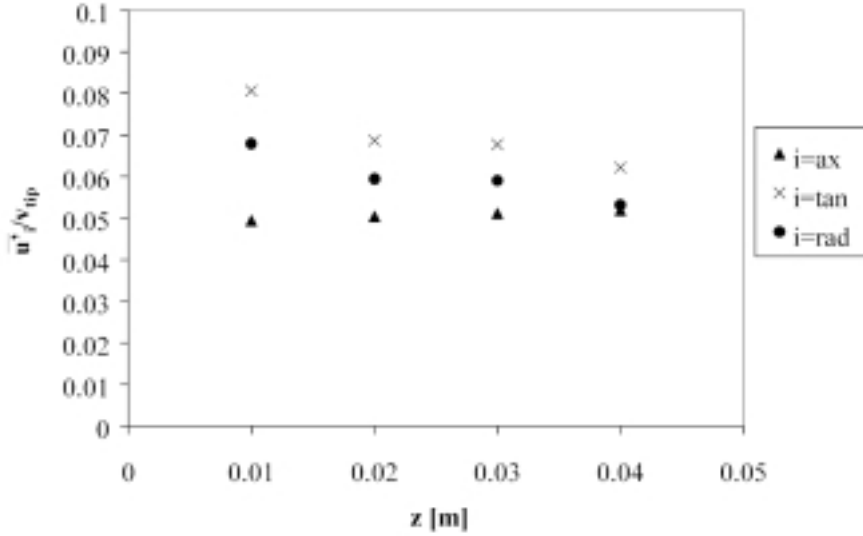


Figure 7: Axial, tangential and radial root-mean-square velocity fluctuations normalized by the tip velocity as a function of the axial coordinate below the feed pipe.

A typical example of an energy spectrum calculated from tangential velocities measured at  $z=0.05$  m below the feed pipe for a stirrer speed of 3.1 Hz is given in Figure 8. The velocity fluctuations related to the large-scale turbulent motions ( $\overline{u}_{i,LS}^2$ ) are assumed to be equal to the area below the horizontal part of an energy spectrum:

$$\overline{u}_{i,LS}^2 = \int_0^{f_h} E_{i,LS}(f) df \quad (21)$$

The value of the horizontal part of an energy spectrum ( $E_{i,LS}(f)$ ) has been approximated by the average of the points obtained in the horizontal part of an energy spectrum. A typical example of  $E_{i,LS}(f)$  is given in Figure 8 by means of a horizontal line.

The velocity fluctuations in radial and tangential direction related to the large-scale turbulent motions are given in Figure 9. From this figure it is concluded that the square root of these velocity fluctuations in both directions are approximately equal to  $0.03v_{tip}$ .

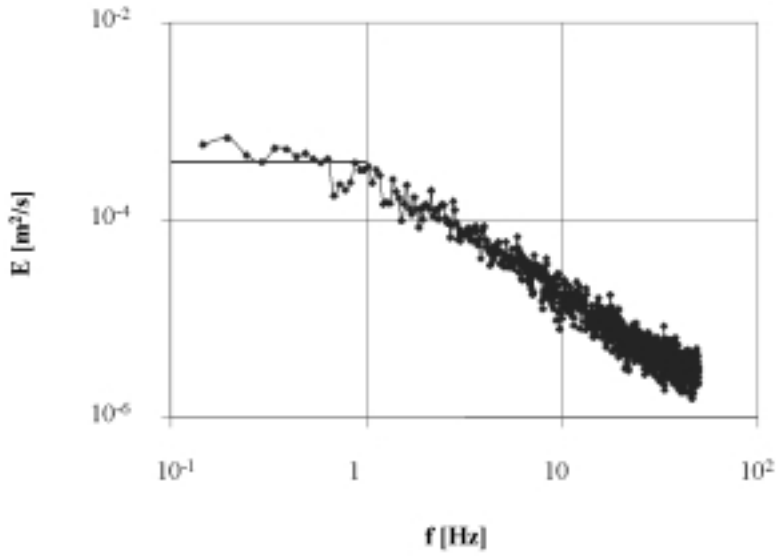


Figure 8: Energy spectrum calculated from tangential velocities measured at a distance of 0.05 m below the feed pipe and for a stirrer speed of 3 Hz.

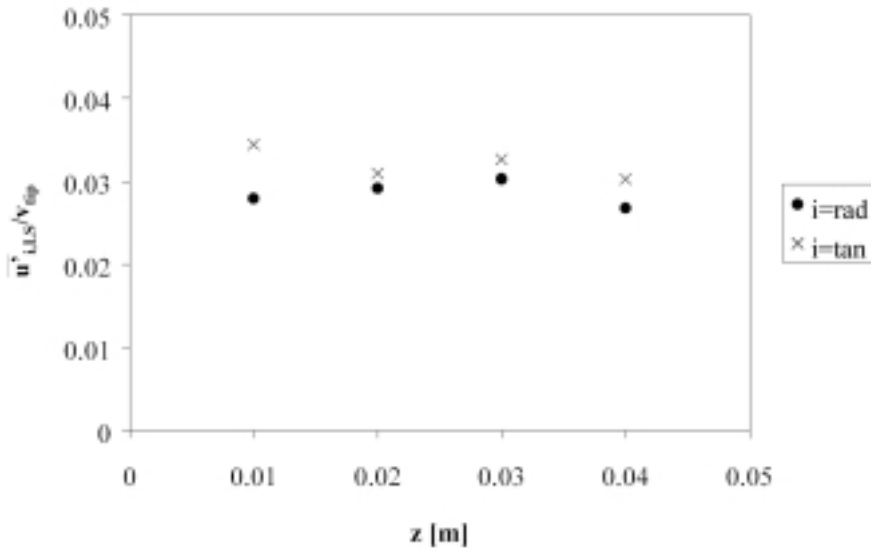
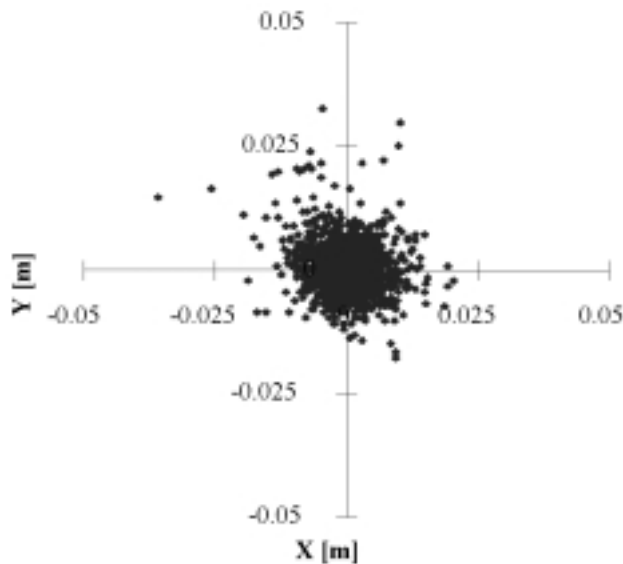


Figure 9: Velocity fluctuations related to the large-scale turbulent motions in radial and tangential direction normalized by the tip velocity as a function of the axial coordinate below the feed pipe.

The X and Y coordinates of the centres-of-mass of a feed stream in a radial cross-section at an axial distance of 0.025m below the feed pipe for a stirrer speed of 3 Hz are given in Figure 10. The rms radius of the displacements is calculated from the X and Y coordinates as given in Figure 10. In Figure 11 the rms radius of the displacements is given as a function of axial distance from the feed pipe, for stirrer speeds of 1.5, 3 and 4 Hz, respectively. In this figure no significant variation of the radius with impeller speed is observed.



*Figure 10: X and Y-coordinates of the centres-of-mass of a feed stream in a radial cross-section at 0.025 m below the feed pipe and a stirrer speed of 3 Hz.*

In Figure 12 the rms radius of the displacements is given as a function of Lagrangian time, for stirrer speeds of 1.5 Hz, 3 Hz and 4 Hz, respectively. The Lagrangian time has been calculated with equation (9) with the average axial velocity equal to  $0.16v_{tip}$ . From this figure it is concluded that the rms radius is directly proportional to time, which corresponds to the “initial growth stage”.



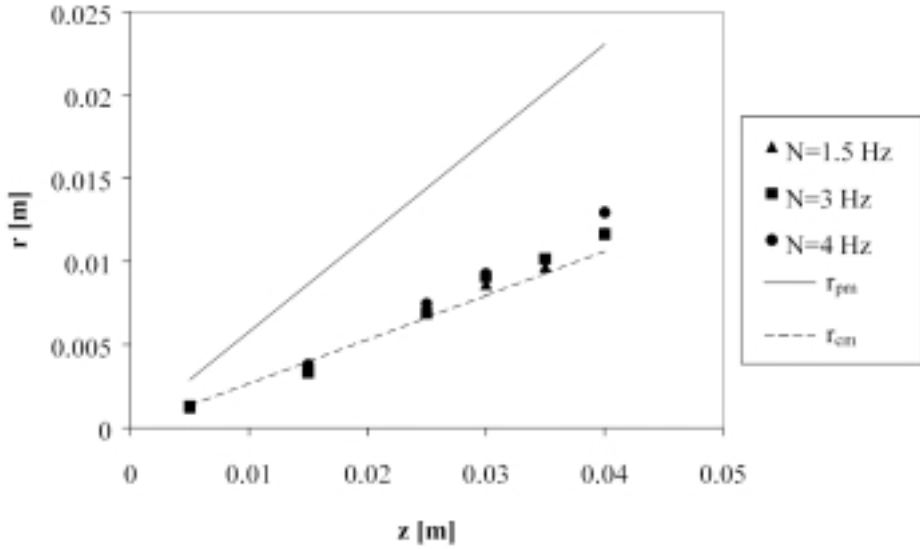


Figure 11: Measured root mean square (rms) radius of the centre-of-mass of a feed stream for stirrer speeds of 1.5, 3 and 4 Hz, calculated rms radius of the centres-of-mass of a feed stream ( $r_{cm}$ ) and calculated rms radius of a passive marker ( $r_{pm}$ ) as a function of axial distance below the feed pipe.

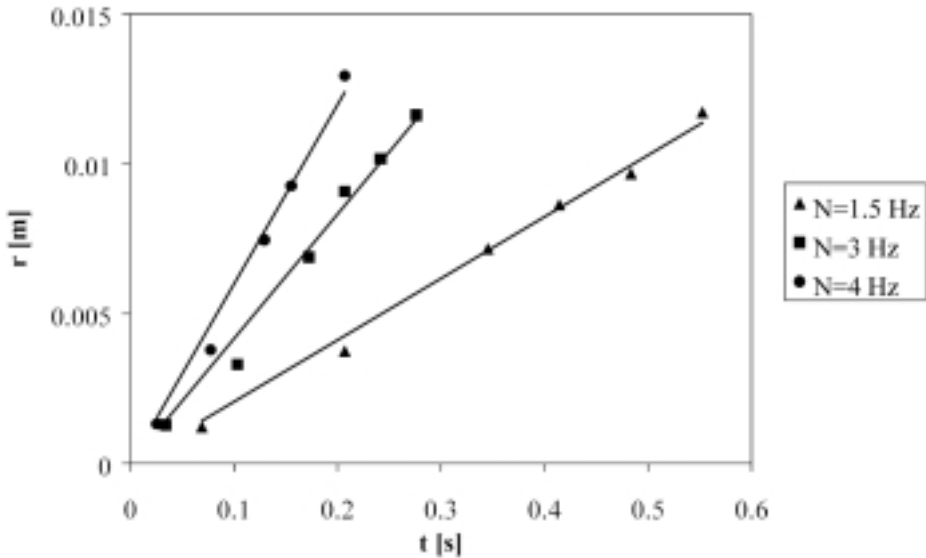


Figure 12: Root mean square radius of the centres-of-mass of a feed stream in radial cross-sections as a function of a Lagrangian time scale for a stirrer speed of 1.5 Hz, 3 Hz and 4 Hz, respectively.

The growth of the mean square radius of the displacements with time in the “initial growth stage” is given by equation (7). Substituting equation (9) for the Lagrangian time scale in equation (7), with the average velocity equal to  $0.16v_{tip}$  and the velocity fluctuations related to large-scale turbulent motions equal to  $0.03v_{tip}$ , yields the following equation for the rms radius of the displacements of the centres-of-mass ( $r_{cm}$ ):

$$r_{cm} = \sqrt{u_{rad,LS}^2 + u_{tan,LS}^2} \frac{z}{u_{ax}} = \sqrt{(0.03v_{tip})^2 + (0.03v_{tip})^2} \frac{z}{0.16v_{tip}} = 0.27z \quad (22)$$

with  $z$  is the axial distance below the feed pipe. From equation (22) follows that  $r_{cm}$  as a function of the axial distance below the feed pipe is independent of stirrer speed, which is in agreement with the results shown in Figure 11.

The rms radius of the displacements of a passive marker ( $r_{pm}$ ) depends on the total velocity fluctuations in radial and tangential direction being equal to  $0.06v_{tip}$  and  $0.07v_{tip}$ , respectively:

$$r_{pm} = \sqrt{u_{rad}^2 + u_{tan}^2} \frac{z}{u_{ax}} = \sqrt{(0.06v_{tip})^2 + (0.07v_{tip})^2} \frac{z}{0.16v_{tip}} = 0.58z \quad (23)$$

Figure 11 shows comparisons between the measured rms radius of the displacements of the centres-of-mass,  $r_{cm}$  calculated with equation (22) and  $r_{pm}$  calculated with equation (23) as a function of the axial distance below the feed pipe. This figure shows that the growth rate of  $r_{pm}$  equal to the total velocity fluctuations is much faster than the growth rate of the rms radius of the displacements of the centres-of-mass. A good agreement is obtained between the measured and calculated rms radius of the displacements of the centres-of-mass, when a growth rate is calculated with velocity fluctuations only related to large-scale turbulent motions. This supports our presumption that large-scale turbulent motions are responsible for the oscillations of a feed stream in a stirred tank reactor.

## 5. Conclusions and practical application

In this study, the increase of the root mean square radius of the displacements of the centres-of-mass of a feed stream with time is shown to be linear, which corresponds to the “initial growth stage”.

The rms radius grows as a function of time with a rate equal to root of the sum of velocity fluctuations related to large-scale turbulent motions, which are apparently responsible for the oscillations of a feed stream in a stirred tank reactor.

In practice, the obtained description for the rms radius of the displacements of the centres-of-mass as a function of time can be used to calculate the minimal distance between feed pipes necessary to prevent the feed streams to overlap. This represents an important feature for the design and scale-up of stirred tank reactors with multiple feed points.

## Nomenclature

$C$	instantaneous tracer concentration	$[\text{mol m}^{-3}]$
$C_{u_i u_i}$	autocovariance of the velocity fluctuations	$[\text{m}^2 \text{s}^{-2}]$
$D_{\text{im}}$	impeller diameter	$[\text{m}]$
$E_i$	energy spectrum	$[\text{m}^2 \text{s}^{-1}]$
$f$	frequency	$[\text{s}^{-1}]$
$G$	instantaneous gray value	$[-]$
$\bar{G}$	average gray value	$[-]$
$N$	impeller speed	$[\text{s}^{-1}]$
$N_q$	pumping capacity	$[-]$
$r$	root mean square radius of the displacements	$[\text{m}]$
$r_c$	circulation ratio	$[-]$
$t$	time	$[\text{s}]$
$t_c$	circulation time	$[\text{s}]$
$t_j$	transit time	$[\text{s}]$
$T_L$	Lagrangian time scale	$[\text{s}]$
$\bar{u}_i$	mean velocity	$[\text{m s}^{-1}]$
$u'_{iL}$	fluid velocity	$[\text{m s}^{-1}]$
$\overline{u_i'^2}$	mean square turbulent velocity fluctuations	$[\text{m}^2 \text{s}^{-2}]$
$V_{\text{reactor}}$	reactor volume	$[\text{m}^3]$
$v_{\text{tip}}$	stirrer tip speed	$[\text{m s}^{-1}]$
$X, Y$	Cartesian positions	$[\text{m}]$
$\bar{X}^2$	mean square displacement	$[\text{m}^2]$
$z$	axial distance below the feed pipe	$[\text{m}]$
$\Delta$	spatial resolution	$[\text{m}]$
$\eta_j$	transit time weighting factor	$[-]$
$\rho_{ii}$	Lagrangian two time velocity autocorrelation coefficient	$[-]$

### subscripts

ax	axial
B	background
$C_{\text{hom}}$	tracer concentration in a homogeneous solution

cm	centre-of-mass
i	coordinate direction
LS	value for the large-scale energy eddies
pm	passive marker
rad	radial
SH	sample hold
tan	tangential
x	x-direction
y	y-direction
z	z-direction
0	initial value

## References

- Adrian, R. J. and C. S. Yao "Power spectra of fluid velocities measured by laser Doppler velocimetry", Exp. In Fluids 5, 17 (1987)*
- Baldyga, J., and J.R. Bourne "Turbulent mixing and chemical reactions", John Wiley, Chichester (1999)*
- Baldyga, J., J.R. Bourne, and S.J. Hearn "Interaction between chemical reactions and mixing on various scales", Chem. Eng. Sci. 52, 457 (1997)*
- Baldyga, J., J.R. Bourne, and Yang Yang "Influence of feed pipe diameter on mesomixing in stirred tank reactors", Chem. Eng. Sci. 48, 3383 (1993)*
- Blackadar, A.K. "Turbulence and Diffusion in the Atmosphere, Lectures in environmental sciences", Springer-Verlag, Berlin Heidelberg, 129 (1996)*
- Houcine, I., E. Plasari, R. David, and J. Villermaux "Feedstream jet intermittency phenomenon in a continuous stirred tank reactor", Chem. Eng. J. 72, 19 (1999)*
- Houcine, I., H. Vivier, E. Plasari, R. David, and J. Villermaux "Planar Laser Induced Fluorescence technique for measurement of concentration fields in continuous stirred tank reactors", Exp. in Fluids 22, 95 (1996)*
- Lesieur, M. "Turbulence in fluids: Stochastic and numerical modeling", Kluwer Academic Publishers, Dordrecht (1990)*
- Rys, P. "The mixing-sensitive product distribution of chemical reactions", Chimia 46, 469 (1992)*

*Schoenmakers, J.H.A., J.G. Wijers, and D. Thoenes "Determination of feed stream mixing rates in agitated vessels", Proc. 8th Europ. Mix. Conf.: Récent Progrès en Génie des Procédés, ed. Lavoisier, 11, 52, 185 (1997)*

*Taylor, G.I. "Diffusion by continuous movements", Proc. London Math. Soc. 20, 196 (1921)*

*Tennekes, H. and J. L. Lumley, "A First Course in Turbulence", MIT Press, Cambridge (1972)*

*Verschuren, I.L.M, J.G. Wijers, and J.T.F. Keurentjes "Effect of mixing on the product quality in semi-batch stirred tank reactors", accepted for publication in A.I.Ch.E. J. (2001)*

# DETERMINATION OF THE MIXING RATE OF A HIGH VELOCITY FEED STREAM IN AGITATED VESSELS

## Abstract

In semi-batch or continuously stirred reactors, often a feed containing one or more reactants has to be mixed with the contents of the vessel. For fast competitive or consecutive reactions the mixing rate of the feed stream with the vessel contents has a large influence on the product quality. The mixing rate is often controlled by the turbulent dispersion process. Therefore, it has been suggested in the literature to keep the turbulent dispersion time constant upon scale-up to obtain a constant product quality. In this study, based on a combination of a theoretical model, Planar Laser Induced Fluorescence experiments and Laser Doppler Velocimetry experiments, the turbulent dispersion coefficient is determined. This has been done for the case that a feed stream is mixed in a stirred vessel by a combination of feed stream and stirrer generated turbulence. The turbulent dispersion coefficient is used to derive an equation for the turbulent dispersion time as function of several design and process variables.

*This chapter has been accepted for publication in Chem. Eng. Commun. as I.L.M. Verschuren, J.G. Wijers and J.T.F. Keurentjes "Determination of the mixing rate of a high velocity feed stream in agitated vessels"*

## 1. Introduction

Agitated vessels with a turbulent flow field and a feed of one or more reactants are frequently used in the chemical industry for the production of fine chemicals or pharmaceuticals. When the occurring reactions are fast relative to the mixing rate, significant reaction occurs before the feed stream is completely mixed with the vessel contents. When a fast reaction system consists of consecutive or competitive reactions, the product quality will depend on the mixing rate (Rys, 1992). Precipitation reactions are examples of feed stream mixing sensitive reaction systems. During a precipitation process nucleation takes place in the feed stream where high supersaturation levels are realized (Leeuwen, 1998). An increase in the mixing rate, at low mixing rates, will increase the supersaturation, thus increasing the amount of nucleation. A further increase of the mixing rate will decrease the supersaturation, which will reduce the amount of nucleation (Baldyga et al., 1990). Since an increase in the nucleation rate results in smaller particles and vice versa, the obtained product quality is affected by the mixing rate (Franke and Mersmann, 1995; Philips et al., 1999; Marcant and David, 1991). Another example of a mixing-sensitive process is the addition of an acid or base to a solution of an organic substrate that degrades in the presence of a low or high pH (Paul et al., 1992).

The mixing of fluids in a turbulent flow is caused by the following processes (Ranada and Bourne, 1991):

1. convection by the average velocity
2. turbulent dispersion by large scale turbulent motions
3. micromixing: mixing on a molecular scale inside small scale turbulent motions by engulfment, deformation and diffusion

For low feed rates the product distribution is controlled by micromixing, whereas, at higher feed rates the product distribution will be determined by turbulent dispersion (Baldyga and Bourne, 1992). When turbulent dispersion controls the mixing rate, scale-up with a constant turbulent dispersion time should be applied to obtain a constant product quality (Thoenes, 1994).

When the velocity of the incoming feed stream is considerably larger than the local circulation flow rate, mixing of the feed stream will be caused by the turbulence



generated by the stirrer and by the turbulence generated by the feed stream (Bourne and Hilber, 1990; Thoenes, 1994). The influence of feed stream generated turbulence on the mixing is especially important at larger scales. In the geometric scale-up of stirred reactors with an equal residence time and equal input of power per unit of mass, the feed velocity increases proportional to the vessel diameter and the circulation stream velocity increases with the cube root of the vessel diameter. In this work the time scale for turbulent dispersion is determined experimentally for a feed stream mixed in a stirred vessel by a combination of feed stream and stirrer generated turbulence. Baldyga and Bourne (1992) and Baldyga et al. (1993) have presented a mechanistic Lagrangian model for the turbulent dispersion process. From this model a time scale for turbulent dispersion is derived. For the calculation of this time scale information is needed about the turbulence characteristics inside the feed stream. In our laboratory, these turbulence characteristics have been obtained from Laser Doppler Velocimetry and Planar Laser Induced Fluorescence experiments. The main objective of this study is to provide a method for the calculation of the time scale for turbulent dispersion of a feed stream with a high velocity inside a stirred vessel.

## 2. Turbulent dispersion of a feed stream

Turbulent dispersion is the dispersion of liquids by large-scale turbulent motions. In this paper the turbulent dispersion of a continuous feed stream in a stirred tank is considered. The flow is assumed to be steady and the fluid density constant. Only radial dispersion is assumed, because in a continuous feed stream, the concentration gradients in the radial direction are much larger than the concentration gradients in the direction of the flow. Baldyga and Bourne (1992) and Baldyga et al. (1993) use Fick's second law to describe the mixing of a feed stream by radial dispersion:

$$\frac{dC}{dt} = D_t \left( \frac{d^2 C}{dr^2} + \frac{1}{r} \frac{dC}{dr} \right) \quad (1)$$

in which  $C$  is the local concentration,  $t$  is time,  $r$  is a radial coordinate and  $D_t$  is the turbulent dispersion coefficient. The solution of equation (1) depends on the initial length scale of the feed stream ( $L_d$ ). The feed pipe is a local finite source if  $L_d$  is smaller than the scale of the system and if the feed pipe radius ( $a$ ) is of the same magnitude or

larger than  $L_d$ . The solution of equation (1) for a local cylindrical finite source and a constant dispersion coefficient (Crank, 1975) is:

$$C(r,t) = \frac{C_0}{2D_t} \exp\left(-\frac{r^2}{4D_t t}\right) \int_0^a \exp\left(-\frac{r'^2}{4D_t t}\right) I_0\left(\frac{rr'}{2D_t t}\right) r' dr' \quad (2)$$

where  $I_0$  is the modified Bessel function of the first kind of order zero. The concentration profile due to turbulent dispersion at the centreline of the jet can be calculated from equation (2):

$$\frac{C}{C_0} = 1 - \exp\left(-\frac{a^2}{4D_t t}\right) \quad (3)$$

The characteristic time scale for turbulent dispersion ( $\tau_{td}$ ) is equal to the time where the relative concentration on the centreline of the feed stream has reached a certain value ( $C_{td}/C_0$ ). The characteristic time scale for turbulent dispersion follows from equation (3):

$$\tau_{td} = \frac{-1}{4 \ln(1 - C_{td}/C_0)} \frac{a^2}{D_t} \quad (4)$$

Feed streams inside stirred tank reactors have been found to oscillate with a period of several seconds (Schoenmakers et al., 1997; Houcine et al., 1999). It must be emphasized that the turbulent dispersion model does not describe these oscillations. In this study the mixing of one feed stream with homogeneous bulk liquid is investigated, therefore, oscillation of the feed stream will have no effect on the mixing rate. However, care should be taken when applying equations (1) to (4), in a double-feed stirred tank reactor, where oscillations of the feed streams can cause regions of high concentrations of reactants to come in contact with each other.

To calculate the turbulent dispersion time with equation (4) the turbulent dispersion coefficient has to be known. The turbulent dispersion coefficient characterizes the spreading of a feed stream by a turbulent motion. The spreading of a fluid element by a turbulent motion is visualized in Figure 1. As shown in this figure the turbulent dispersion coefficient depends on the velocity of the eddies and the length scale of the eddies taking part in the turbulent dispersion process. The dispersion coefficient is given by (Tennekes and Lumley, 1972):

$$D_t = \alpha \cdot \lambda \cdot u(\lambda) \quad (5)$$

assuming the length scales and the velocities of the eddies to be described by a single characteristic length scale ( $\lambda$ ) and characteristic velocity ( $u(\lambda)$ ), respectively.

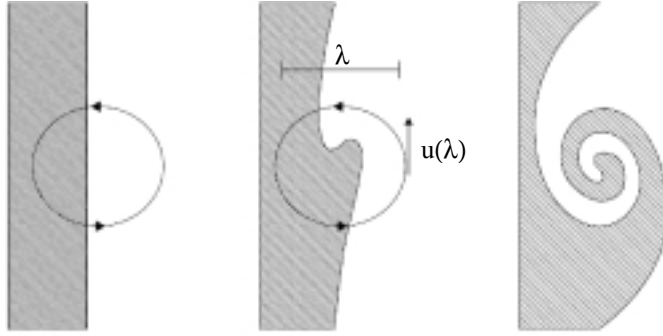


Figure 1: Generalized picture of the spreading of a fluid element by a turbulent motion.

The characteristic length scale for turbulent dispersion ( $\lambda$ ) is equal to the length scale of the concentration fluctuations ( $L_c$ ) when the length scale of the concentration fluctuations is of the same magnitude or smaller than the length scale of the velocity fluctuations ( $L_v$ ). The characteristic length scale is equal to the length scale of the velocity fluctuations when  $L_c$  is larger than  $L_v$  (Lesieur, 1990).

The characteristic velocity of a turbulent motion is given by (Tennekes and Lumley, 1972):

$$u(n) = (n \cdot E(n))^{1/2} \quad (6)$$

in which  $n$  is the wavenumber of a turbulent motion and  $E(n)$  is the energy spectrum. The wave number of a turbulent motion with a length scale equal to  $\lambda$  is  $2\pi/\lambda$ . The energy spectrum for large scale turbulent motions causing turbulent dispersion (Tennekes and Lumley, 1972) is:

$$E(n) = 1.5 \cdot \varepsilon^{2/3} \cdot n^{-5/3} \quad (7)$$

where  $\varepsilon$  is the energy dissipation rate.

Substituting equation (6) and (7) in equation (5) leads to the following equation for the turbulent dispersion coefficient:

$$D_t = A \cdot \varepsilon^{1/3} \cdot L_v^{2/3} \quad (8)$$

with A being a constant, equal to  $\alpha(2\pi)^{-1/3}(1.5)^{1/2}$ .

To calculate the dispersion coefficient with equation (8) the characteristic length scale for turbulent dispersion and the energy dissipation rate have to be known. The energy dissipation rate is related to the turbulent kinetic energy (k) and the length scale of the velocity fluctuations ( $L_v$ ) by:

$$\varepsilon = \beta \frac{k^{3/2}}{L_v} \quad (9)$$

in which  $\beta$  is a constant, equal to unity (Kusters, 1991).

The turbulent kinetic energy and the length scale of the velocity fluctuations are measured with Laser Doppler Velocimetry. The diameters of the feed pipes used for the experiments were much smaller than the length scale of the velocity fluctuations. Therefore, the length scale of the concentration fluctuations will be smaller than the length scale of the velocity fluctuations and the characteristic length scale for turbulent dispersion will be equal to the length scale of the concentration fluctuations. The characteristic length scale for turbulent dispersion is determined from the size of the large-scale structures visible in the pictures of the feed stream taken with Planar Laser Induced Fluorescence. The measured turbulent kinetic energy, the length scale of the velocity fluctuations and the characteristic length scale for turbulent dispersion are used to derive an equation for the turbulent dispersion time as function of several design and process variables. Turbulent dispersion times are also determined from concentration profiles measured with PLIF, in which the length scale is replaced by a Lagrangian time with the velocity measured with LDV. These measured turbulent dispersion times are used to verify the equation for the turbulent dispersion time.

### 3. Experimental

#### 3.1 Determination of the turbulent kinetic energy and the length scale of the velocity fluctuations

Laser Doppler Velocimetry (LDV) experiments were performed in stirred tanks of different sizes (19, 44, 196, 400 l, respectively), shown schematically in Figure 2. A commercially available set-up (Dantec, Denmark) was used, consisting of a 2W-argon laser, a 2D-laser probe with fibre optics, photomultipliers and Burst Spectrum Analyzers. The wavelengths of the laser beams were 514.5 and 488 nm, respectively. The focal length was 400 mm and the beam separation was 38 mm. The measurement volume, created by the intersection of two laser beams, was an ellipsoid with a diameter of about 0.15 mm and a length of about 3 mm. The vessels were made of perspex and had a flat bottom and top. The stirrer was a standard six-bladed Rushton turbine impeller, shown schematically in Figure 3. The position of the feed pipe is given in Figure 2. The vessels were entirely filled with water and placed in square containers of glass, also filled with water to reduce diffraction of the laser light. For seeding an in-house produced polystyrene latex was used with an average particle size of 4  $\mu\text{m}$ . The LDV measurements were performed at ten positions on a vertical line below the feed pipe. Three orthogonal velocity components were measured in each grid point. For the determination of one single velocity component 30000 velocity samples were used, acquired with an average rate of 0.3 kHz. For each vessel size studied, the impeller speed, feed velocity and feed pipe diameter were varied. The inner diameters of the feed pipes are given in Table 1. The wall thickness of these feed pipes was approximately equal to 1 mm.

Table 1: Inner diameters of the feed pipes

$V_{\text{vessel}}$ [L]	feed pipe diameters [mm]		
19	8	6	4
44	6		
196	12		
400	23	16	

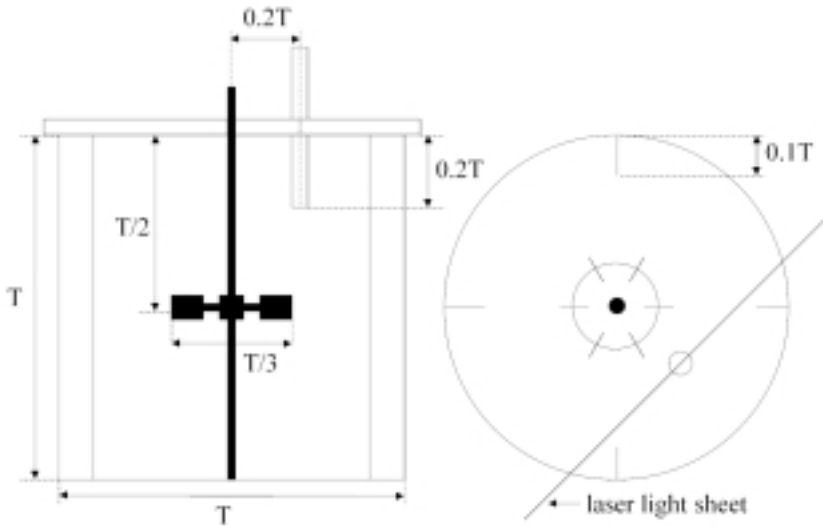


Figure 2: Geometry of the vessels used for the LDV and the PLIF experiments.

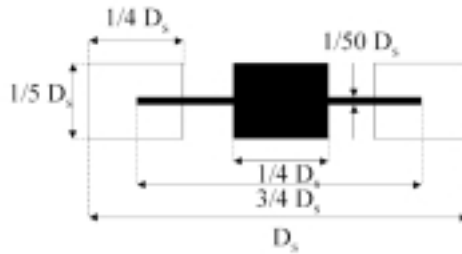


Figure 3: Geometry of the Rushton turbine stirrer used in this study.

During LDV-experiments the data rate of particles with a higher velocity is higher than the data rate of particles with a lower velocity. Therefore, inter arrival time weighting was applied in the calculation of the average velocity ( $U_i$ ) and fluctuating velocity ( $u'_i$ ) (Barnett and Bentley, 1979):

$$U_i = \frac{\sum_{j=1}^M u_i(j) \Delta t(j)}{\sum_{j=1}^M \Delta t(j)} \quad (10)$$

$$u_i'^2 = \frac{\sum_{j=1}^M (u_i(j) - U_i)^2 \Delta t(j)}{\sum_{j=1}^M \Delta t(j)} \quad (11)$$

in which  $u_i(j)$  is the velocity of particle  $j$  in the  $i$  direction,  $\Delta t(j)$  is the time between the arrival times of particle  $j$  and  $j+1$  and  $M$  is the total number of velocity measurements. The LDV measurements were performed at data rates  $(N) N \cdot T_i > 5$ , necessary to make inter arrival time weighting effective (Kusters et al., 1990).

The turbulent kinetic energy ( $k$ ) was calculated from the fluctuating velocities ( $u_i'$ ) in the three orthogonal directions:

$$k = 1/2 \sum_{i=1}^3 u_i'^2 \quad (12)$$

The integral length scale of the velocity fluctuations was calculated from the integral time scales ( $T_i$ ) using Taylor's hypothesis:

$$L_v = \left( \sum_{i=1}^3 U_i^2 \right)^{1/2} \sum_{i=1}^3 T_i \quad (13)$$

with  $U_i$  as the average velocity. The integral time scales were calculated from the energy spectrum of the velocity fluctuations (Mujumdar et al., 1970):

$$T_i = \frac{1}{4u_i'^2} \lim_{f \rightarrow 0} E_i(f) \quad (14)$$

The energy spectrum was calculated from the autocovariance of the velocity fluctuations ( $C_{u_i u_i}(\tau)$ ) using Fast Fourier Transformation (FFT):

$$C_{u_i u_i}(\tau) = \lim_{T \rightarrow \infty} \frac{1}{T} \int_0^T (u_i(t) - U_i)(u_i(t + \tau) - U_i) dt \quad (15)$$

$$E_i(f) = 4 \int_0^{\infty} C_{u_i u_i}(\tau) e^{-2\pi f \tau} d\tau \quad (16)$$

To calculate the energy spectrum, the discrete velocity samples have to be evenly distributed in time. To obtain evenly distributed velocity samples from the LDV-measurements, the

Sample-Hold technique proposed by Adrian and Yao (1987) was used. The integral time scale was approximated from the average of the first points obtained in the horizontal part of the energy spectrum (Schoenmakers et al., 1997).

### 3.2 Determination of the characteristic length scale for turbulent dispersion and the turbulent dispersion time

The local concentration field of a feed stream in an agitated vessel was measured using Planar Laser Induced Fluorescence (PLIF). The PLIF experiments were performed in the same vessels as used for the LDV experiments. A laser sheet with a thickness of 0.5 mm and uniform intensity was generated from a laser beam with a wavelength of 476.5 nm with a cylindrical lens (Dantec 9080XO.21). The laser sheet was placed in the vessel as shown in Figure 2. A fluorescent dye (disodium fluorescein) was added to the feed in such a low concentration (5  $\mu\text{mol/l}$ ) that the intensity of the fluorescence was linearly dependent on the concentration of the dye. A high speed CCD camera (JAI CV-M30) positioned perpendicularly to the laser sheet was used to record images of the feed stream and to convert the intensity of the fluorescent light into a grey level. The images acquired had a size of 216 \* 216 pixels. The spatial resolution ( $\Delta x$ ) of the pixels depended on the vessel size as given in Table 2. During a single experiment the CCD camera recorded 685 images in 11.4 seconds. The 685 images per PLIF experiment were averaged to obtain a time-averaged image. During the PLIF-experiments described in this paper, visual observations of the feed stream showed a periodic oscillation of the feed stream with an average frequency significantly lower than the stirrer frequency. As described above these oscillations are not included in the turbulent dispersion model. Therefore, in order to avoid overestimation of the turbulent dispersion rate due to these oscillations, every instantaneous image was corrected by assuming that for each line at a certain axial position the centre of the mass was located at the centreline of the feed stream (Lozano et al., 1986; Schoenmakers et al., 1997). PLIF-experiments with a horizontal laser sheet showed that the oscillations usually occurred in the vertical plane in which the laser sheet was placed. The conservation of mass was determined in the time-averaged images and showed to be valid within a few percent. These results showed that the oscillation of the feed stream out of the plane of measurement was not significant.



Table 2: Spatial resolution of the PLIF-experiments

$V_{\text{vessel}}$ [L]	$\Delta x$ [mm]
19	0.4
44	0.5
196	0.9
400	1.1

The characteristic length scale for turbulent dispersion was determined from the instantaneous images. Normalized averaged concentration profiles at the centreline of the feed stream were derived from the time-averaged pictures. The length coordinate in the concentration profiles was replaced by a Lagrangian time scale with the time-averaged velocity measured with LDV. The turbulent dispersion time was taken equal to the time where the relative concentration on the centreline of the feed stream had reached an arbitrary chosen value of 0.091 (dilution 1 to 10). This time was determined from the measured averaged concentration profiles at the centreline of the feed stream.

## 4. Results and Discussion

### 4.1 Turbulent kinetic energy, length scale of the velocity fluctuations and the characteristic length scale for turbulent dispersion

Typical values for the turbulent kinetic energy measured with LDV are given in Figure 4. In this figure, the turbulent kinetic energy, for a feed velocity of 1.9 m/s, increases with increasing distance from the feed pipe, because kinetic energy of the mean flow of the feed stream is converted to turbulent kinetic energy. From Figure 4 it follows that the turbulent kinetic energy increases with increasing tip velocity ( $v_{\text{tip}}$ ) and feed velocity ( $v_{\text{feed}}$ ). In equation (9), the turbulent kinetic energy averaged over the axial distance is used to calculate the turbulent dispersion coefficient with equation (8). The same trend as observed in the local values for the turbulent kinetic energy as plotted in Figure 4 is also seen in averaged turbulent kinetic energies.

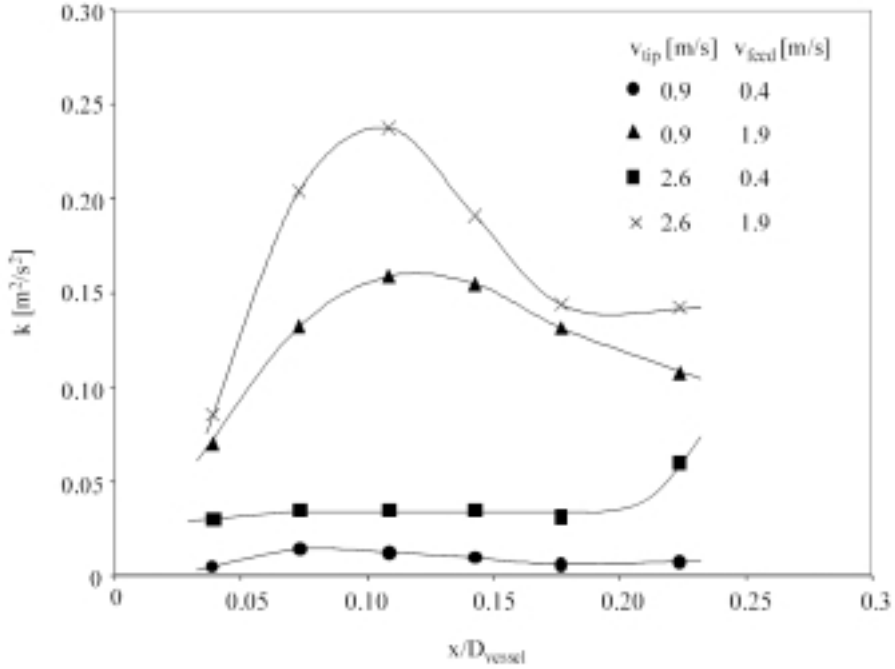


Figure 4: Turbulent kinetic energy as a function of the axial coordinate for a vessel with a diameter of 288 mm and a feed pipe diameter of 6 mm.

To obtain a correlation for the average turbulent kinetic energy, this energy is assumed to be a function of the feed stream velocity, the circulation velocity ( $v_{circ}$ ) and an interaction between these velocities:

$$k = f(v_{feed}^2, v_{circ}^2, v_{feed} \cdot v_{circ}) \quad (17)$$

in which  $v_{circ}$  is the mean velocity beneath the feed pipe when no feed stream is present. With a fitting procedure applied to all measured values of the average turbulent kinetic energy, the following equation for the average turbulent kinetic energy in the feed stream is obtained:

$$k = 0.15 \cdot v_{circ}^2 + 0.025 \cdot v_{feed}^2 + 0.045 \cdot v_{feed} \cdot v_{circ} \quad (18)$$

Equation (18) describes the measured averaged turbulent kinetic energy reasonably well, as shown by Figure 5.

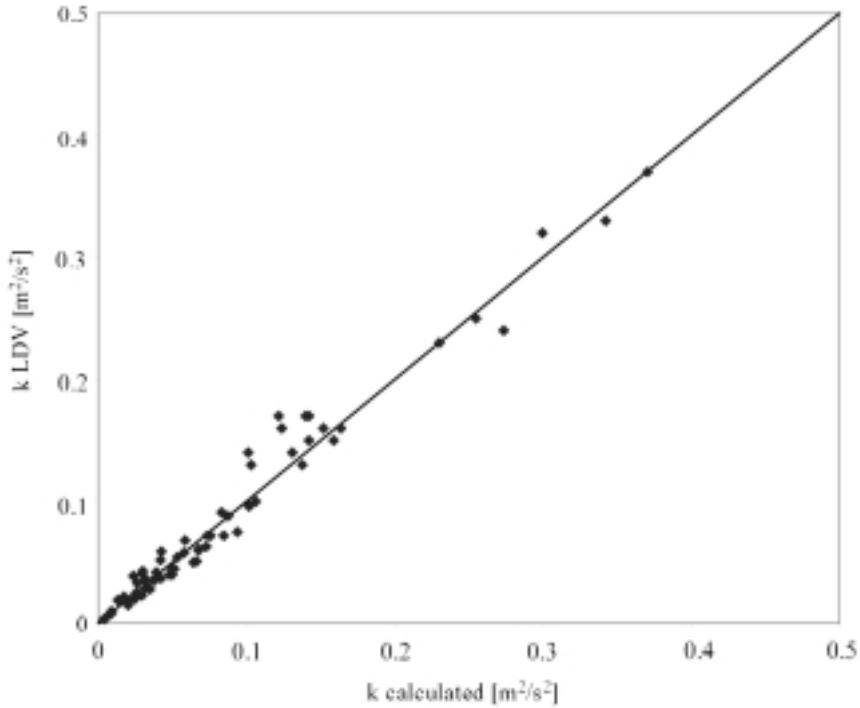


Figure 5: Turbulent kinetic energy from LDV measurements as a function of the turbulent kinetic energy calculated with equation 18.

In Figure 6 measured circulation velocities normalized to the stirrer tip speed ( $v_{tip}$ ) are given as a function of the axial coordinate. The circulation velocities have been measured in the absence of a feed pipe. From Figure 6 it is concluded that in a large part of the vessel and independent of the vessel size, the circulation velocity is equal to  $0.15v_{tip}$ . This result is used in equation (18).

Figure 7 shows two representative examples of energy spectra obtained from the measured velocity data. These energy spectra show the typical characteristics of a turbulence energy spectrum (Wu and Patterson, 1989), which are that most of the energy is contained in the lower frequency eddies, in the low frequency range the spectrum is almost horizontal and in the higher frequency range a slope proportional to  $-5/3$  on a log-log scale is visible.

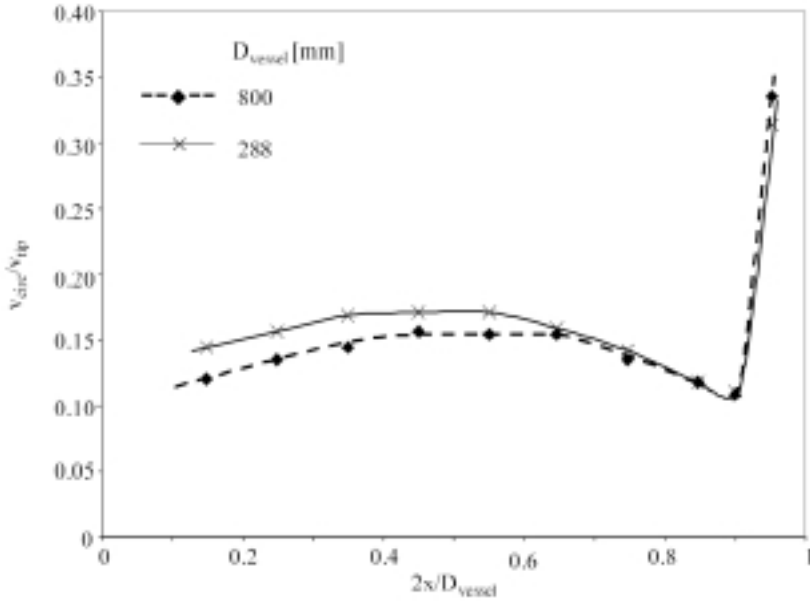


Figure 6: Circulation velocity normalized to the stirrer tip speed as a function of the axial coordinate, for a vessel with a diameter of 288 mm at a stirrer tip speed of 2.1 m/s and a vessel with a diameter of 800 mm at a stirrer tip speed of 3.1 m/s.

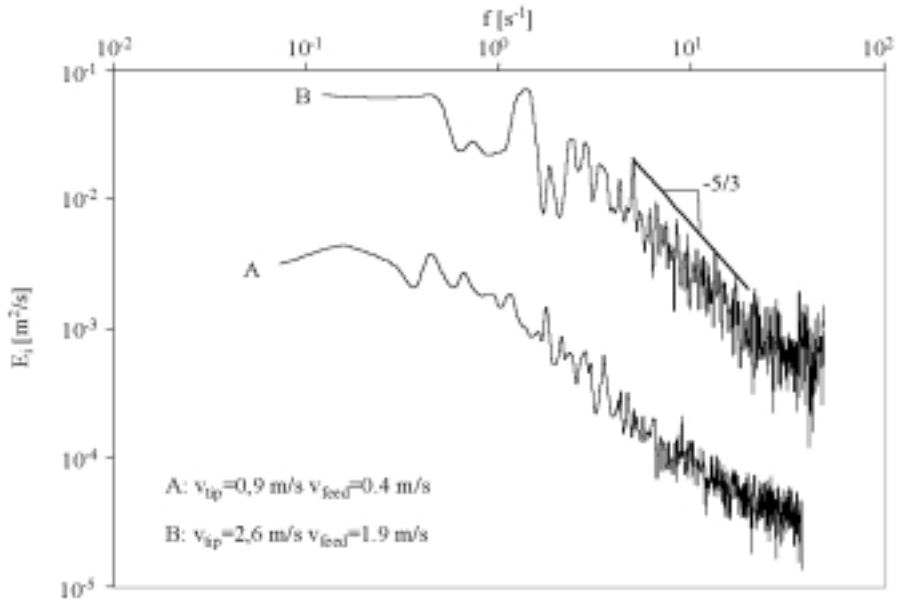


Figure 7: Energy spectra for axial velocity components at 0.1 times the vessel diameter below the feed pipe, a vessel diameter of 288 mm and a feed pipe diameter of 4 mm.

Integral length scales of the velocity fluctuations have been calculated from integral time scales, which have been approximated from the average of the first points obtained in the horizontal part of an energy spectrum. Integral length scales of the velocity fluctuations measured in the 288 mm vessel with a feed pipe diameter of 4 mm are given in Figure 8. Integral length scales of the velocity fluctuations measured in vessels with a diameter of 288 mm and 800 mm, respectively, and without a feed pipe present are given in Figure 9. Figure 8 in combination with Figure 9 shows that for  $v_{\text{feed}}/v_{\text{circ}} \leq 5$  the influence of the feed velocity on the integral length scale is small. For these values of  $v_{\text{feed}}/v_{\text{circ}}$  the integral velocity length scale is approximately equal to  $0.15D_{\text{vessel}}$ . For  $v_{\text{feed}}/v_{\text{circ}}=14$  the integral length scale of the velocity fluctuations is approximately equal to the feed pipe diameter. An intermediate value of  $v_{\text{feed}}/v_{\text{circ}}=10$  has been chosen as a value below which the integral length scale is equal to  $0.15D_{\text{vessel}}$ .

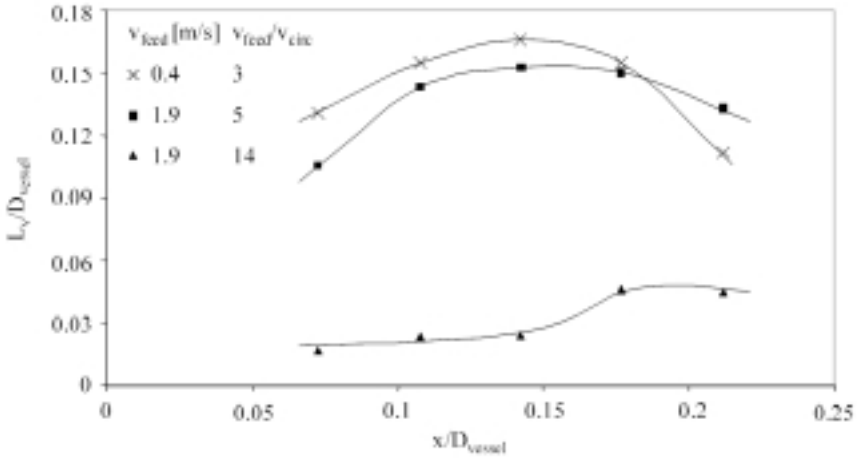


Figure 8: Integral length scales of the velocity fluctuations as a function of the axial coordinate for a vessel with a diameter of 288 mm and a feed pipe diameter of 4 mm.

Substituting equation (18) for the turbulent kinetic energy in equation (9), with the integral length scale of the velocity fluctuations equals  $0.15D_{\text{vessel}}$ , leads to the following equation for the energy dissipation rate for  $v_{\text{feed}}/v_{\text{circ}} < 10$ :

$$\varepsilon = \frac{\left(0.15 \cdot v_{\text{circ}}^2 + 0.025 \cdot v_{\text{feed}}^2 + 0.045 \cdot v_{\text{feed}} \cdot v_{\text{circ}}\right)^{3/2}}{0.15 \cdot D_{\text{vessel}}} \quad (19)$$

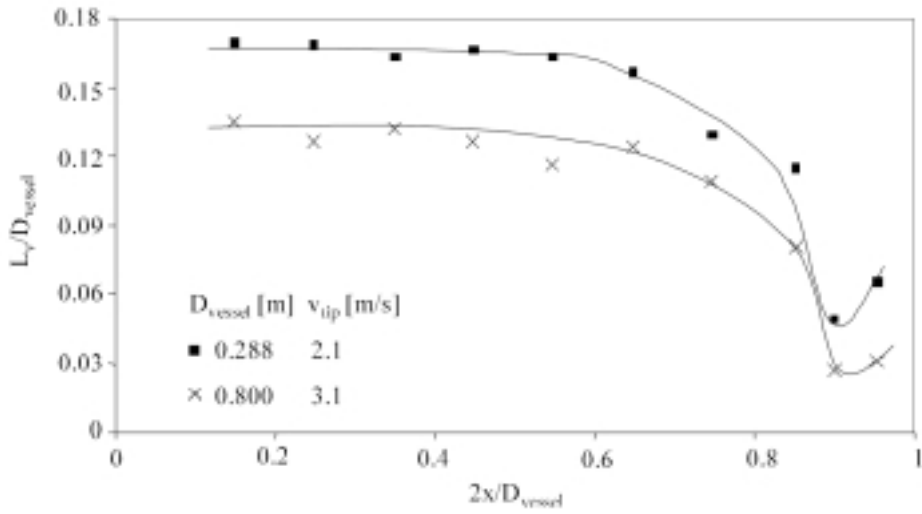


Figure 9: Integral length scales of the velocity fluctuations as a function of the axial coordinate measured in the absence of a feed pipe.

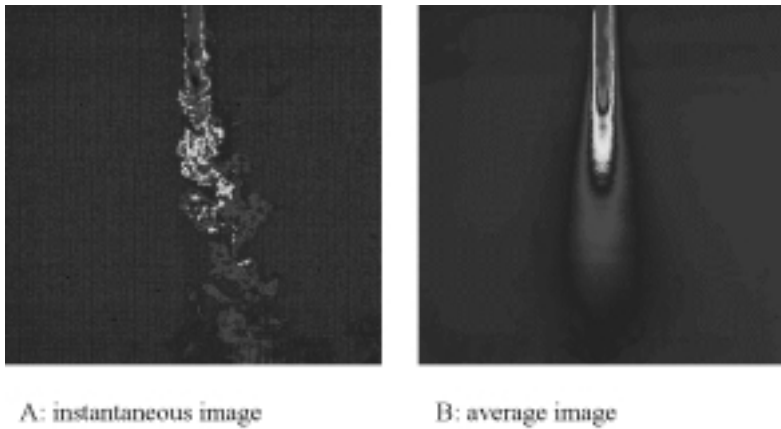


Figure 10: Examples of an instantaneous (a) and a time-averaged image (b) obtained with PLIF in a vessel with a diameter of 382 mm, a feed pipe diameter of 6 mm, a feed velocity of 0.4 m/s and a stirrer speed of 0.8 m/s.

The characteristic length scale for turbulent dispersion is determined from the instantaneous images obtained with PLIF. A typical example of an instantaneous image obtained with PLIF is given in Figure 10a. The instantaneous picture shows large-scale coherent structures with a size comparable to the feed pipe diameter. Therefore, it is concluded that the length scale for turbulent dispersion is approximately equal to the feed pipe diameter.

Combining equations (8) and (19), with the characteristic length scale for turbulent dispersion equal to the feed pipe diameter ( $d_{\text{feed}}$ ), yields the following equation for the turbulent dispersion coefficient as function of process and design variables:

$$D_t = A \cdot \frac{(0.15 \cdot v_{\text{circ}}^2 + 0.025 \cdot v_{\text{feed}}^2 + 0.045 \cdot v_{\text{feed}} \cdot v_{\text{circ}})^{1/2}}{(0.15 \cdot D_{\text{vessel}})^{1/3}} \cdot d_{\text{feed}}^{4/3} \quad (20)$$

#### 4.2 Turbulent dispersion time

The turbulent dispersion time is defined as the time where the relative concentration on the centreline of the feedstream has reached the arbitrarily chosen value of 0.091. This concentration corresponds to one volume element of feed liquid mixed with ten volume elements of bulk liquid. Substituting equation (20) for the turbulent dispersion coefficient in equation (4) for the turbulent dispersion time, with the relative concentration equal to 0.091, gives the following equation for the turbulent dispersion time.

$$\tau_{\text{td}} = \frac{0.55}{A} \cdot \frac{a^{2/3} \cdot D_{\text{vessel}}^{1/3}}{(0.15 \cdot v_{\text{circ}}^2 + 0.025 \cdot v_{\text{feed}}^2 + 0.045 \cdot v_{\text{feed}} \cdot v_{\text{circ}})^{1/2}} \quad (21)$$

Turbulent dispersion times are also determined experimentally from the time-averaged images obtained with PLIF. These turbulent dispersion times are used to verify equation (21). An example of a time-averaged image is given in Figure 10b. Examples of normalized averaged concentration profiles at the centreline of the feed stream obtained from the time-averaged pictures are given in Figures 11 and 12. Figure 11 shows normalized averaged concentration profiles for three feed velocities and a tip velocity of 0.9 m/s.

In this figure an increasing turbulent dispersion rate is observed when the feed velocity is increased. Averaged normalized concentration profiles for a feed velocity of 1 m/s, a tip velocity of 0.9 m/s and a feed pipe diameter of 4 mm and 8 mm, respectively, are given in Figure 12. A lower turbulent dispersion rate is observed for the larger feed pipe diameter. The influences of feed velocity and feed pipe diameter on the turbulent dispersion rate, as illustrated in figures 11 and 12, respectively, are in agreement with equation (21).

The turbulent dispersion times, defined as the time where the relative concentration on the centreline of the feed stream has reached a value of 0.091, are determined from the concentration profiles. In Figure 13 measured turbulent dispersion times are plotted against calculated turbulent dispersion times with equation (21). Figure 13 shows a good agreement between the measured and calculated turbulent dispersion times. The constant A in equation (21) proved to be equal to 0.36 from comparison between the measured and calculated turbulent dispersion times.

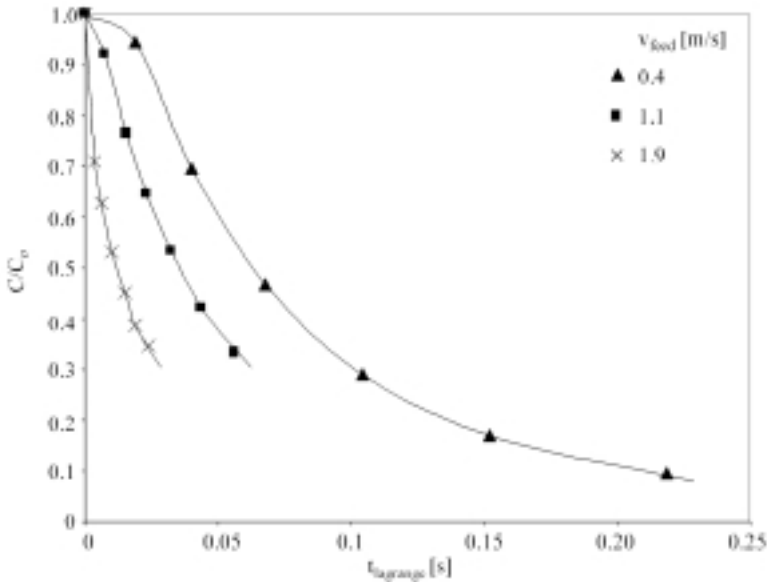


Figure 11: Relative concentration as a function of Lagrangian time for three feed velocities, a stirrer tip speed of 0.9 m/s, a vessel diameter of 288 mm and a feed pipe diameter of 6 mm.



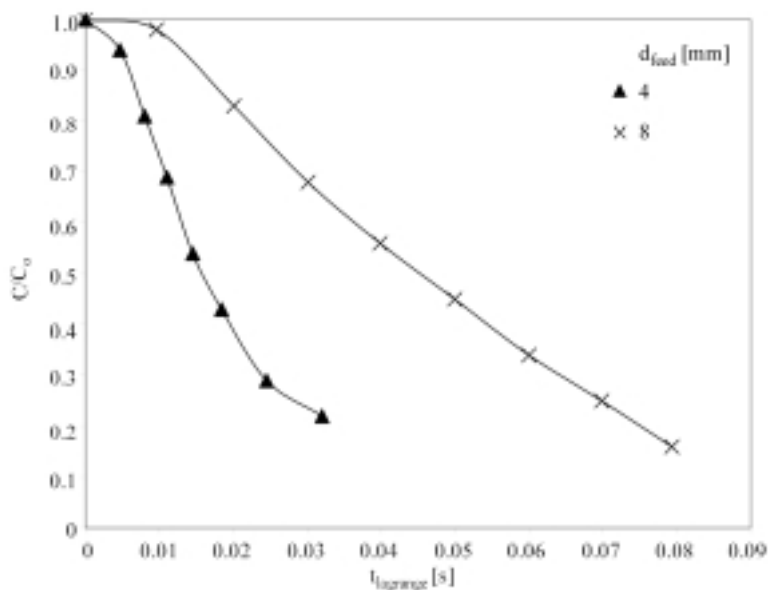


Figure 12: Relative concentration as a function of Lagrangian time for a stirrer tip speed of 1.9 m/s, a feed velocity of 1.1 m/s, a vessel diameter of 288 mm and feed pipe diameters of 4 mm and 8 mm, respectively.

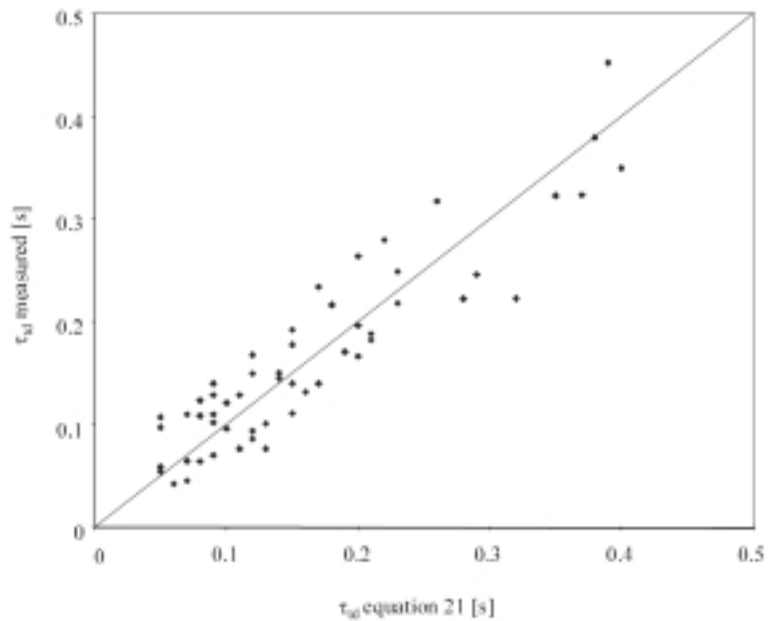


Figure 13: Measured turbulent dispersion times as function of calculated turbulent dispersion times with equation (21).

## 5. Conclusions

Based on a theoretical model for turbulent dispersion and LDV and PLIF measurements an equation for the turbulent dispersion time as function of several design and process variables is derived. This equation can be used to maintain a constant turbulent dispersion time during the scale-up of a stirred tank reactor. Scaling-up with a constant turbulent dispersion time will result in a constant product quality when turbulent dispersion controls the mixing rate. Both the model and the experiments showed that the turbulent dispersion time decreases with an increasing stirrer speed or feed stream velocity. The turbulent dispersion time for a constant feed velocity and stirrer speed is shorter when a smaller feed pipe is used.

## Nomenclature

$a$	internal radius of the feed pipe	[m]
$A$	constant	[-]
$C$	local concentration	[mol m <sup>-3</sup> ]
$C_0$	initial feed concentration	[mol m <sup>-3</sup> ]
$C_{u_i u_i}(\tau)$	autocovariance of the velocity fluctuations	[m <sup>2</sup> s <sup>-2</sup> ]
$d_{\text{feed}}$	feed pipe diameter	[m]
$D_t$	turbulent dispersion coefficient	[m <sup>2</sup> s <sup>-1</sup> ]
$D_{\text{vessel}}$	vessel diameter	[m]
$E$	energy spectrum	[m <sup>2</sup> s <sup>-1</sup> ]
$I_0$	modified Bessel function of the first kind of order zero	[-]
$k$	turbulent kinetic energy	[m <sup>2</sup> s <sup>-2</sup> ]
$L_c$	length scale of the concentration fluctuations	[m]
$L_d$	initial length scale of the feed stream	[m]
$L_v$	length scale of the velocity fluctuations	[m]
$M$	total number of velocity measurements	[-]
$n$	wave number of a turbulent motion	[m <sup>-1</sup> ]
$N$	data rate	[s <sup>-1</sup> ]
$r$	radial coordinate	[m]
$t$	time	[s]
$T_i$	integral time scale of the velocity fluctuations	[s]
$u(n)$	characteristic velocity of a turbulent motion	[m s <sup>-1</sup> ]
$u_i(j)$	velocity of particle $j$ in the $i$ -direction	[m s <sup>-1</sup> ]
$U_i$	average velocity in the $i$ -direction	[m s <sup>-1</sup> ]
$u_i'$	rms velocity fluctuation in the $i$ -direction	[m s <sup>-1</sup> ]
$v_{\text{circ}}$	mean velocity beneath the feed pipe when no feed stream is present	[m s <sup>-1</sup> ]
$v_{\text{feed}}$	feed velocity	[m s <sup>-1</sup> ]
$v_{\text{tip}}$	stirrer tip velocity	[m s <sup>-1</sup> ]
$V_{\text{vessel}}$	vessel volume	[m <sup>3</sup> ]
$x$	axial coordinate	[m]

$\alpha$	constant	[-]
$\beta$	constant	[-]
$\varepsilon$	energy dissipation rate	[m <sup>2</sup> s <sup>-3</sup> ]
$\lambda$	characteristic length scale for turbulent dispersion	[m]
$\tau_{td}$	characteristic time scale for turbulent dispersion	[s]
$\Delta t(j)$	time between the arrival times of particle $j$ and $j+1$	[s]

## References

- Adrian, R. J. and C.S. Yao "Power spectra of fluid velocities measured by laser Doppler velocimetry", *Exp. In Fluids* 5, 17 (1987)
- Baldyga, J. and J.R. Bourne "Interactions between mixing on various scales in stirred tank reactors", *Chem. Eng. Sci.* 47, 1837 (1992)
- Baldyga, J., J.R. Bourne, and Y. Yang "Influence of feed pipe diameter on mesomixing in stirred tank reactors", *Chem. Eng. Sci.* 48, 3383 (1993)
- Baldyga, J., R. Pohorecki, W. Podgorska, and B. Marcant "Micromixing effects in semi-batch precipitation", *Proc. 11th Symp. on Industrial Crystallization (Garmisch Partenkirchen)* (1990)
- Barnett, D.O. and H.T. Bentley "Statistical bias of individual realization laser velocimeters", *Proc. 2nd Int. Workshop Laser Velocimetry*, ed. Thompson and Stevenson, 428-444 (1979)
- Bourne, J. R. and C.P. Hilber "The productivity of micromixing-controlled reactions: effect of feed distribution in stirred tanks", *Trans. I.Chem.E.* 68, 51 (1990)
- Crank, J. "Mathematics of Diffusion", Oxford University Press, Oxford (1975)
- Franke, J., and A. Mersmann "The influence of the operational conditions on the precipitation process", *Chem. Eng. Sci.* 50, 1737 (1995)
- Houcine, I., E. Plasari, R. David, and J. Villiermaux "Feedstream jet intermittency phenomenon in a continuous stirred tank reactor", *Chem. Eng. J.* 72, 19 (1999)
- Kusters, K.A. "The influence of turbulence on the aggregation of small particles in agitated vessels", *Ph.D. thesis, Eindhoven University of Technology, The Netherlands* (1991)
- Kusters, K.A., C.J.G. van Strien, J.G. Wijers, and D. Thoenes "Effect of velocity bias on integral time scale", *Proc. 3rd Int. Conf. on Laser Anemometry*, ed. Turner, BHRA/Springer Verlag, 557 (1990)

Leeuwen, M. L. J. van "Precipitation and Mixing" Ph.D. thesis, Delft University of Technology, The Netherlands (1998)

Lesieur, M. "Turbulence in fluids: Stochastic and numerical modelling", Kluwer Academic Publishers, Dordrecht (1990)

Lozano, I., I. van Cruyningen, I., P. Danehy, and R.K. Hanson "Planar Laser Induced Scalar Measurements in a turbulent jet, Applications of Laser Techniques to Fluid Mechanics", Adrian, R.J., Durao, D. F. G. and Durst, F. (eds), Springer, 19 (1986)

Marcant, B., and R. David, R. "Experimental evidence for and prediction of micromixing effects in precipitation", *A.I.Ch.E. J.* 37, 1698 (1991)

Mujumdar, A. R., B. Huang, D. Wolf, M.E. Weber, and W.J.M. Douglas "Turbulence parameters in a stirred tank", *Can. J. Chem. Eng.* 48, 475 (1970)

Paul, E. L., J. Mahadevan, J. Foster, and M. Kennedy Midler "The effect of mixing on scale-up of a parallel reaction system", *Chem. Eng. Sci.* 47, 2837 (1992)

Philips, R., S. Rohani, and J. Baldyga "Micromixing in a single feed semi-batch precipitation process", *A.I.Ch.E.J.* 45, 82 (1999)

Ranada, V.V. and J.R. Bourne "Reactive mixing in agitated tanks", *Chem. Eng. Commun* 99, 33 (1991)

Rys, P. "The mixing-sensitive product distribution of chemical reactions", *Chimia* 46, 469 (1992)

Schoenmakers, J.H.A., J.G. Wijers, and D. Thoenes "Determination of feed stream mixing rates in agitated vessels", *Proc. 8th Europ. Mix. Conf.: Récent Progrès en Génie des Procédés*, ed. Lavoisier, 11, 52, 185 (1997)

Tennekes, H. and J.L. Lumley "A First Course in Turbulence", MIT Press, Cambridge (1972)

Thoenes, D. "Chemical Reactor Development", Kluwer Academic Publishers, Dordrecht (1994)

Schoenmakers, J.H.A., J.G. Wijers, and D. Thoenes "Non steady-state behaviour of the flow in agitated vessels" *Proc. 4th World Conf. on Exp. Heat Transfer, Fluid Mech. and Thermodynamics*, ed. Giot, Mayinger and Celata, *ExHFT* 4, 1, 477 (1997)

Wu, H. and G.K. Patterson "Laser Doppler measurements of turbulent-flow parameters in a stirred mixer", *Chem. Eng. Sci.* 44, 2207 (1989)



## **SCALE-UP OF A STIRRED TANK REACTOR EQUIPPED WITH A PFAUDLER TYPE IMPELLER**

### Abstract

Micromixing in a reactor equipped with a Pfaudler impeller-type agitator is investigated with the objective to obtain a scale-up rule, when micromixing controls the mixing rate. For this purpose selectivities of mixing-sensitive reactions have been determined experimentally and have been calculated with the engulfment model, requiring information on local energy dissipation rates. Using Laser Doppler Velocimetry and torque measurements it is shown that the distribution of the energy dissipation rate inside a baffled reactor equipped with a Pfaudler impeller is relatively homogeneous. Selectivities calculated using average energy dissipation rates are in good agreement with measured selectivities for a broad range of process conditions in these reactors. From these results it is concluded that when a constant energy input per unit volume is used, a constant micromixing rate is obtained in a baffled reactor with a Pfaudler impeller.

*This chapter has been submitted for publication as I.L.M. Verschuren, J.G. Wijers and J.T.F. Keurentjes "Scale-up of a stirred tank reactor equipped with a Pfaudler type impeller"*

## 1. Introduction

The degree of mixing in a stirred tank reactor affects the yield and selectivity of a broad range of chemical processes. Examples of these mixing-sensitive processes are various types of polymerizations (Fields and Ottino, 1987), precipitations (Franke and Mersmann, 1995) and fermentations (Larsson et al., 1992). Stirred tank reactors with a Pfaudler impeller-type agitator (also called retreat curve impeller) are frequently used in the chemical industry for the production of fine chemicals and pharmaceuticals. The shape of a retreat curve impeller permits a glass lining to be applied, which makes this type of impeller particularly useful in corrosive environments. Although the Pfaudler impeller is widely used in the chemical industry, information on the mixing performance of this type of impeller is limited.

The mixing in a stirred vessel consists of three processes: macromixing, mesomixing and micromixing (Ranada and Bourne, 1991). Macromixing is the convection of fluid by the average velocity. Mesomixing refers to the turbulent dispersion of a feed stream by large-scale turbulent motions. Micromixing is mixing inside small-scale turbulent motions by engulfment, deformation and diffusion. In the production of fine chemicals usually low feed rates are used to prevent a thermal runaway and to control the product distribution. For sufficiently low feed rates the product distribution is controlled by micromixing and scale-up with a constant micromixing rate should be applied to obtain a constant product quality (Bourne and Hilber, 1990). The objective of this study is to obtain a scale-up rule for a stirred tank reactor with a Pfaudler impeller-type agitator, which can be used to obtain a constant micromixing rate. To obtain our goal, selectivities of mixing sensitive reactions have been measured and calculated with a micromixing model. Application of the model requires information about local energy dissipation rates and the circulating flow rate. These parameters have been obtained from Laser Doppler Velocimetry and torque measurements.

## 2. Micromixing model

The complete micromixing process, which is diffusion within shrinking laminated structures formed by engulfment, is described by the EDD (engulfment, deformation



and diffusion) model (Baldyga and Bourne, 1984). Baldyga and Bourne have shown that for systems having a Schmidt number less than 4000, engulfment is the rate-determining step of the micromixing process and the EDD-model simplifies to the engulfment model (E-model) (Baldyga and Bourne, 1989a). The growth of the micromixed volume according to the E-model is described by:

$$\frac{dV_{mi}}{dt} = EV_{mi} \quad (1)$$

$$E = 0.058 \sqrt{\frac{\epsilon}{\nu}} \quad (2)$$

where E is the engulfment rate,  $\nu$  is the kinematic viscosity and  $\epsilon$  is the local energy dissipation rate.

The E-model can be used to calculate the selectivity of a chemical process in a semi-batch reactor in which a reagent is slowly added to a reagent already present in the vessel (Baldyga and Bourne, 1989b). A volume containing feed liquid will grow according to equation (1). The mass balance for a component i in this fluid element is:

$$\frac{dc_i}{dt} = E(\langle c_i \rangle - c_i) + R_i \quad (3)$$

in which  $c_i$  is the concentration of i in the micro-mixed volume,  $\langle c_i \rangle$  is the concentration of i in the surrounding fluid near the micro-mixed volume and  $R_i$  is the specific reaction rate.

No macroscopic concentration gradients are included in the model. The concentration of a reactant in the surrounding fluid ( $\langle c_i \rangle$ ) is assumed to be constant during one circulation time and added feed liquid is assumed to be homogeneously mixed after one circulation. Due to this assumption the history of all fluid elements, added to the reactor during one circulation time ( $t_c$ ), will be the same. Therefore, the total feed volume is discretized into  $\sigma$  equal parts, with:

$$\sigma = \frac{t_{feed}}{t_c} \quad (4)$$

in which  $t_{feed}$  is the feed time defined as the total feed volume divided by the feed flow rate.

The circulation time inside a stirred tank reactor is:

$$t_c = \frac{V_{\text{reactor}}}{Q_c} \quad (5)$$

where  $V_{\text{reactor}}$  is the volume of the reactor contents and  $Q_c$  is the circulating flow rate of the stirrer. The circulating flow rate of a stirrer is usually given as:

$$N_c = \frac{Q_c}{ND_{\text{im}}^3} \quad (6)$$

in which  $N_c$  is the circulation number of the stirrer,  $N$  is the stirrer speed, and  $D_{\text{im}}$  is the impeller diameter.

To calculate the selectivity of a mixing-sensitive reaction with the E-model, information on the energy dissipation rate in the reaction zone and on the circulation number needs to be available. In this study, local energy dissipation rates and the circulation number for a stirred tank reactor equipped with a Pfaudler impeller-type agitator have been measured with Laser Doppler Velocimetry (LDV). The average energy dissipation rate for the same reactor as used for the LDV experiments has been obtained from torque measurements. To validate the simulations and to investigate micromixing inside reactors equipped with a Pfaudler impeller selectivities of mixing sensitive reactions have been determined experimentally. The LDV experiments, torque measurements and reactive experiments are discussed in more detail below.

### 3. Experiments

#### 3.1 Experimental determination of the energy dissipation rate

The stirred tank reactor used for the LDV and torque measurements is shown schematically in Figure 1. The internal tank diameter was 0.2 m. The impeller was a commercially available glass-lined Pfaudler impeller-type agitator. The tank was partially baffled with a beavertail baffle and a feed pipe.

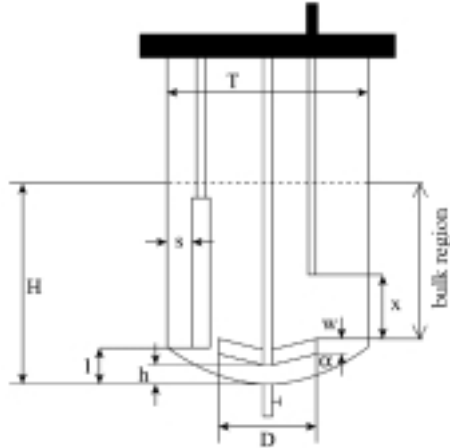


Figure 1: Geometry of the vessel and the Pfaudler impeller-type agitator, with  $T=H=0.2$  m,  $D=0.120$  m,  $h=0.018$  m,  $w=0.035$  m,  $s=0.022$  m,  $l=0.036$  m and  $\alpha=10^\circ$

Laser Doppler Velocimetry was used to determine local energy dissipation rates in the bulk region of the stirred tank reactor (see Figure 1). The LDV set-up and method of data processing used to determine these energy dissipation rates have already been described (Verschuren et al., 2001a). LDV measurements were not possible in the stirrer region due to diffraction of the laser light by the curvature of the tank wall. The energy dissipated in the stirrer region was determined by subtracting the measured amount of energy dissipated in the bulk region from the total amount of energy dissipated in the reactor. The total amount of energy dissipated in the reactor is equal to the volume of the reactor times the average energy dissipation rate. The average turbulent energy dissipation rate ( $\bar{\epsilon}$ ) was estimated with:

$$\bar{\epsilon} = \frac{P}{\rho V_{\text{reactor}}} \quad (7)$$

in which  $V_{\text{reactor}}$  is the liquid volume in the vessel,  $\rho$  is density and  $P$  is the total power input. The total power input was determined from torque measurements. The total power input will be given as the power number of the impeller ( $P_o$ ):

$$P_o = \frac{P}{\rho N^3 D_{\text{im}}^5} \quad (8)$$

with  $N$  the stirrer speed and  $D_{\text{im}}$  the impeller diameter.

No circulation loop was assumed to be present below the impeller. With this assumption the circulating flow rate was determined by the liquid drawn in from the upper side of the impeller:

$$Q_c = \int_{r_1}^{r_2} \int_0^{2\pi} r \bar{u}_{ax} d\theta dr \quad (9)$$

with  $r_1$  the radial position of the impeller shaft,  $r_2$  the radial position where the mean axial velocity is zero and  $\bar{u}_{ax}$  the mean axial velocities just above the impeller. These mean axial velocities were measured with LDV for an impeller speed of 3 Hz in a plane just above the impeller, i.e. at a height of 0.35 times the vessel diameter from the bottom of the tank. The circulating flow rate was used to calculate the circulation number of the stirrer with equation (6).

### 3.2 Experimental determination of the product distribution of a mixing-sensitive reaction set

The product distribution of a mixing-sensitive reaction was measured for various feed point locations, feed times and stirrer speeds in the same reactor as used for the LDV and torque measurements. The feed point locations are given in Figure 2 and Table 1. The feed pipe internal diameter was 5 mm. The stirrer speeds used were 1.12 Hz, 2.97 Hz and 6.67 Hz. The feed times were in the range of 30-1020 s.

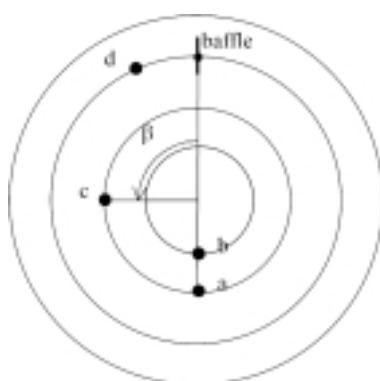


Figure 2: Top view of the vessel with the various feed point locations used.

Table 1: Co-ordinates of the feed points illustrated in Figure 2.

feed point	R [m]	$\beta$	x/T		
A	0.50	90°	0.19	0.44	0.62
B	0.29	90°	0.19		
C	0.50	45°	0.19		
D	0.78	29°	0.19		

The mixing-sensitive reaction set used was the third Bourne reaction (Bourne and Yu, 1994):



For each experiment the vessel was filled with a solution of 0.09 M ethyl chloroacetate (ECA) and 0.09 M hydrochloric acid (HCl). The feed stream was a solution of 1.8 M sodium hydroxide (NaOH). The feed volume was 1/20 of the initial volume of  $5.74 \cdot 10^{-3} \text{ m}^3$  present in the vessel. When the mixing is fast, all NaOH will be neutralised by HCl and no ethanol will be produced. More ethanol will be produced at lower mixing rates, thus being a direct measure of the reaction selectivity.

## 4. Results and Discussion

### 4.1 Results of the LDV and torque measurements

In Figure 3 measured power numbers in the partially baffled reactor and power numbers provided by the Pfaudler company for a fully baffled and unbaffled reactor are given as a function of Reynolds number. For the partially baffled reactor and Reynolds numbers between the  $1.4 \cdot 10^4$  and  $10^5$  a constant power number of 0.64 is measured. For higher Reynolds numbers the power number decreases with increasing Reynolds number. This decrease in the power number is caused by vortex formation at high stirrer speeds as could also be observed visually (Rushton et al., 1950). The circulation number of the Pfaudler impeller, calculated from the mean axial velocities measured in a plane just above the impeller as described in section 3.1, is equal to 0.4.

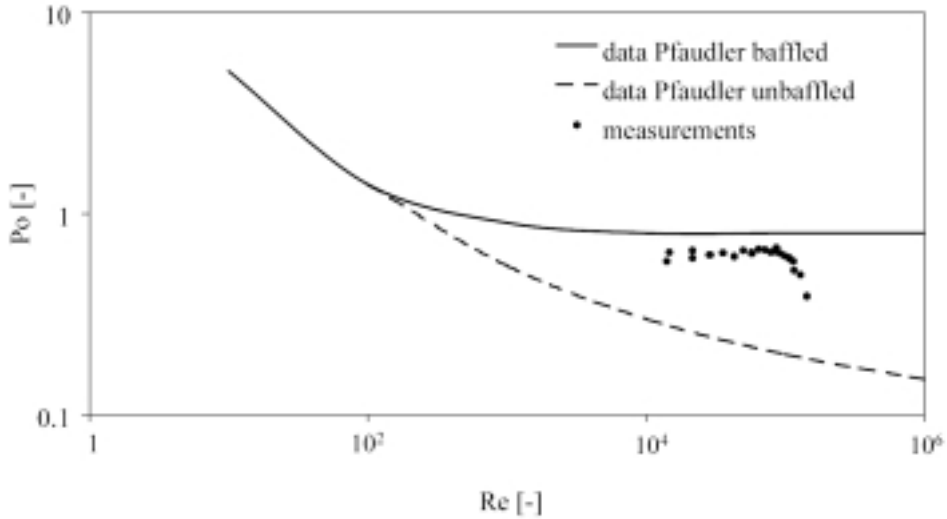


Figure 3: Power numbers measured in a partially baffled reactor and power numbers provided by the Pfaudler company for a fully baffled and unbaffled reactor as function of Reynolds number.

Figure 4 represents the spatial distribution of the energy dissipation rate inside a stirred tank reactor equipped with a Pfaudler impeller. This figure shows that three characteristic regions can be distinguished, i.e. an upper bulk region, a lower bulk region and a stirrer region. From Figure 4 it is concluded that the distribution of the energy dissipation rate inside the stirred vessel equipped with the Pfaudler impeller is relatively homogeneous, especially when compared to the distribution of the energy dissipation rate inside a reactor equipped with a Rushton turbine impeller as illustrated in Figure 5 (Verschuren et al., 2001b).

No significant variation in product distribution with feed point position is to be expected, seen the homogeneous distribution of the energy dissipation rate in the reactor equipped with the Pfaudler impeller. To verify this assumption the selectivity of a mixing-sensitive reaction set has been determined for various feed point locations. The results of these reactive experiments are discussed in section 4.2.

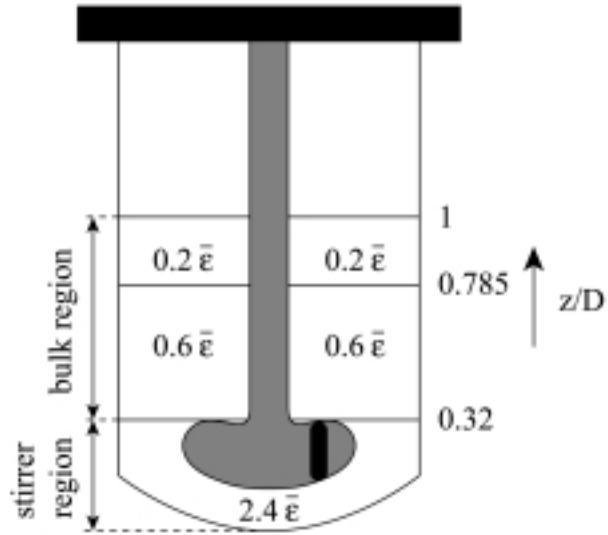


Figure 4: Spatial distribution of the energy dissipation rate in a stirred tank reactor equipped with a Pfaudler type impeller.

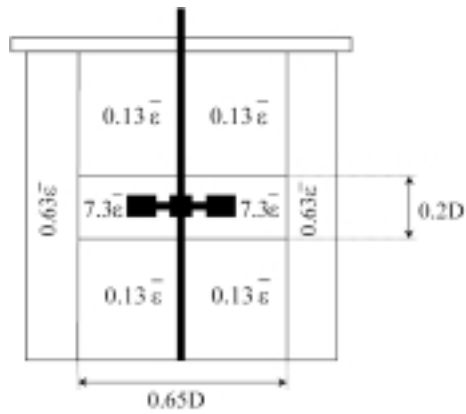


Figure 5: Spatial distribution of the energy dissipation rate in a stirred tank reactor equipped with a Rushton turbine impeller (based on Verschuren et al., 2001b).

## 4.2 Results of the reactive experiments

In Figure 6 the ethanol yield, defined as the total amount of ethanol at the end of an experiment divided by the amount of ECA present at the beginning of an experiment ( $X_{\text{EtOH}}$ ), is given as a function of feed time normalised by the circulation time for a stirrer speed of 1.12 Hz, 2.97 Hz and 6.67 Hz, respectively. Figure 6 shows that a smaller amount of ethanol is obtained when a higher stirrer speed is used. For short feed times the ethanol yield decreases with decreasing feed time, whereas for longer feed times the ethanol yields are independent of feed time. The product distribution is expected to be independent of feed time when micromixing controls the mixing rate (Bourne and Hilber, 1990). From Figure 6 it is concluded that the product quality is controlled by micromixing when the feed time is larger than about 50 times the circulation time for a stirrer speed of 1.12 Hz and when the feed time is larger than about 80 times the circulation time for stirrer speeds of 2.97 Hz and 6.67 Hz.

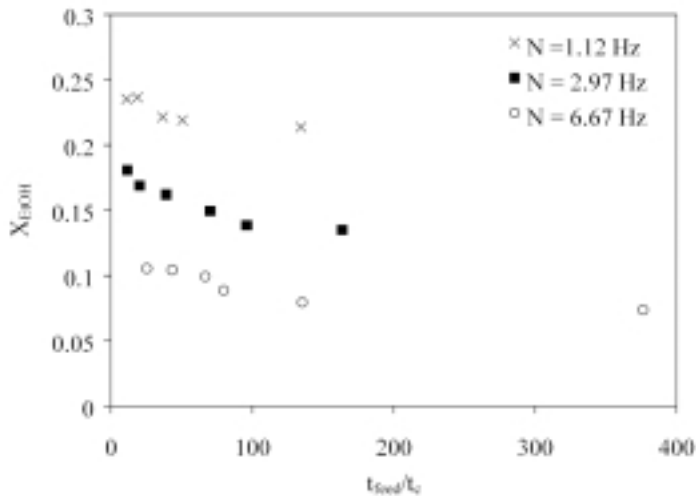


Figure 6: Ethanol yield as a function of feed time for stirrer speeds of 1.12 Hz, 2.97 Hz and 6.67 Hz, respectively.

Figure 7 shows product distributions as a function of stirrer speed for three different heights of the feed point above the impeller. The feed point at the highest location above the impeller yields a larger amount of ethanol compared to the lower feed points. Nevertheless, the differences between the amount of ethanol formed for the different feed point locations are relatively small.



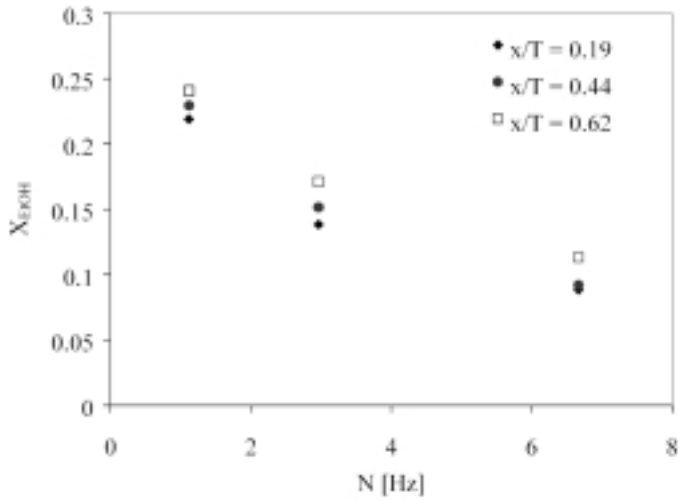


Figure 7: Ethanol yield as a function of stirrer speed for feed points located at different heights above the impeller.

In Figure 8 the product distribution ( $X_{EtOH}$ ) is given as a function of stirrer speed for four different feed point locations all at a height of  $0.19T$  above the upper edge of the impeller. From these results it follows that no significant differences between the amounts of ethanol obtained for the different feed point locations can be observed.

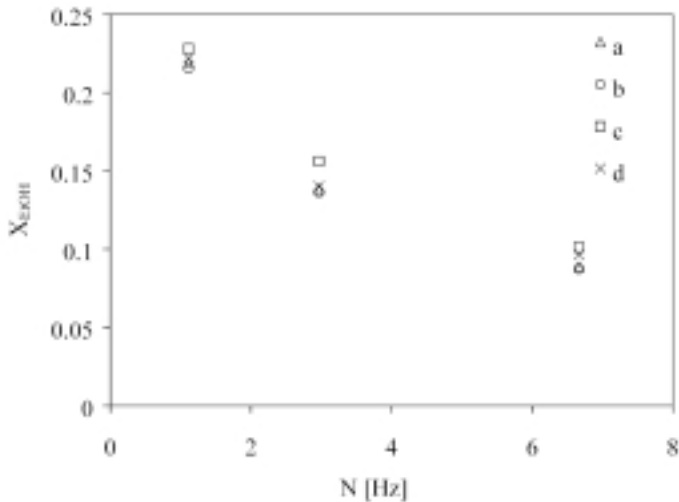


Figure 8: Ethanol yield as a function of stirrer speed for different feed point locations.

Because of the even distribution of the energy dissipation rate, the average energy dissipation rate, as obtained from the experimentally determined power numbers, is used to calculate the product distribution with the E-model as described in section 2. In Figure 9 the calculated product distributions are plotted together with the measured product distributions, which are independent of feed time, as a function of stirrer speed. A good agreement is obtained between the calculated and measured product distributions for stirrer speeds of 2.97 Hz and 6.67 Hz. However, a relatively large deviation is observed between the measurements and the simulations for a stirrer speed of 1.12 Hz. This discrepancy may be caused by not fully developed turbulence at this low stirrer speed. From Figure 9 it can be concluded that under turbulent flow conditions, the E-model with an average energy dissipation rate can effectively be used to calculate the selectivity of a mixing-sensitive reaction in a partially baffled reactor equipped with a Pfaudler impeller-type agitator.

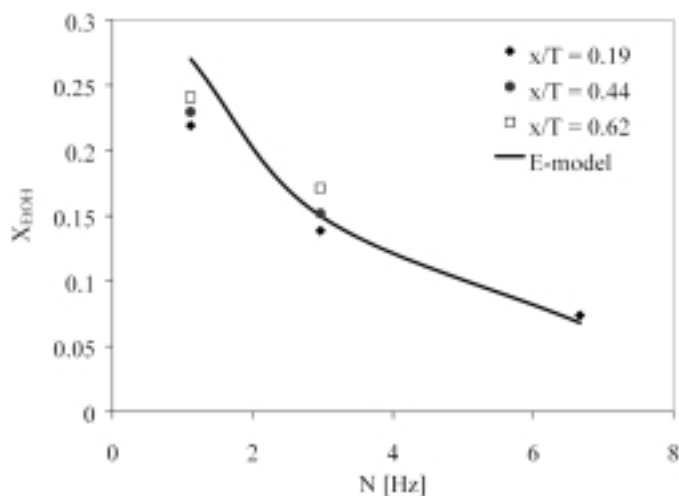
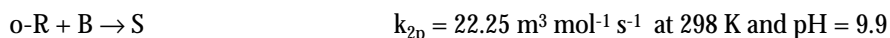
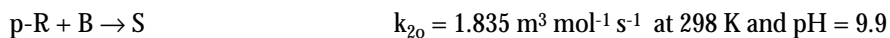
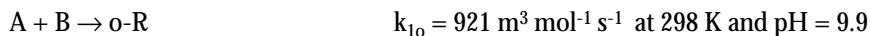
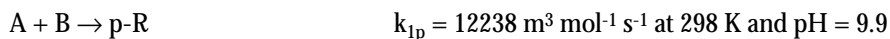


Figure 9: Ethanol yields, which are independent of feed time, as a function of stirrer speed for feed points at different heights above the impeller. The curve represents the calculated ethanol yield with the E-model.

To verify this conclusion for a broader range of experimental conditions, measurements of micromixing in a commercial scale reactor with a Pfaudler impeller-type agitator are used from literature (Angst et al., 1979). In this study the product distribution of the first Bourne reaction was measured in a tank with a working volume of 0.63 m<sup>3</sup>. These product distributions were determined for various feed point locations in a partially

baffled and unbaffled reactor, respectively. The reaction mechanism of the first Bourne reaction, along with the second order kinetic constants (Baldyga and Bourne, 1999), is given below.



where A is 1-naphtol, B is diazotized sulfanilic acid, o-R is ortho monoazo dye from 1-naphtol, p-R is para monoazo dye from 1-naphtol and S is bisazo dye from 1-naphtol.

In Table 2 the product distributions of the first Bourne reaction measured by Angst et al. (1979) in the commercial scale reactor are given. No significant variation in the product distribution with feed point position is observed for the feed point positions just above the impeller and below a height of 0.42T above the upper edge of the impeller.

To calculate the product distribution with the E-model, average energy dissipation rates are used as given in (Angst et al., 1979). The calculated product distributions are given in Table 2. The model and the experiments are in good agreement for the partially baffled reactor with feed points located between the upper edge of the impeller and 0.42T above the upper edge of the impeller. The deviation between the model and the experiments is larger for the unbaffled reactor. This indicates that the E-model with an average energy dissipation rate is not suitable to predict the selectivity of a mixing-sensitive reaction set in an unbaffled reactor equipped with a Pfaudler impeller-type agitator.

Table 2: Product distribution of the 1e bourne reaction measured in a commercial scale reactor (Angst et al., 1979) and calculated with the E-model.

Position feed pipe	$\varepsilon$ [m <sup>2</sup> /s <sup>3</sup> ]	tank base	position above the impeller [x/T]				E-model
			0.025	0.175	0.425	0.715	
baffled: % mono	0.07	65	97	97.5	96.5	92	97.2
Unbaffled: % mono	0.05	57	94		93	91	96.7

The scale-up criterion for constant product distribution, which follows from the E-model, is a constant energy dissipation rate in the reaction zone (Bourne and Dell'ava, 1987). In this study, the average energy dissipation rate has been used to calculate the product distribution with the E-model.

A good agreement is obtained between the calculated product distributions and measured product distributions in partially baffled reactors for a broad range of process conditions. From these results it can be concluded that a constant energy input per unit volume will be a reasonable scale-up rule for a partially baffled reactor equipped with a Pfaudler impeller-type agitator.

## 5. Conclusions

The spatial distribution of the energy dissipation rate inside a partially baffled reactor equipped with a Pfaudler impeller-type agitator has been shown to be relatively homogeneous. As expected from the homogeneous distribution of the energy dissipation rate, no significant variation in the product distribution with feed point position in a large part of a partially baffled reactor has been obtained. The E-model, in which an average energy dissipation rate is used, proved to be well suited to predict the product distribution of mixing-sensitive reaction sets for a broad range of process conditions in these reactors. From these results it is concluded that a constant energy input per unit volume is a reasonable scale-up rule for a baffled reactor with a Pfaudler impeller-type agitator, when micromixing controls the product distribution. Using literature data, less correspondence is obtained between calculated product distributions using an average energy dissipation rate and measured product distributions in an unbaffled reactor with a Pfaudler impeller. This indicates that a constant energy input per unit volume is not a suitable scale-up rule for an unbaffled reactor with a Pfaudler impeller-type agitator.

## Nomenclature

$c_i$	concentration of $i$ in the micromixed volume	$[\text{mol m}^{-3}]$
$\langle c_i \rangle$	concentration of $i$ in the surrounding fluid	$[\text{mol m}^{-3}]$
$D_{im}$	impeller diameter	$[\text{m}]$
$E$	engulfment rate	$[\text{s}^{-1}]$
$N$	stirrer speed	$[\text{s}^{-1}]$
$N_c$	circulation number	$[-]$
$P$	power input	$[\text{W}]$
$Po$	power number	$[-]$
$Q_c$	circulating flow rate	$[\text{m}^3 \text{s}^{-1}]$
$r$	radial coordinate	$[\text{m}]$
$R$	reaction rate	$[\text{mol m}^{-3} \text{s}^{-1}]$
$t$	time	$[\text{s}]$
$t_{\text{feed}}$	feed time	$[\text{s}]$
$t_c$	circulation time	$[\text{s}]$
$T$	vessel diameter	$[\text{m}]$
$\bar{u}_{ax}$	mean axial velocity	$[\text{m s}^{-1}]$
$V_{mi}$	micromixed volume	$[\text{m}^3]$
$V_{\text{reactor}}$	volume of the reactor	$[\text{m}^3]$
$\varepsilon$	energy dissipation rate	$[\text{m}^2 \text{s}^{-3}]$
$\nu$	kinematic viscosity	$[\text{m}^2 \text{s}^{-1}]$
$\theta$	angle	$[\text{°}]$
$\rho$	density	$[\text{kg m}^{-3}]$
$\sigma$	number of feed parts	$[-]$

## References

- Angst, W., Bourne J.R. and F. Kozicki "Some measurements of micromixing in commercial-scale stirred reactors" *Proc. third Europ. Conf. on Mixing, Paper A4, York, U.K., (1979)*
- Baldyga, J., and J.R. Bourne "A fluid mechanical approach to turbulent mixing Part II Micromixing in the light of turbulence theory", *Chem. Eng. Commun.*, 28, 243 (1984)

Baldyga, J., and J.R. Bourne "Simplification of micromixing calculations I. Derivation and Application of new model", *Chem. Eng. J.*, 42, 83 (1989a)

Baldyga, J., and J.R. Bourne "Simplification of micromixing calculations II. New Applications", *Chem. Eng. J.*, 42, 93 (1989b)

Baldyga, J., and J.R. Bourne "Turbulent mixing and chemical reactions", John Wiley, Chichester (1999)

Bourne, J.R., and C.P. Hilber "The productivity of micromixing-controlled reactions: Effect of feed distribution in stirred tanks" *Trans. I. Chem. E.* 68, 51 (1990)

Bourne, J.R., Kozicki, F., and P. Rys "Mixing and Chemical Reaction-I: Test reactions to determine segregation", *Chem. Eng. Sci.* 36, 1643 (1981)

Bourne, J.R., and P. Dell'ava "Micro- and macro-mixing in stirred tank reactors of different sizes", *Chem. Eng. Res. Des.* 65, 180 (1987)

Bourne, J.R., and S. Yu "Investigation of micromixing in stirred tank reactors using parallel reactions", *Ind. Eng. Chem. Res.*, 33, 41 (1994)

Fields, S.D. and Ottino, J.M. "Effect of segregation on the course of unpremixed polymerization" *A.I.Ch.E.J.*, 33, 959 (1987)

Franke, J. and A. Mersmann "The influence of the operation conditions on the precipitation process", *Chem. Eng. Sci.*, 50, 1737 (1995)

Larsson, G., S. George, and S.O. Enfors "Scale-down reactor model to simulate insufficient mixing conditions during fed batch operation using a biological test system", *A.I.Ch.E. Symp. Series*, 293, 151 (1992)

Paul, E. L., J. Mahadevan, J. Foster, and M. Kennedy Midler "The effect of mixing on scale-up of a parallel reaction system", *Chem. Eng. Sci.* 47, 2837 (1992)

Ranade, V.V., and J.R. Bourne "Reactive mixing in agitated tanks", *Chem. Eng. Commun.* 99, 33 (1991)

Rushton, J.H., E.W. Costich, and H.J. Everett "Power characteristics of mixing impellers" *Chem. Eng. Prog.* 46, 395 (1950)

Verschuren, I.L.M., J.G. Wijers and J.T.F. Keurentjes "Flow and turbulence characteristics in a stirred tank reactor equipped with a Pfaudler type impeller" submitted for publication to *Ind. Eng. Chem. Res.* (2001a)

Verschuren, I.L.M., J.G. Wijers and J.T.F. Keurentjes "Effect of mixing on the product quality in semi-batch stirred tank reactors" accepted for publication in *A.I.Ch.E.J* (2001b)

## DESIGN AND SCALE-UP OF INDUSTRIAL MIXING PROCESSES

### Abstract

In this chapter scale-up rules are derived from the model presented in chapter 2. These scale-up rules are shown to be only applicable when no large gradients in the hydrodynamic parameters are present in the reaction zone. The presumed PDF method can be used to calculate the selectivity of a mixing-sensitive reaction set once the probability density function (PDF) of the passive tracer concentration is known. In this chapter it is shown that the PDF of an passive tracer fed to a stirred tank reactor can reasonable be approximated by the beta-distribution. Finally, some areas which need further development are discussed, including the modelling of a turbulent flow field in a stirred tank reactor, the effect of large scale-oscillations of a feed stream on the selectivity of a mixing-sensitive process, the instability of the flow pattern in a stirred tank reactor and multiphase mixing.

*This chapter is based on I.L.M. Verschuren, J.G. Wijers and J.T.F. Keurentjes "Determination of the turbulent flow parameters in a stirred tank reactor equipped with a Pfaudler type impeller" and I.L.M. Verschuren, J.G. Wijers and J.T.F. Keurentjes "The Probability Density Function of passive tracer concentrations in a stirred tank reactor", submitted for publication.*

## 1. Introduction

Mixing has a large influence on the product quality of a broad range of chemical reactions. Therefore, a model for the mixing of reacting flows is a helpful tool in the design of a chemical reactor. In principle, the mixing of fluids is completely described by the partial differential equations describing the momentum, mass and species balances. However, turbulent flows of practical interest exhibit a wide range of time and length scales. Consequently, these so-called Direct Numerical Simulations (DNS) of practical turbulent reacting flows require computational resources far exceeding the most powerful computers available today. Therefore, simplified but tractable models are proposed in this thesis to describe the mixing in stirred tank reactors with a turbulent flow field. The applicability of these models depends on the type of flow and chemical reactions under consideration. The second section of this chapter deals with the practical application of these models for the design and scale-up of industrial mixing processes. The third section discusses some suggestions for future research.

## 2. Practical application of mixing models

### 2.1 Lagrangian mechanistic mixing model

A Lagrangian mechanistic mixing model for the calculation of the selectivity of fast mixing-sensitive reactions creating a localized reaction zone in semi-batch stirred tank reactors has been described in chapter 2. The reaction zone will be localized when the characteristic time scale for chemical reaction is much smaller than the circulation time ( $t_c$ ):

$$t_c = \frac{V}{r_c N_q N D_{im}^3} \quad (1)$$

with  $N_q$  the pumping capacity,  $r_c$  circulation ratio,  $N$  impeller speed,  $D_{im}$  impeller diameter and  $V$  the vessel volume.

In chapter 2, the following mixing mechanisms are used to describe the mixing of fluids in a semi-batch stirred tank reactor (see Figure 1):



1. macromixing: convection of the reaction zone through the vessel by the average velocity.
2. mesomixing: spatial evolution of the reaction zone due to turbulent dispersion by large-scale turbulent motions.
3. micromixing: mixing on a molecular scale inside small-scale turbulent motions by engulfment, deformation and diffusion.

Equations for the characteristic time scales for these mixing mechanisms can be derived from the model presented in chapter 2. These equations are presented below and their applicability for the scale-up of a stirred tank reactor with a defined product quality will be discussed.

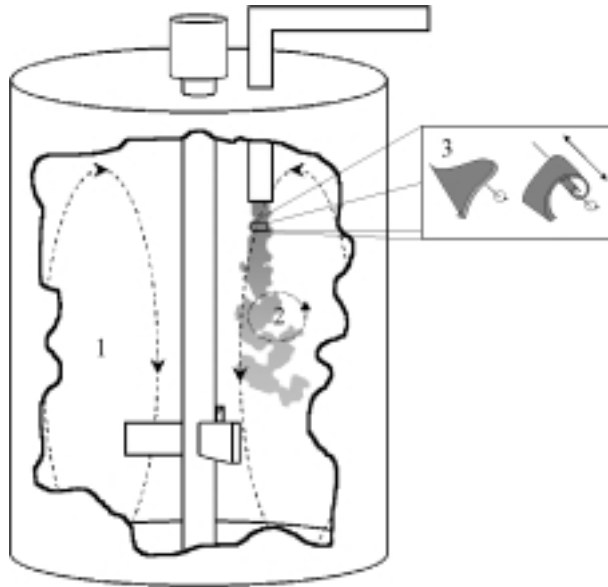


*Figure 1: Schematic representation of the mixing mechanism inside a stirred tank reactor.*

A characteristic time scale for macromixing is the circulation time (equation 1):

$$t_{\text{macro}} \approx t_c \quad (2)$$

The mesomixing rate depends on the size of the turbulent motions taking part in the dispersion process (Lesieur, 1990). The size of these turbulent motions depends on the radius of the feed stream compared to the integral velocity length scale ( $L_v$ ). When the radius of the feed stream is larger than  $L_v$ , a characteristic length scale for the turbulent motions taking part in the dispersion process is  $L_v$ . In that case the characteristic time scale for the turbulent dispersion process equals:

$$t_{\text{meso}} \approx \frac{Q}{u_c \varepsilon^{1/2} L_v^{1/2}} \quad (3)$$

in which  $Q$  is the feed flow rate,  $u_c$  is the local circulation velocity just below the feed pipe,  $\varepsilon$  is the local energy dissipation rate and  $L_v$  is the integral velocity length scale. Usually, inside a stirred tank reactor the radius of the feed stream is smaller than the integral velocity length scale. For this situation, the characteristic length scale for turbulent dispersion is the radius of the feed stream and the characteristic time scale for the turbulent dispersion process equals:

$$t_{\text{meso}} \approx \left( \frac{Q}{u_c \varepsilon} \right)^{1/2} \quad (4)$$

Micromixing is mixing by engulfment, deformation and diffusion inside small-scale turbulent motions. As shown by Baldyga and Bourne (1989) for  $Sc \ll 4000$ , engulfment is the rate-limiting step of the micromixing process. In that case the characteristic time scale for micromixing is:

$$t_{\text{micro}} = \frac{l}{E} = 17.3 \sqrt{\frac{\nu}{\varepsilon}} \quad (5)$$

with  $E$  the engulfment rate,  $\nu$  the kinematic viscosity and  $\varepsilon$  the local energy dissipation rate.

The micromixing time scale is a function of the local energy dissipation rate. The mesomixing time scales are a function of the local energy dissipation rate, integral velocity length scale and circulation velocity. When no large gradients of these hydrodynamic parameters are present in the reaction zone, the energy dissipation rate, integral velocity length scale and circulation velocity can be assumed to be a constant fraction of the average energy dissipation rate, vessel diameter and tip velocity, respectively:

$$\bar{\varepsilon} \propto \bar{\varepsilon} \quad (6)$$

$$L_v \propto D \quad (7)$$

$$u_c \propto u_{tip} \quad (8)$$

For the average energy dissipation rate in geometrically similar stirred tank reactors with a turbulent flow field the following relationship exists:

$$\bar{\varepsilon} \propto N^3 D^2 \quad (9)$$

The tip velocity ( $u_{tip}$ ) is proportional to stirrer speed (N) and vessel diameter (D):

$$u_{tip} \propto ND \quad (10)$$

The general method used in the scale-up of a chemical reactor consists of the identification of the mixing mechanism controlling the product quality and keeping the characteristic time scale of the controlling mechanism constant during scale-up. Substituting equations (6)-(10) into equations (2)-(4) gives the following scale-up rules for geometrically similar vessels with a relatively homogeneous turbulent flow field:

$$\text{micromixing: } N \propto D^{-2/3} \quad (11)$$

$$\text{mesomixing: } N \propto \sqrt{QD^{-3}} \quad r > L_v \quad (12)$$

$$N \propto (QD^{-3})^{1/4} \quad r < L_v \quad (13)$$

Note that for a constant residence time ( $Q \propto D^3$ ) the scale-up criteria derived for mesomixing-limited processes with  $r > L_v$  is equal to the scale-up criteria for  $r < L_v$ , i.e. a constant stirrer speed. The scale-up rule for a constant macromixing time, which follows from equation (1) is also a constant stirrer speed.

Based on the scale-up rules given above one may conclude that a conservative scaling rule for a stirred tank reactor is to keep stirrer speed and residence time constant on scale-up.

In that case, the micromixing time scale decreases and the mesomixing and macromixing time scales are constant. This implies that the following trends are anticipated:

- a) When micromixing controls the product quality, the increase in the micromixing rate will decrease the amount of by-products.
- b) When mesomixing or macromixing controls the product quality no change in product distribution is to be expected.

It should be noticed that the scale-up rules described above are not applicable when large gradients of the hydrodynamic parameters are present in the reaction zone. In chapter 2 large gradients of the energy dissipation rate have been shown to be present in a stirred tank reactor equipped with a Rushton turbine impeller. Figure 2 shows the amount of by-product of the third Bourne reaction for two geometrically similar vessels equipped with a Rushton turbine impeller as a function of stirrer speed. The amounts of by-product at a constant stirrer speed have been measured using a constant residence time. More details about these experiments can be found in chapter 2. Figure 2 shows that for a stirrer speed larger than 1 Hz, more by-product is formed in the larger reactor at a constant stirrer speed and residence time. Therefore, it can be concluded that a constant stirrer speed and residence time is not a general conservative scale-up criterion. In general, a mixing model, which takes the gradients of the hydrodynamic parameters into account (e.g. the model presented in chapter 2) should be used for the effective design and scale-up of stirred tank reactors.

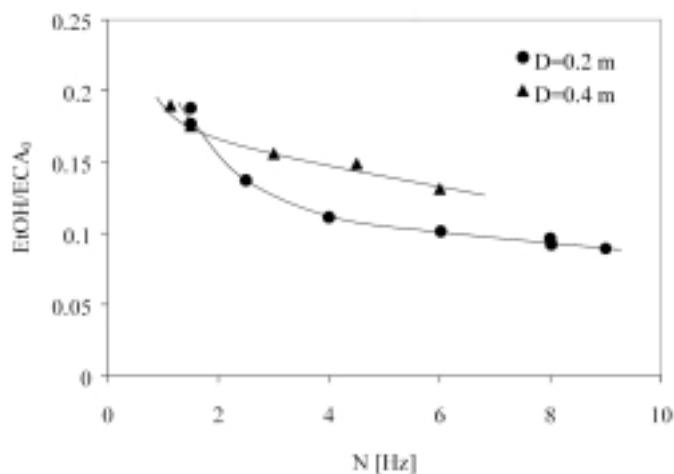


Figure 2: Ethanol yields as a function of stirrer speed for two geometrically similar vessels equipped with a Rushton turbine impeller.

## 2.2 Model based on Reynolds decomposition

A Lagrangian mechanistic mixing model cannot be used for complex inhomogeneous flows, where the environment contains partially reacted fluids. For this situation models based on Reynolds decomposition are proposed. Reynolds decomposition consists of describing a property of the turbulent flow with a mean and fluctuating value. In chapter 3 models for the calculation of the mean and fluctuating concentration of an passive tracer fed to a stirred tank reactor have been presented. How these equations can be extended to describe the mixing of turbulent reacting flows is discussed in more detail below.

Reynolds decomposition and time averaging applied to the mass transfer equation of a reactant results in:

$$\frac{D\bar{c}}{Dt} = \frac{\partial}{\partial x_j} \left[ D_m \frac{\partial \bar{c}}{\partial x_j} \right] - \frac{\partial}{\partial x_j} \overline{u'_j c'} + \bar{R} \quad (14)$$

In equation (14) the term  $\overline{u'_j c'}$  is unclosed. This term is usually approximated using the concept of turbulent diffusivity:

$$-\overline{u'_j c'} = D_T \frac{\partial \bar{c}}{\partial x_j} \quad (15)$$

The turbulent dispersion coefficient ( $D_T$ ) depends on the radius of the feed stream ( $r$ ) compared to the size of the large scale turbulent motions ( $L_v$ ) (Lesieur, 1990):

$$D_T = 0.1 \varepsilon^{-1/2} \lambda^{4/3} \quad (16)$$

with  $\lambda = r$  when  $r < L_v$  (chapter 2) and  $\lambda = L_v$  when  $r \geq L_v$  (Baldyga and Pohorecki, 1995).

The reaction term in equation (14) is unclosed when the reaction kinetics are nonlinear. Consider for example the following reaction:



with a reaction rate equal to:

$$R = k_p c_A c_B \quad (18)$$

Reynolds decomposition and averaging generates the unclosed term  $\overline{c'_A c'_B}$ :

$$\overline{R} = k_p \overline{c_A c_B} = \overline{c_A c_B} + \overline{c'_A c'_B} \quad (19)$$

The model required to close the chemical reaction term depends on the rates of decay of the concentration variances, i.e.  $t_s^{-1}$ , E and G, (see chapter 3) compared to the chemical reaction rate (Baldyga and Bourne, 1999; Fox, 1996):

- When chemical reaction rates are slow compared to the rates of decay of the concentration variance, the concentration fluctuations can be neglected:

$$\overline{R} = R(\overline{c}) \quad (20)$$

- In the case of very fast reaction rates compared to the rates of decay of the concentration variance, the chemical reaction term can be closed using a presumed Probability Density Function (PDF) method (Toor, 1962; Li and Toor, 1986).
- Between these limits of very fast and very slow reaction rates there is a wide range of reaction rates called “finite rate chemistry”. To close the chemical reaction term for “finite rate chemistry” presumed and full PDF closure methods are proposed in the literature.

Presumed PDF methods were first used to close the chemical reaction term for very fast chemical reactions (Toor, 1962; Li and Toor, 1986). Baldyga (1994) has extended this method to reactions with finite rate chemistry. In presumed PDF methods local species concentrations are expressed as a function of normalized passive tracer concentrations ( $f=c/c_0$ ), so that the mean reaction rate can be calculated from:

$$\overline{R} = \int_0^1 R(f) p(f) df \quad (21)$$

once the probability density function (PDF) of the passive tracer concentration ( $p(f)$ ) is known.

Usually, this PDF is approximated by the beta-distribution (Li and Toor, 1986):

$$p(f) = \frac{f^{\alpha-1} (1-f)^{\beta-1}}{\int_0^1 u^{\alpha-1} (1-u)^{\beta-1} du} \quad (22)$$

$$\alpha = \bar{f} \left[ \frac{\bar{f}(1-\bar{f})}{\sigma^2} - 1 \right] \quad (23)$$

$$\beta = (1-\bar{f}) \left[ \frac{\bar{f}(1-\bar{f})}{\sigma^2} - 1 \right] \quad (24)$$

The beta-distribution is determined uniquely by the normalized mean concentration of an passive tracer ( $\bar{f}$ ) and the variance of the normalized concentration of an passive tracer ( $\sigma^2 = (\overline{f^2}) - (\bar{f})^2$ ). The mean concentration and concentration variance of an passive tracer fed to a stirred tank reactor can be calculated with the models described in chapter 3.

PDFs of an passive tracer fed to a stirred tank reactor equipped with a Rushton turbine impeller have been measured with Planar Laser Induced Fluorescence (PLIF) (Verschuren et al., 2001a). The PLIF set-up and stirred tank configuration used to determine these PDFs have already been described in chapter 3 of this thesis. Figure 3 shows a comparison between a measured PDF and the beta-distribution calculated with the mean and variance obtained from the measured PDF. This figure shows that the measured PDF in a stirred tank reactor can be approximated reasonably by the beta-distribution.

Full PDF methods predict the shape of the one-point joint velocity-composition PDF or the one-point joint composition PDF. An important feature of these methods is that the chemical reaction kinetics appear in closed form. Full PDF methods are more generally applicable than the presumed PDF methods. However, due to their complexity they require very long calculation times (Baldyga, 1997), which makes them impractical for engineering calculations. Elaborate information about these full PDF methods can be found in various review papers, e.g. Pope (1985) and Fox (1996).

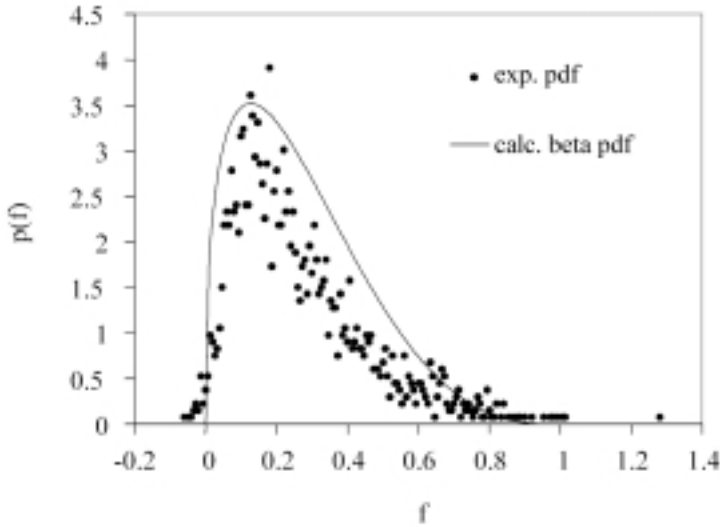


Figure 3: Probability density function (PDF) of normalized passive tracer concentrations ( $f$ ) measured at an axial distance of 0.04 m below the feed pipe ( $\bullet$ ) and the beta-distribution calculated with the mean and variance of the measured PDF ( $\text{—}$ ) (Verschuren et al., 2001a).

### 3. Suggestions for future research

#### **Modeling of a turbulent flow field in a stirred tank reactor**

Application of the mixing models presented in this thesis requires information on local turbulent flow parameters, e.g. energy dissipation rates, integral velocity length scales and average velocity. Therefore, these models need to be combined with models for the turbulent flow parameters to obtain a general design tool for stirred tank reactors.

Various models for the turbulent flow parameters in stirred tank reactors are presented in the literature, e.g. models based on Reynolds Averaged Navier Stokes (RANS) equations (Ng et al., 1998; Hui Meng and Fox, 1998), Large Eddy Simulations (LES) (Eggels, 1996; Derksen and van den Akker, 1999, Bakker 2000) and Direct Numerical Simulations (DNS) (Bartels et al., 2000). DNS is only applicable for relatively low Reynolds numbers and not yet capable of simulating turbulent flows of practical interest. In general, models based on RANS equations predict the mean velocity field rather well, although, they underpredict the turbulent kinetic energy and energy dissipation rate, especially in the flow discharge region of the impeller (Ng et al., 1998; Hui Meng and Fox, 1998). LES in stirred tank configurations have been successfully used to describe



phase-averaged velocity measurements (Eggels, 1996), phase-resolved velocity measurements and turbulent kinetic energy levels (Derksen and van den Akker, 1999). Therefore, it is expected that LES can be used to calculate the turbulent flow parameters required by the mixing models, although, energy dissipation rates predicted by LES need to be validated against experimental data.

### **Effect of large-scale oscillations of feed streams on the selectivity of a mixing-sensitive process**

Feed streams inside stirred tank reactors have been shown to oscillate. These oscillations are ignored in the Lagrangian model presented in chapter 2 and the model based on Reynolds decomposition presented in chapter 3, because these models have been used to describe the mixing of one single feed stream with relatively homogeneous bulk liquid. Under these circumstances the large-scale oscillations have no effect on the mixing rate. When multiple feed points are used in a stirred tank reactor the large-scale oscillations of the feed streams can cause feed streams to overlap. In that case the large-scale oscillations will have to be included in the mixing models. A description for the large-scale oscillations has been given in chapter 4. Additional research will have to be performed to include this description for the large-scale oscillation in mixing models for the calculation of the selectivity of mixing-sensitive reactions in stirred tank reactors with multiple feed points.

### **Instability of the flow pattern in stirred tank reactors**

Large-scale, low-frequency variations of the flow pattern have been shown to be present in stirred tank reactors (Chapple and Kresta, 1994; Montes et al., 1997; Schoenmakers et al., 1997). These large-scale flow instabilities (also called macro-instabilities) are visible by means of peaks in the horizontal part of an energy spectrum. Examples of energy spectra calculated from radial velocities measured in a stirred tank reactor equipped with a Pfaudler impeller-type agitator for stirrer speeds of 1 Hz, 3 Hz and 4 Hz, respectively, are given in Figure 4 (Verschuren et al., 2001b). In this figure three peaks are visible in the horizontal part of the energy spectra at frequencies of  $0.4N$ ,  $0.6N$  and  $0.8N$ , with  $N$  the stirrer frequency. From Figure 4 it is concluded that the frequency of the large-scale variations of the flow pattern scale with impeller speed. Although recent publications have demonstrated the existence of the instability, its origin and influence on chemical processes is unknown yet. Therefore, more research is necessary to determine its origin and effect on chemical processes.

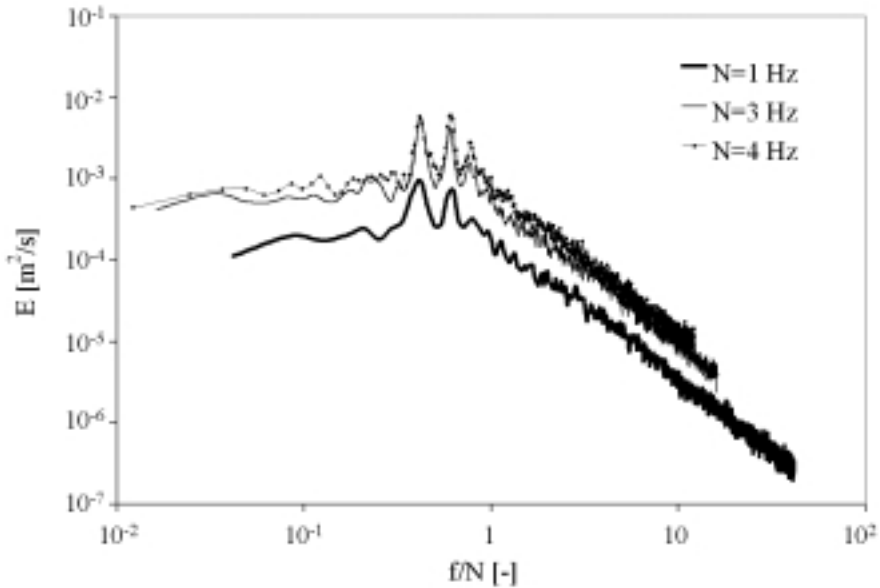


Figure 4: Energy spectra calculated from radial velocities measured in a stirred tank reactor equipped with a Pfaudler impeller-type agitator for stirrer speed of 1 Hz, 3 Hz and 4 Hz, respectively (Verschuren et al., 2001b).

Macro-instabilities are large-scale and low frequency phenomena. The kinetic energy of the flow is dissipated at the flow's micro scale and phenomena like droplet break up, agglomeration, cell damage and mixing are controlled by processes taking place on a small-scale. Therefore, to quantify the instabilities, to determine its dynamics and its effect on chemical processes, measurement techniques able to determine the properties of the flow locally and simultaneously at multiple positions and for a long period of time are required. Examples of possible measurement techniques are Particle Image Velocimetry (PIV) and Laser Induced Fluorescence (LIF). PIV can be used to measure the flow field and LIF can be used for the visualization of flow structures and the measurement of passive and reactive scalar mixing. Furthermore, a combination of PIV and LIF makes it possible to measure the flow field and scalar mixing simultaneously, which may be used to uncover the cross-correlation between the flow instabilities and chemical processes.

The measurement techniques mentioned above have some inherent limitations, e.g. they can only be used with transparent vessels and transparent liquids. When investigating high Reynolds number flows, the smallest scales are not accessible for these techniques and the instantaneous measurement of the complete flow field inside a stirred tank reactor is impossible. As a consequence, computational modeling is necessary to provide the additional information, which cannot be measured experimentally. Additionally, the results of the computational modeling can be used to refine the measurement techniques. It is expected that LES can be used to study the large-scale low-frequency variations of the flow field inside stirred tank reactors, given the fact that flow patterns predicted with LES have shown to exhibit these variations (Bakker, 2000).

### **Multiphase mixing**

The models proposed in this thesis have been used to describe single-phase liquid mixing in stirred tank reactors. These models require information about the turbulent flow parameters, which have been measured with Laser Doppler Velocimetry (LDV). However, stirred vessels are not only widely used for single-phase liquid mixing but also for multiphase mixing. For very low volume fractions of the dispersed phase (solid, gas and or liquid), the models and turbulent flow parameters proposed in this study can be used to describe the mixing of reactants in the liquid phase. As an example, in the modeling of precipitation reactions the effect of the solid particles on the mixing is usually neglected (Phillips et al., 1999; van Leeuwen, 1998). However, at higher volume fractions the interaction between the turbulent liquid flow and the dispersed phase should be taken into account. As an example, it has been shown that solid particles can cause either an increase or a decrease of the turbulence intensity, depending on the size of the particles compared to the fluid length scale (Gore and Crowe, 1989). However, turbulence modification in multiphase flows and the effect of a dispersed phase on chemical processes are areas that still need further development. To ascertain the effect of suspended solids on turbulence, LDV can be used to measure the turbulent flow parameters in a flow containing suspended particles with a refractive index matched to the refractive index of the liquid (Kajbic, 1995). The effect of suspended solids on chemical reactions can be studied using the same mixing sensitive test reactions as employed in single-phase liquid mixing investigations (Bennington and Bourne, 1990; Barresi, 1997).

## Nomenclature

$c$	concentration	$[\text{mol m}^{-3}]$
$D$	vessel diameter	$[\text{m}]$
$D_{\text{im}}$	impeller diameter	$[\text{m}]$
$f$	normalized passive tracer concentration	$[-]$
$k_{\text{R}}$	kinetic constant	$[\text{m}^3 \text{mol}^{-1} \text{s}^{-1}]$
$L_{\text{v}}$	integral velocity length scale	$[\text{m}]$
$N$	stirrer speed	$[\text{s}^{-1}]$
$N_{\text{q}}$	pumping capacity	$[-]$
$p$	probability density function	$[-]$
$Q$	feed flow rate	$[\text{m}^3 \text{s}^{-1}]$
$r$	radius of the feed stream	$[\text{m}]$
$r_{\text{c}}$	circulation ratio	$[-]$
$R$	reaction rate	$[\text{mol m}^{-3} \text{s}^{-1}]$
$t$	time	$[\text{s}]$
$t_{\text{c}}$	circulation time	$[\text{s}]$
$t_{\text{macro}}$	macromixing time	$[\text{s}]$
$t_{\text{meso}}$	mesomixing time	$[\text{s}]$
$t_{\text{micro}}$	micromixing time	$[\text{s}]$
$u$	velocity	$[\text{m s}^{-1}]$
$u_{\text{c}}$	circulation velocity	$[\text{m s}^{-1}]$
$u_{\text{tip}}$	tip velocity	$[\text{m s}^{-1}]$
$V$	vessel volume	$[\text{m}^3]$
$x$	coordinate	$[\text{m}]$
$\varepsilon$	energy dissipation rate	$[\text{m}^2 \text{s}^{-3}]$
$\lambda$	length scale	$[\text{m}]$
$\nu$	kinematic viscosity	$[\text{m}^2 \text{s}^{-1}]$
$\sigma$	variance of the normalized passive tracer concentration	$[-]$

subscripts

A,B

reactants

j

coordinate direction

superscripts

‘

fluctuation

—

average

## References

Bakker A. "The use of Large Eddy Simulations to study stirred vessel hydrodynamics" *Proc. 10th Europ. Conf. on Mixing (Delft, The Netherlands)*, 247 (2000)

Baldyga, J. "A closure model for homogeneous chemical reactions" *Chem. Eng. Sci.* 44, 1985 (1994)

Baldyga, J., and J.R. Bourne "Simplification of micromixing calculations I. Derivation and Application of new model", *Chem. Eng. J.*, 42, 83 (1989a)

Baldyga, J. and J.R. Bourne "Turbulent mixing and chemical reactions" *John Wiley, Chichester* (1999)

Baldyga, J. and M. Henczka "Turbulent mixing and parallel chemical reactions in a pipe: application of a closure model" *9th Europ. Conf. on Mixing, Paris* (1997)

Baldyga, J., and R. Pohorecki "Turbulent micromixing in chemical reactors. a review", *Chem. Eng. J.* 58, 183 (1995)

Barresi, A.A. "Experimental investigation of interaction between turbulent liquid flow and solid particles and its effect on fast reactions" *Chem. Eng. Sci.* 52, 807 (1997)

Bennington, C.P.J. and Bourne, J.R. "Effect of suspended fibres on macro-mixing and micro-mixing in a stirred tank reactor" *Chem. Eng. Commun.* 92, 183 (1990)

Chapple, D. and S.M. Kresta "The effect of geometry on the stability of flow patterns in stirred tanks" *Chem Eng Sci* 49, 3651 (1994)

Derksen, J. and H.E.A. van den Akker "Large Eddy Simulation on the flow driven by a Rushton turbine" *A.I.Ch.E. J.* 45, 209 (1999)

Eggels, J.G.M. "Direct and Large-Eddy Simulations of turbulent fluid flow using the Lattice-Boltzmann scheme" *Int. J. Heat and Fluid Flow* 17, 307 (1996)

Fox, R.O. "Computational methods for turbulent reacting flows in the chemical process industry", *Revue de L'Institut Français du Pétrole*, 51, 215 (1996)

Gore, R.A. and C.T. Crowe "Effect of particle size on modulating turbulence intensity" *Int. J. Multiphase Flow* 15, 279 (1989)

Hui Meng, J.S. and R.O. Fox "Validation of CFD simulations of a stirred tank using particle image velocimetry data" *Can. J. Chem. Eng.* 76, 611 (1998)

Kajbic, A.F. "Distribution of energy dissipation in stirred vessels for liquids and suspensions" (in Dutch), Eindhoven University of Technology, Institute for Continuing Education, ISBN 90-5282-543-3 (1995)

Leewen van, M. "Precipitation and Mixing" Ph.D. Thesis, Delft University of Technology, The Netherlands (1998)

Lesieur, M. "Turbulence in fluids: Stochastic and numerical modeling", Kluwer Academic Publishers, Dordrecht (1990)

Li, K.T. and H.L. Toor "Chemical indicators as mixing probes. A possible way to measure micromixing simply" *Ind. Eng. Chem. Fundam.* 25, 719 (1986)

Montes, J. L., H.C. Boisson, I. Fort, and M. Jahoda "Velocity field macro-instabilities in an axially agitated mixing vessel" *Chem Eng J* 67, 139 (1997)

Ng, K., N.J. Fentiman, K.C. Lee and M. Yianneskis "Assessment of sliding mesh CFD prediction and LDA measurements of the flow in a tank stirred by a Rushton impeller" *Trans. I.Chem.E.* 76, Part A, 737 (1998)

Phillips R., S. Rohani and J. Baldyga "Micromixing in a single feed semibatch precipitation process" *A.I.Ch.E. J.* 45, 82 (1999)

Pope, S.B. "PDF methods for turbulent reactive flows" *Prog. Energy Combust. Sci.* 11, 119 (1985)

Schoenmakers, J. H. A., J.G. Wijers, and D. Thoenes "Non steady-state behavior of the flow in agitated vessels", *Proc fourth World Conf on Exp Heat Transfer, Fluid Mechanics and Thermodynamics, ExHFT 4*, (Brussels, Belgium), 477 (1997)

Toor, H.L. "Mass transfer in dilute turbulent or nonturbulent systems with rapid irreversible reactions and equal diffusivities" *A.I.Ch.E.J.* 8, 70 (1962)

Verschuren, I.L.M., J.G. Wijers and J.T.F. Keurentjes "Probability Density Function of passive tracer concentration in a stirred tank reactor" submitted (2001a)

Verschuren I.L.M., J.G. Wijers and J.T.F. Keurentjes "Determination of the flow and turbulence characteristics in a stirred vessel equipped with a Pfaudler type impeller", submitted (2001b)



## Summary

Inefficient mixing has large negative effects on the yield and selectivity of a broad range of chemical reactions, because slow mixing can retard desired reactions and promote undesired side reactions. Therefore, a better designed and controlled mixing process leads to significant pollution prevention, better usage of raw materials and avoids expensive separation costs downstream in the process. Examples of mixing-sensitive processes are various types of polymerizations, precipitations and fermentations. Stirred tank reactors are frequently used in the chemical and biochemical industry to accomplish mixing tasks. In this study the interaction between mixing and chemical reactions is investigated for stirred tanks operated under turbulent flow conditions. The objective of this study is to obtain models and rules applicable for the design and scale-up of stirred tank reactors yielding a defined product quality.

A Lagrangian mechanistic mixing model has been developed to calculate the selectivity of a mixing-sensitive reaction in a semi-batch stirred tank reactor based on descriptions of the mixing processes in a turbulent flow. The model is validated by determining the effects of stirrer speed, vessel size, feed point position and feed flow rate on the selectivity of a mixing-sensitive reaction set. Application of the model requires information on the local hydrodynamic parameters of the stirred vessel studied, i.e. energy dissipation rate, integral velocity length scale and the mean velocity. The required detailing in the description of these hydrodynamic parameters to obtain a good agreement between measured and calculated selectivities has been determined. The model proved to be successful in predicting the product distribution of a competitive reaction, making it useful for the design and scale-up of stirred tank reactors.

Since the Lagrangian mechanistic mixing model describes the mixing of a fluid element with homogeneous bulk liquid, it cannot be used for complex inhomogeneous flows, where the environment contains partially reacted fluids. For inhomogeneous flows, Eulerian models based on Reynolds decomposition are proposed. Reynolds decomposition consists of describing a property of the turbulent flow with a mean and a fluctuating value. In this study, models from the literature have been integrated to describe the mean and fluctuating concentration of a feed stream in a stirred tank reactor. Planar Laser Induced Fluorescence (PLIF) and Laser Doppler Velocimetry (LDV) experiments have been performed to validate these models and to determine the model parameters. To calculate the mean concentration, the turbulent dispersion coefficient



has to be known. In this study, a combination of a theoretical model, measured mean concentrations and LDV experiments is used to determine this turbulent dispersion coefficient. A model described in the literature is adapted to calculate the concentration variance. Compared to the literature the model requires adjustment of the constant in the production term of the concentration variance to fit the measured concentration variances correctly. The models proved to be able to describe the mean concentration and concentration variance of an passive tracer stream fed to a stirred tank reactor. A next step would be to integrate these models with the presumed Probability Density Function (PDF) method proposed in the literature. This method enables the calculation of the yield of mixing-sensitive reactions from mean concentrations and concentration variances of an passive tracer.

Feed streams inside stirred tank reactors have been shown to oscillate. These large-scale oscillations are ignored in the models described above, because the models have been used to describe the mixing of one single feed stream with relatively homogeneous bulk liquid. Under these circumstances the large-scale oscillations have no effect on the mixing rate. However, when multiple feed points are used, the large-scale oscillation can cause the feed streams to overlap. In this study large-scale oscillations have been shown to be caused by turbulent motions with a size larger than the diameter of the feed stream. In addition, an equation describing the root-mean-square displacements of the centre-of-mass of a feed stream caused by the large-scale oscillations has been derived. This equation can be used to calculate the minimal distance between feed pipes to prevent overlap of the feed streams.

The models described above have been used to describe the mixing inside stirred tank reactors due to turbulence generated by the stirrer. When the velocity of the feed stream is much higher than the local circulation velocity, mixing of the feed stream will be caused by a combination of stirrer and feed stream generated turbulence. For these feed stream velocities it has been suggested in the literature to keep the turbulent dispersion time constant upon scale-up to obtain a constant product quality. To obtain an equation for the turbulent dispersion time a theoretical model, PLIF experiments and LDV experiments have been combined. This has been done for the case that a feed stream is mixed in a stirred vessel due to a combination of stirrer and feed stream generated turbulence. The equation as well as the experiments showed that the turbulent dispersion time decreases with an increasing stirrer speed or feed stream velocity or with a decreasing feed pipe diameter.

Pfaudler impeller-type agitators are frequently used in the chemical industry for the production of fine chemical and pharmaceuticals. Information on the hydrodynamic parameters in these reactors is limited. The hydrodynamic parameters in a baffled reactor equipped with a Pfaudler impeller-type agitator, which are required to predict selectivities of mixing-sensitive processes, have been determined. For low feed rates, often used to control the product distribution or to prevent a thermal runaway, the selectivity is controlled by micromixing. A micromixing model from the literature has been used to calculate the selectivity of mixing sensitive reactions in reactors equipped with a Pfaudler impeller. The calculated selectivities have been validated against measured selectivities of mixing-sensitive reactions. Calculated selectivities using an average energy dissipation rate are in good agreement with measured selectivities for a broad range of process conditions. From these results it is concluded that a constant energy input per unit volume is a reasonable scale-up rule for a baffled reactor equipped with a Pfaudler impeller-type agitator, when micromixing controls the product distribution.

In this study various models from the literature describing the mixing in a turbulent flow have been validated against detailed experimental data. To make the models suitable for stirred tank reactors various refinements have been suggested. It has been shown that the models can be used to describe local mixing phenomena and are able to predict the selectivity of mixing sensitive reactions in stirred tank reactors operated under turbulent flow conditions.



## Samenvatting

Voor een groot aantal chemische reacties is de snelheid van menging van de reactanten van invloed op de productsamenstelling. Zo kan bijvoorbeeld langzame menging de gewenste reactie vertragen, waardoor ongewenste reacties de kans krijgen op te treden. Onderzoek naar de menging in reactoren is dus van groot belang voor de reductie van de hoeveelheid bijproducten, hetgeen niet alleen leidt tot een versnelling van de productie en verlaging van de kostprijs, maar bovendien beter is voor het milieu. Precipitaties, polymerisaties en fermentaties zijn slechts enkele voorbeelden van menggevoelige reacties. Zowel de chemische als de biochemische industrie maakt veelvuldig gebruik van geroerde reactoren voor menggevoelige processen. Dit onderzoek is gericht op de interactie tussen menging in geroerde reactoren en de selectiviteit van chemische reacties. Het doel van het onderzoek is het ontwikkelen van modellen en regels die toepasbaar zijn bij het ontwerpen en opschalen van geroerde reactoren met behoud van productkwaliteit.

Een Lagrangiaans mengmodel, waarmee de opbrengst van chemische reacties voorspeld kan worden, is ontwikkeld op basis van modellen uit de literatuur voor de verschillende mengprocessen in een turbulente stroming. In dit model is de snelheid van menging een functie van de lokale energiedissipatie, de lokale lengteschaal van het turbulente snelheidsveld en de lokale gemiddelde snelheid. Tevens is de vereiste detaillering van de beschrijving van deze modelparameters om de selectiviteit van een chemische reactie te kunnen voorspellen bepaald. Dit is gedaan door selectiviteiten, berekend met verschillende beschrijvingen van de modelparameters, te vergelijken met gemeten selectiviteiten als functie van toerental, vatgrootte, locatie van de voedingsbuis en toevoersnelheid. Het model blijkt zeer goed in staat de selectiviteit van een menggevoelige reactie te voorspellen en is dus bruikbaar voor het ontwerpen en opschalen van geroerde reactoren.

Het Lagrangiaans mengmodel beschrijft de menging van een vloeistofelement met een homogene bulkvloeistof, waardoor het model niet toepasbaar is als een reactie niet gelocaliseerd plaatsvindt. In die situatie is het beter gebruik te maken van een Euleriaans model gebaseerd op Reynolds-decompositie. Reynolds-decompositie is het opsplitsen van een instantane variabele in een gemiddelde en een fluctuatie. In dit onderzoek is de gemiddelde en fluctuerende concentratie van een niet-reagerende scalair geïnjecteerd in een geroerd vat beschreven door verschillende modellen uit de literatuur te combineren.

De modellen zijn gevalideerd en de modelparameters zijn bepaald met behulp van concentratiemetingen met Laser Geïnduceerde Fluorescentie en Laser Doppler snelheidsmetingen. Zo is onder andere de turbulente dispersiecoëfficiënt, vereist om de gemiddelde concentratie te kunnen berekenen, bepaald aan de hand van een model uit de literatuur, gemeten gemiddelde concentraties en Laser Doppler snelheidsmetingen. Ook blijkt uit de experimenten dat een kleinere constante dan voorgesteld in de literatuur in de productieterm van de concentratiefluctuaties gebruikt moet worden, om een goede overeenkomst te krijgen tussen de gemeten en berekende fluctuerende concentraties. De modellen uit de literatuur, gecombineerd met de in dit onderzoek bepaalde turbulente dispersiecoëfficiënt en constante in de productieterm van de concentratiefluctuaties, blijken in staat te zijn de gemiddelde en fluctuerende concentratie van een niet-reagerende scalair geïnjecteerd in een geroerd vat te beschrijven. Het combineren van deze modellen met de “presumed Probability Density Function method” uit de literatuur zou een volgende stap kunnen zijn. Met behulp van deze methode is het namelijk mogelijk om de selectiviteit van een menggevoelige reactie te berekenen uit de gemiddelde en fluctuerende concentratie van een niet-reagerende scalair.

Een voedingsstroom in een geroerd vat oscilleert. Deze grootschalige oscillaties zijn niet meegenomen in de hierboven beschreven modellen, omdat deze modellen de menging van één voedingsstroom met relatief homogene bulkvloei stof beschrijven. In die situatie hebben de oscillaties van een voedingsstroom geen invloed op de menging. Echter in een geroerde reactor met meerdere toevoerpunten kunnen voedingsstromen met elkaar in contact komen ten gevolge van de grootschalige oscillaties. In dit onderzoek is aangetoond dat de grootschalige oscillaties worden veroorzaakt door turbulente wervels groter dan de breedte van de voedingsstroom. Een model is ontwikkeld voor de verspreiding van het massazwaartepunt van een voedingsstroom veroorzaakt door de grootschalige oscillaties. Met dit model kan de minimale afstand tussen twee toevoerpunten berekend worden die nodig is om te voorkomen dat de voedingsstromen met elkaar in contact komen.

Bovenstaande modellen zijn toegepast op situaties waarin de menging van een voedingsstroom wordt veroorzaakt door de turbulentie gegenereerd door de roerder. Echter wanneer de snelheid van de voedingsstroom groter is dan de lokale circulatiesnelheid wordt de menging niet alleen veroorzaakt door de turbulentie

gegenereerd door de roerder, maar ook door de turbulentie gegenereerd door de voedingsstroom. Verder geldt voor deze toevoersnelheid dat het turbulente dispersieproces vaak de snelheidsbepalende stap is van het mengproces, hetgeen betekent dat de turbulente-dispersie-mengtijd constant gehouden moet worden tijdens het opschalen van een reactor. In dit onderzoek is een vergelijking voor de turbulente-dispersie-mengtijd als functie van verschillende ontwerpparameters bepaald voor een snelle voedingsstroom in een geroerd vat. Uit zowel deze vergelijking als de experimenten blijkt dat de turbulente-dispersie-mengtijd afneemt bij een verhoging van het toerental of toevoersnelheid of wanneer een kleinere toevoerbuisdiameter wordt toegepast.

De opbrengst van een chemische reactie kan berekend worden met een mengmodel, mits de turbulente stromingsparameters van de gebruikte reactor bekend zijn. Reactoren met een Pfaudler-roerder worden in de chemische industrie vaak toegepast voor de productie van o.a. fijnchemicaliën en farmaceutica. In dit onderzoek zijn de turbulente stromingsparameters in een reactor met een Pfaudler-roerder bepaald met behulp van Laser Doppler snelheidsmetingen en koppelmetingen. Om de productkwaliteit en warmteontwikkeling van processen te beheersen wordt de voeding vaak zeer langzaam aan de reactor toegevoerd. Voor lage toevoersnelheden geldt dat micromenging de snelheidsbepalende stap van het mengproces is en kan de opbrengst van een chemische reactie berekend worden met een micromengmodel. Selectiviteiten van menggevoelige reacties in een reactor met een Pfaudler-roerder zijn berekend met een micromengmodel uit de literatuur en de experimenteel bepaalde stromingsparameters. Vervolgens zijn de berekende selectiviteiten gevalideerd met experimenteel bepaalde selectiviteiten. Selectiviteiten berekend met een gemiddelde energiedissipatie komen goed overeen met de gemeten selectiviteiten. Dit impliceert dat het constant houden van het door de roerder toegevoerde vermogen per volume-eenheid een goede opschaalregel is voor een reactor met een Pfaudler-roerder, als micromenging de snelheidsbepalende stap is.

In dit onderzoek zijn verschillende modellen uit de literatuur voor de mengprocessen in een turbulente stroming gevalideerd met experimentele data. Om de modellen toepasbaar te maken voor geroerde reactoren zijn diverse aanpassingen gemaakt. Deze modellen kunnen worden gebruikt worden om locale mengprocessen te beschrijven en om de selectiviteit van menggevoelige reacties te berekenen in geroerde reactoren.



## Dankwoord

In de eerste plaats wil ik alle medewerkers van de capaciteitsgroep SPD bedanken voor de prettige sfeer en collegialiteit in de afgelopen jaren.

Jos Keurentjes wil ik bedanken voor zijn in mijn gestelde vertrouwen. Jos, ik had me geen betere promotor kunnen wensen. Johan Wijers ben ik veel dank verschuldigd voor de vele vruchtbare discussies, prettige gesprekken en voor het onvermoeibaar nakijken van mijn manuscripten.

Een bijzonder woord van dank ook aan mijn (ex-)kamergenoten, Willem-Jan, Sjoerd, Frank en Henny voor de gezellige afleiding en de plezierige tijd. Marc, je bent naast een collega ook een zeer goede vriend, bedankt voor al je steun en natuurlijk niet te vergeten de koffie.

Verder wil ik de leden van mijn begeleidingscommissie (Frank Jeurissen (Akzo Nobel), Gert Colenbrander (Shell), Jos Derksen (TuDelft), Remko Bakker (DSM) en Thomas Martin (DSM)) bedanken voor hun constructieve opmerkingen en suggesties.

De afstudeerders Donald, Dominique, Bjorn, Patrick en Martijn en de stagiaires Bram en Diana ben ik zeer dankbaar voor al het waardevolle werk dat ze verricht hebben, hun enthousiasme en gezellige samenwerking.

Tenslotte wil ik het thuisfront inclusief vrienden bedanken voor al hun steun in de afgelopen jaren, in het bijzonder Dion, mijn ouders, Edwin, Bouwe, Marga en Joannie.

*Iris*





## Curriculum vitae

- |                                |   |
|--------------------------------|---|
| February 11 1974               | Born in Beek en Donk, The Netherlands   |
| August 1986 - August 1992      | Secondary school (V.W.O.) at the Dr. Knippenbergcollege, Helmond  |
| September 1992 - June 1997     | Chemical Engineering at the Eindhoven University of Technology Graduated Cum Laude at the Process Development Group on mesomixing in agitated vessels supervised by ir. J.G. Wijers and prof. dr. ir. A.A.H. Drinkenburg. |
| September 1997- September 2001 | Ph.D. project at the Process Development Group on feed stream mixing in stirred tank reactors supervised by ir. J.G. Wijers and prof. dr. ir. J.T.F. Keurentjes   |

## Publications

- I.L.M. Verschuren, J.G. Wijers and J.T.F. Keurentjes, Turbulent feed stream mixing in agitated vessels: mixing effects on chemical reaction selectivity, full paper annual A.I.Ch.E.-meeting (Miami, Florida), 1998, 185 g, 17 p.
- I.L.M. Verschuren, J.G. Wijers and J.T.F. Keurentjes, Turbulent feed stream mixing in agitated vessels: mixing effects on chemical reaction selectivity, A.I.Ch.E. annual meeting abstracts (Miami, Florida), published on CD, 1998
- I.L.M. Verschuren, J.G. Wijers, G.J.H.A. Schoenmakers, F. Jeurissen and J.T.F. Keurentjes, Determination of the mixing rate of a high velocity feed stream in agitated vessels, accepted for publication in Chem. Eng. Commun.
- I.L.M. Verschuren, J.G. Wijers and J.T.F. Keurentjes, Mixing with a Pfaudler type impeller; The effect of micromixing on reaction selectivity in the production of fine chemicals, Proc. 10th Europ. Conf. on Mixing (Delft), Elsevier, 2000

I.L.M. Verschuren, J.G. Wijers and J.T.F. Keurentjes, Effect of mixing on the product quality in semi-batch stirred tank reactors, accepted for publication in A.I.Ch.E.J.

I.L.M. Verschuren, J.G. Wijers and J.T.F. Keurentjes, Mean concentrations and concentration fluctuations in a stirred tank reactor, submitted for publication

I.L.M. Verschuren, J.G. Wijers and J.T.F. Keurentjes, Large-scale oscillations of a feed stream inside a stirred tank reactor, submitted for publication

I.L.M. Verschuren, J.G. Wijers and J.T.F. Keurentjes, Scale-up of a stirred tank reactor equipped with a Pfaudler type impeller, submitted for publication

I.L.M. Verschuren, J.G. Wijers and J.T.F. Keurentjes, A study of the flow and turbulence characteristics in a stirred vessel equipped with a Pfaudler type impeller, submitted for publication

I.L.M. Verschuren, J.G. Wijers and J.T.F. Keurentjes, Probability Density Function of the mixture fraction in a stirred tank reactor, submitted for publication

## Presentations

Experimental investigation of feed stream mixing in agitated vessels, SON-meeting, 1998

Turbulent feed stream mixing in agitated vessels: mixing effects on chemical reaction selectivity, A.I.Ch.E.-annual meeting, NAME, Industrial Mixing & Scale-up (Miami, Florida), November 15-20, 1998

Determination of the mixing rate of a high velocity feed stream in agitated vessels, 17th Biennial North American Mixing Conference (Banff, Canada), August 15-20, 1999

Mixing with a Pfaudler type impeller; The effect of micromixing on reaction selectivity in the production of fine chemicals, 10th Europ. Conf. on Mixing (Delft), July 2-5, 2000

Mixing and chemical selectivity in stirred tank reactors, A.I.Ch.E.-annual meeting, NAME, November (Los Angeles), November 12-17, 2000

# Stellingen

behorende bij het proefschrift "Feed stream mixing in stirred tank reactors" van Iris Verschuren

1. De grootschalige oscillaties van een toevoerstroam in een geroerde reactor worden veroorzaakt door wervels groter dan de straal van de toevoerstroam.

*dit proefschrift*

2. Een toevoerstroam met een straal kleiner dan de grootste wervels wordt verspreid door wervels van dezelfde orde grootte als de straal van de toevoerstroam. Daarom geldt in die situatie, in tegenstelling tot wat in de literatuur wordt aangenomen (o.a. Baldyga and Pohorecki, 1995), dat de karakteristieke tijdschaal voor turbulente dispersie op dezelfde manier afhankelijk is van de lengteschaal van de concentratie-fluctuaties als de karakteristieke tijdschaal voor het inertial-convective mengmechanisme.

*dit proefschrift*

*Baldyga, J. and R. Pohorecki, Turbulent mixing in chemical reactors; a review, Chem. Eng. J. 58, 183 (1995)*

3. Gezien het limiterende effect van turbulente dispersie op de mengsnelheid is het aan te bevelen om voor het opschalen van geroerde reactoren niet de diameter van de toevoerbuus op te schalen, maar juist het aantal toevoerbuizen.

*dit proefschrift*

4. In de berekening van de turbulente kinetische energie uit gemeten snelheidsfluctuaties in een geroerde reactor dient niet alleen een correctie gemaakt te worden voor de fluctuaties veroorzaakt door de roerderbladen, maar ook voor de fluctuaties veroorzaakt door de grootschalige instabiliteiten van het stromingsprofiel.

*Verschuren, I.L.M., Wijers J.G. and J.T.F. Keurentjes, Determination of the flow and turbulence characteristics in a stirred vessel equipped with a Pfaudler type impeller, submitted for publication*

5. In het onderzoek naar de invloed van stroming op chemische processen is er te weinig samenwerking tussen natuurkundigen en chemisch technologen.

6. Des te groter de welvaart, des te meer probeert men deze in zijn vrije tijd te ontvluchten.

7. In Barbershop hoor je de bariton pas als hij niet zingt.

8. De mate van emancipatie hangt niet zozeer af van het aantal huishoudelijke taken die de man op zich neemt als wel de verantwoordelijkheid die hij in deze draagt.

9. Aangezien smaak voor een belangrijk deel gebaseerd is op reuk is roken tussen de gangen van een maaltijd een belediging voor de kok. Omdat sterke drank zorgt voor het lamleggen van smaakpapillen geldt hetzelfde voor het nuttigen van sterke drank als aperitief.

10. Voor multidisciplinaire opleidingen is het van belang de terminologie van de verschillende disciplines beter op elkaar af te stemmen.

11. Je leert nooit iets voor niets.

*mijn wijze moeder*